Master's thesis

NTNU
Norwegian University of Science and Technology
Faculty of Natural Sciences
Department of Chemistry

Malene Fikseth Jakobsen

Synthesis of steroid analogs as potential CDK8 inhibitors using *(S)*-hydroxyalkyl azide in a stereoselective ring expansion

Master's thesis in Natural Science with Teacher Education
Supervisor: Eirik Johansson Solum

June 2021

NTNU
Norwegian University of
Science and Technology

Malene Fikseth Jakobsen

Synthesis of steroid analogs as potential CDK8 inhibitors using *(S)*-hydroxyalkyl azide in a stereoselective ring expansion

Master's thesis in Natural Science with Teacher Education
Supervisor: Eirik Johansson Solum
June 2021

Norwegian University of Science and Technology
Faculty of Natural Sciences
Department of Chemistry

NTNU
Norwegian University of
Science and Technology

Preface

This master´s thesis with the title *"Synthesis of steroid analogs as potential CDK8 inhibitors using (S)-hydroxyalkyl azide in a stereoselective ring expansion"* is based on work executed at the Department of Chemistry at NTNU during autumn and spring 2020-21. The thesis is a part of my education in the Master´s degree program Natural Science with Teacher Education. The supervisor of the thesis has been Associate Professor Eirik Johansson Solum.

I want to thank my supervisor, Associate Professor Eirik Johansson Solum, for good advice and for supporting me during working at the laboratory. I have learned a lot during these months in the lab. In the writing process, your advice has been highly valuable.

I would also like to thank Inga Haugsvær, who has been a big support during my time at NTNU. Her master´s thesis is on the same subject, but with a different regioisomer of the compound. Thank you for helping me with lab-related frustrations.

I would also like to thank Senior Engineer Susana Villa Gonzales, who has run the analyses for the MS-samples in this project, and staff engineer Roger Aarvik for ordering and providing chemicals applied in this thesis.

Lastly, I would like to thank family and friends for their encouragement and support last year.

Abstract

CDK8 plays an important role in regulating cell transcription either through the enzymes attachment to the mediator complex or through phosphorylation of transcription factors. CDK8-mediated activation of oncogenes is important in several cancers, including acute myelogenous leukemia (AML). Several compounds with a steroid core have been reported to have anticancer effects and can act as CDK8 inhibitors. Examples of effective CDK8 inhibitors are cortistatin A and CCT251545. The similarity between these compounds and the steroid structure suggests that the A-ring and the D-ring potentially can form interactions with CDK8. The compounds were therefore simplified by modifying the A- and D-ring in the steroidal structure. The A-ring was extended to a heterocyclic seven-membered ring in a regioselective ring expansion. The D-ring was introduced to various aromatic heterocycles that prior had shown promising result in biological evaluation.

In the first step, a hydroxyalkyl azide was synthesized in an S_N2 reaction. The A-ring in the steroid core was extended to a seven-membered ring by converting the ketone in 5α-dihydrotestosterone to an amide in a Schmidt reaction with the hydroxyalkyl azide. The hydroxyl groups were oxidized using PCC, and an β-elimination of the aryl alkyl ketone was performed with NaH. The D-ring was applied to a triflate in a synthesis with NaHMDS and *N*-phenyl-bis (trifluoromethanesulfonimide). The 17-position was further introduced to various heterocyclic rings in a Suzuki-Miyaura cross-couplings. The synthesis resulted in the formation of five potential inhibitors to be biologically evaluated as CDK8 inhibitors.

Sammendrag

CDK8 har en viktig rolle i regulering av celletranskripsjon gjennom enzymets tilknytning til mediatorkomplekset eller ved fosforylering av transkripsjonsfaktorer. CDK8-mediert aktivering av onkogener har vist seg å være viktig i en rekke krefttyper, inkludert akutt myelogen leukemi (AML). Det har vært rapportert om at flere forbindelser med steroid-struktur har antikrefteffekter, og kan fungere som CDK8-hemmere. Eksempler på CDK8 hemmere er cortistatin A og CCT251545. Likheten mellom forbindelsene og steroid-strukturen tyder på at at A-ringen og D-ringen kan danne interaksjoner med CDK8. Forbindelsene ble derfor forenklet ved å ta utgangspunkt i steroid-strukturen, samtidig som A- og D-ringen ble modifisert. A-ringen ble utvidet til en heterosyklisk syv-ring i en regioselektiv ringutvidelse, og D-ringen ble påsatt ulike aromatiske heterosykler som tidligere har vist lovende resultater under biologisk testing.

I det første trinnnet ble et hydroksylalkylazid syntetisert i en S_N2 reaksjon. A-ringen i steroid-strukturen ble utvidet til en syvring ved at ketonet i 5a-dihydrotestosteron ble omgjort til et amid i en Schmidt reaksjon med hydroksylalkylazidet. Hydroksyl-gruppene ble oksidert av PCC, for så å kunne utføre β-eliminasjon av aryl alkyl ketonet med NaH som base. D-ringen ble påsatt et triflat i en syntese med NaHMDS og *N*-fenyl-bis(trifluormetansulfonimid). 17-posisjonen ble videre påsatt ulike heterosykliske ringer i en Suzuki-Miyaura krysskobling. Syntesen resulterte i dannelse av fem forbindelser, som skal testes biologisk som mulige CDK8-hemmere.

Table of content

Abbreviations

$[\alpha]_D^{20}$	Specific Rotation [Measured at 589 nm (D-Line) and 20 °C]
δ	Chemical shift in NMR spectrums
λ	Wavelength in nano millimeters
AML	Acute Myelogenous Leukemia
ADP	Adenosine diphosphate
ATP	Adenosine triphosphate
Bcl-2	B-cell lymphoma 2
br	Broad Signal
CDK	Cyclin Dependent Kinases
d	Doublet
DCM	Dichloromethane
DMF	Dimethylformamide
EtOAc	Ethyl Acetate
equiv.	Equivalents
Flt3	FMS-like tyrosine kinase 3
g	Grams
h	Hour(s)
Hz	Hertz
IDH	Isocitrate Dehydrogenases
INF	Interferon
IR	Infrared
J	Coupling Constant

JAK	Janus kinase
LiAlH$_4$	Lithium Aluminium Hydride
M	Molar concentration given in moles/litres
m	Multiplet
MeOH	Methanol
mg	Milligrams
MS	Mass Spectroscopy
NMR	Nuclear Magnetic Resonance Spectroscopy
PCC	Pyridinium Chlorochromate
pK$_a$	Acid Dissociation Constant
ppm	Parts Per Million
q	Quartet
R$_f$	Retention Factor
rt	Room Temperature
s	Singlet
S$_N$2	Bimolecular Nucleophilic Substitution
STAT	Signal Transducer and Activator of Transcription
t	Triplet
THF	Tetrahydrofuran
TLC	Thin Layer Chromatography
UV	Ultraviolet

Numbered compounds
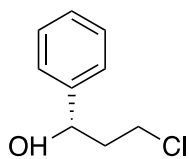
1
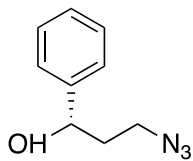
2
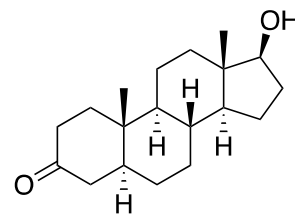
3
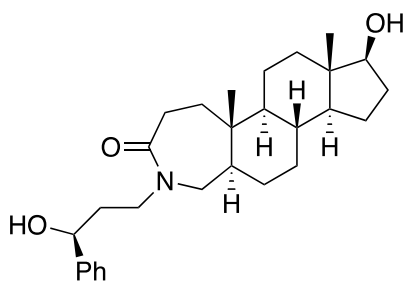
4
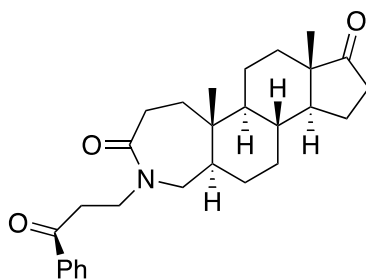
5
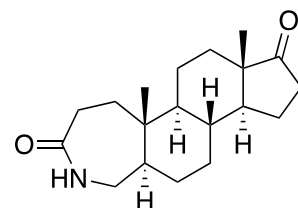
6
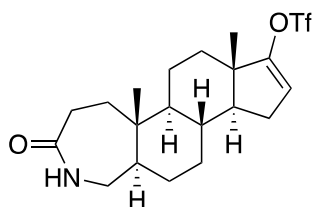
7
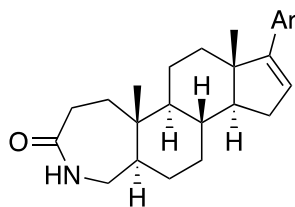
8
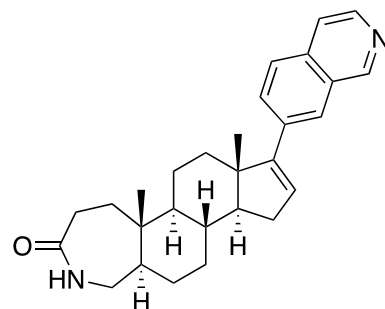
8a
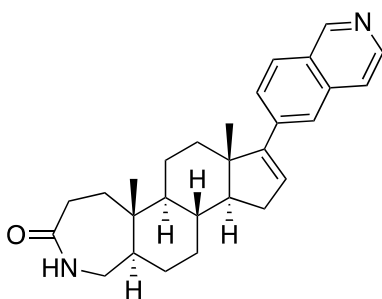
8b
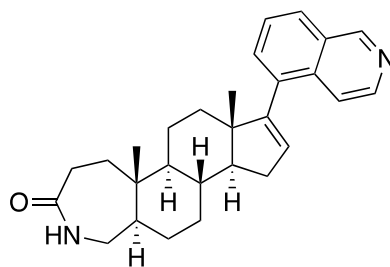
8c
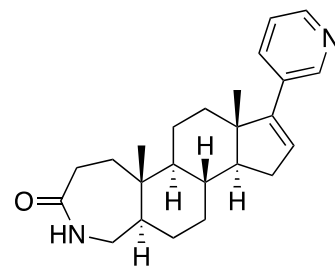
8d
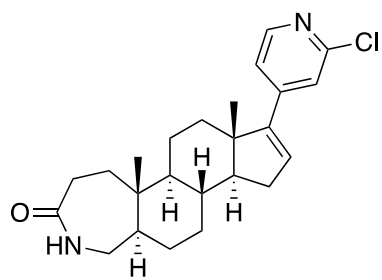
8e
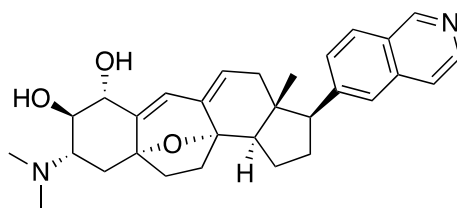
9
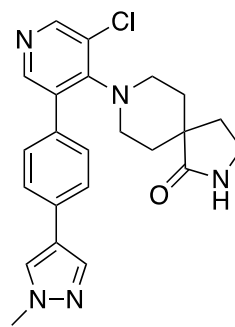
10
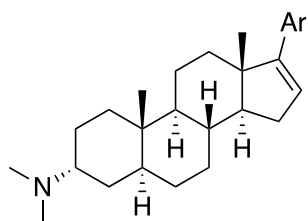
11
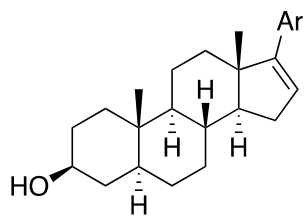
12
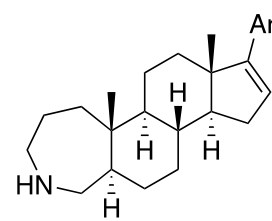
13
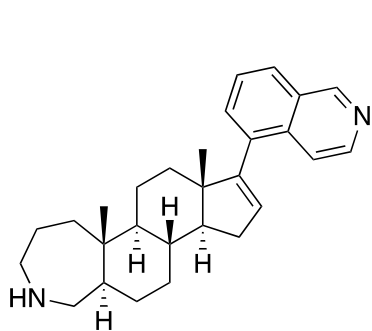
13a
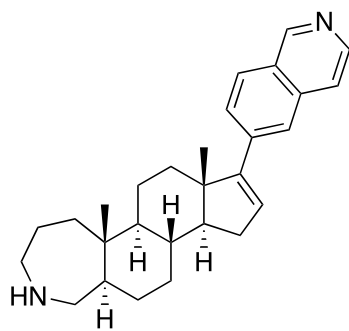
13b
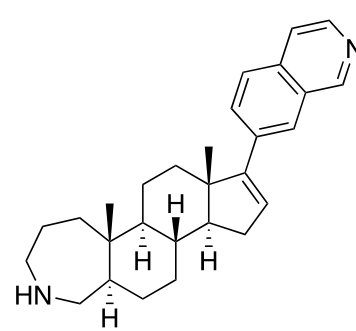
13c
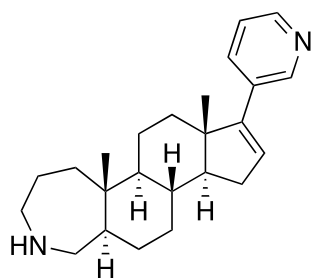
13d
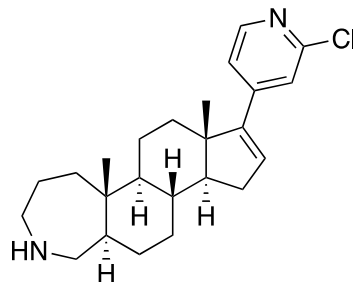
13e
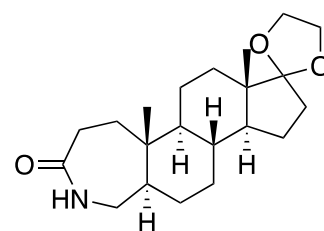
14
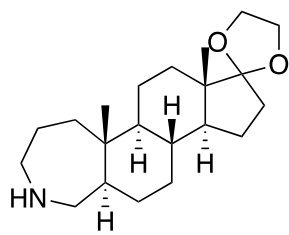
15
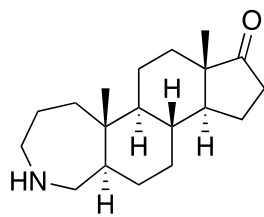
16
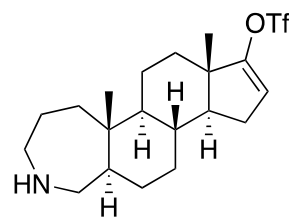
17
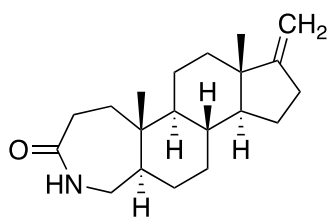
18
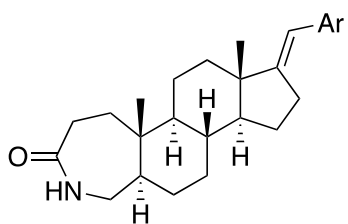
19
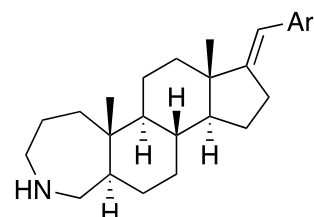
20

1 Introduction

In 2015, acute myelogenous leukaemia (AML) affected about one million people and resulted in 147.000 deaths globally[1]. AML is a heterogeneous and aggressive hematopoietic malignancy due to recurrent gene mutation and is the most common form of acute leukaemia in adults and the second most common form in children[2,3]. In the last few decades, much progress has been made toward improving treatment-related mortality rates. Despite this, long-term overall survival has stagnated[2]. Exciting developments of gene mutation-targeted therapeutic agents are now changing the perspective in AML treatment. Target therapy is a commonly used approach to treat AML. This type of therapy can be helpful even when standard chemotherapy has stopped working. Another option is to use targeted drugs along with chemotherapy to increase the therapeutic outcome[4].

There is growing interest in the use of novel and effective, target-directed therapies. Some of the targeted drugs developed are inhibitors of proteins like Bcl-2 (B-cell lymphoma 2), IDH (Isocitrate dehydrogenases), Flt3 (FMS-like tyrosine kinase 3)[5]. Flt3 is a receptor tyrosine kinase. When the ligand activates the receptor, it phosphorylates a tyrosine-residue on STAT-proteins. However, additional serine phosphorylation is needed for STAT-proteins to mediate their transcriptional effects. CDK8 mediates this serine-phosphorylation[6].

1.1 CDK8

Cyclin dependent kinases (CDKs) are a family of serine-threonine protein kinases that control critical regulatory events during cell cycle and transcription[7]. Different types of CDKs exist, and each kinase has a role to play at different stages of the cell cycle. Binding of a cyclin with its associated kinase activates the enzyme and serves to move the cell from one phase of the cell cycle to another[7]. CDK8 is particularly interesting because the kinase is found to be either mutated or amplified in a variety of human cancers[8, 9]. CDK8-mediated activation of oncogenes has proved to be important in various cancer types, including hematological malignancies[6]. CDK8 has a vital role in cell transcription regulation either by association with the mediator complex or phosphorylation of transcription factors[10-12]. As a serine-threonine kinase, CDK8 phosphorylates the alcohol group of serine and threonine residues, see Scheme 1.

1
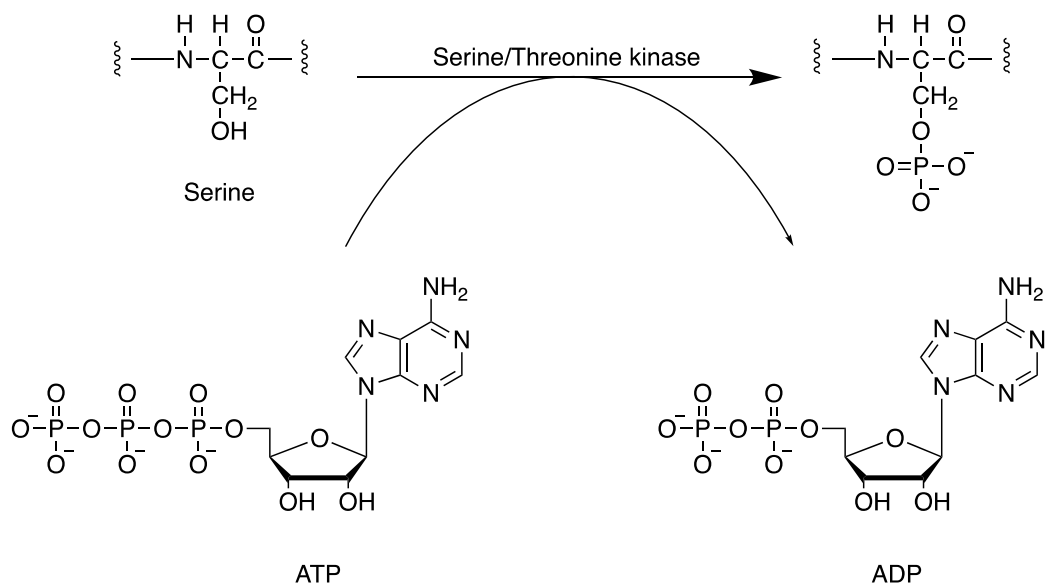
Scheme 1: Phosphorylation of a serine residue catalysed by serine/threonine kinase. The phosphate group is donated from ATP.

To get an understanding in CDK8s role in cell transcription, it is necessary to look at the JAK/STAT-pathway. The JAK/STAT pathway starts with interferon (INF)[13, 14]. INF is often referred to as a group of proteins and glycoproteins with the common property of inhibiting virus replication[15]. INF activates the transmembrane ligand-activated receptor tyrosine kinase named Flt3[16]. When the ligand activates the receptor, the non-receptor tyrosine kinase Janus kinase (JAK) is activated, leading to tyrosine phosphorylation of several STAT proteins, including STAT1[17]. However, additional serine phosphorylation is needed for STAT-proteins to mediate their transcriptional effects. Data from Bancerek *et al.* identify CDK8 as a key regulator of STAT1 and antiviral responses and suggest a general role for CDK8 in STAT-mediated transcription[18]. CDK8 is a transcription-regulating kinase and has shown to be responsible for INF-induced STAT1 serine phosphorylation[19]. The CDK8 module of the Mediator complex phosphorylated regulatory sites within the transactivation domains on STAT1. This suggests that CDK8 is a promising target for the therapeutic manipulation of cytokine responses. An illustration of the relationship between INF, the JAK-STAT1-pathway, and CDK8 is given in Figure 1.
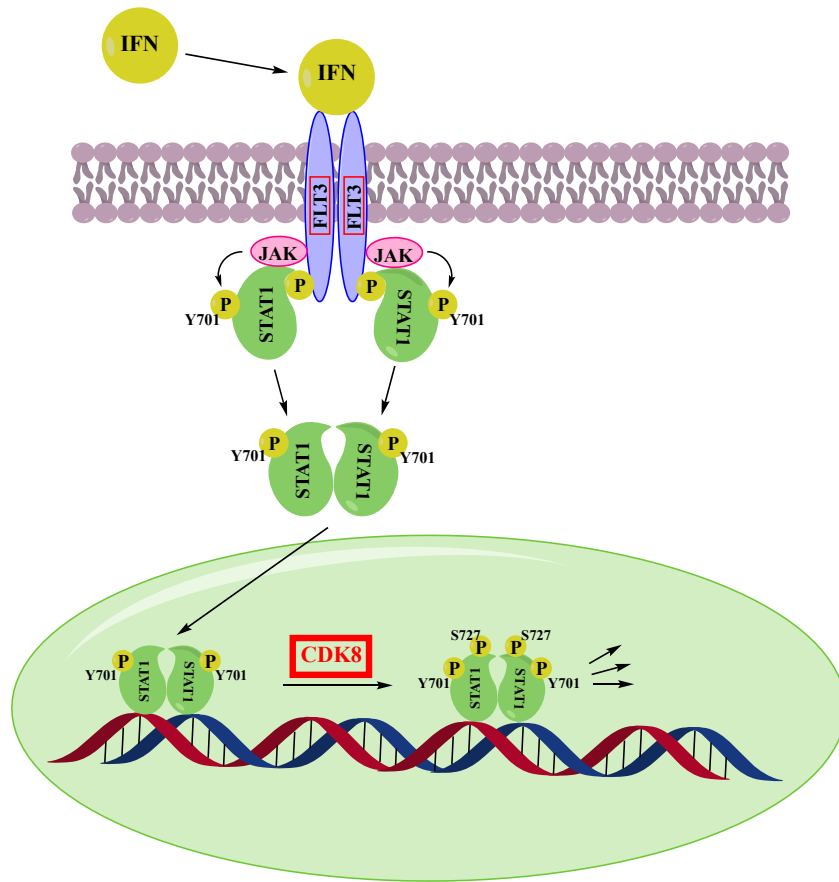
Figure 1: CDK8´s role in cell transcription adopted from refrences[18, 20].

CDK8 inhibitors can restrain the activity of CDK8. The majority of CDK8 inhibitors have been shown to consistently repress phosphorylation of the transactivation domains of STATs[21-23]. CDK inhibitors can downregulate the progression through the cell cycle. The whole process usually is tightly controlled. An accumulation of a relevant cyclin-CDK complex is followed by a rapid degradation of the cyclin once its task is complete[7]. Since these structures are closely involved in the signal transduction process that drives cell growth and cell division, protein kinase inhibitors are useful as anticancer agents[7].

1.2   Objective of the Project

The aim of this project is to simplify and combine the binding modes of previously reported inhibitors of CDK8 cortistatin A (**9**) and CCT252545 (**10**) (Figure 2).

<div align="center">

Cortistatin A (**9**)   CCT251545 (**10**)

</div>
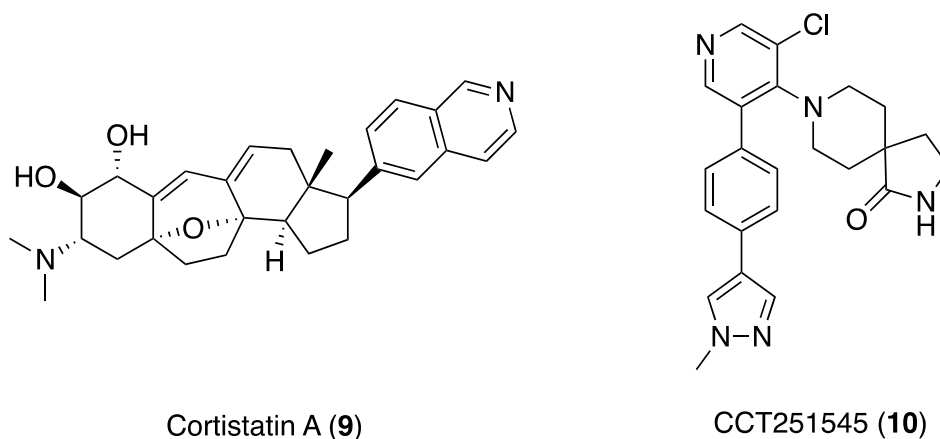
Figure 2: Example of reported CDK8 inhibitors cortistatin A (**9**) and CCT251545 (**10**)[24,25].

Hatcher, Wang, Johannessen, Kwiatkowski, Sim, and Gray have demonstrated that several steroidal cortistatin A analogs were effective inhibitors of CDK8[24]. Cortistatin A (**9**) is a naturally occurring steroidal alkaloid isolated from the marine sponge Corticum simplex[24, 26]. The steroidal-like core in cortistatin A (**9**) makes extensive contact with the ATP-binding cavity. It is a high-affinity binder with Kd = 17 nM toward CDK8. According the binding model, an important hydrogen bonding between nitrogen in the isoquinoline chain and Ala100 in CDK8 was observed. In addition to its strong binding affinity, the compound showed a high level of selectivity for CDK8. CCT251545 (**10**) is a heterocyclic compound that studies identifies CDK8/CDK19 as its primary targets[25]. The pyridine nitrogen in CCT251545 interacts with the kinase hinge segment by a similar interaction to the N-H of Ala100 as the isoquinoline´s nitrogen in cortistatin A. From this interaction, the pyrazole substituent of CCT251545 (**10**) is orientated towards the ATP-binding cavity in similarity to the steroidal core of cortistatin A. The chlorine-atom increased the affinity by interaction with Phe97[12, 25]. An illustration of the binding modes for **9** and **10** is given in Figure 3.
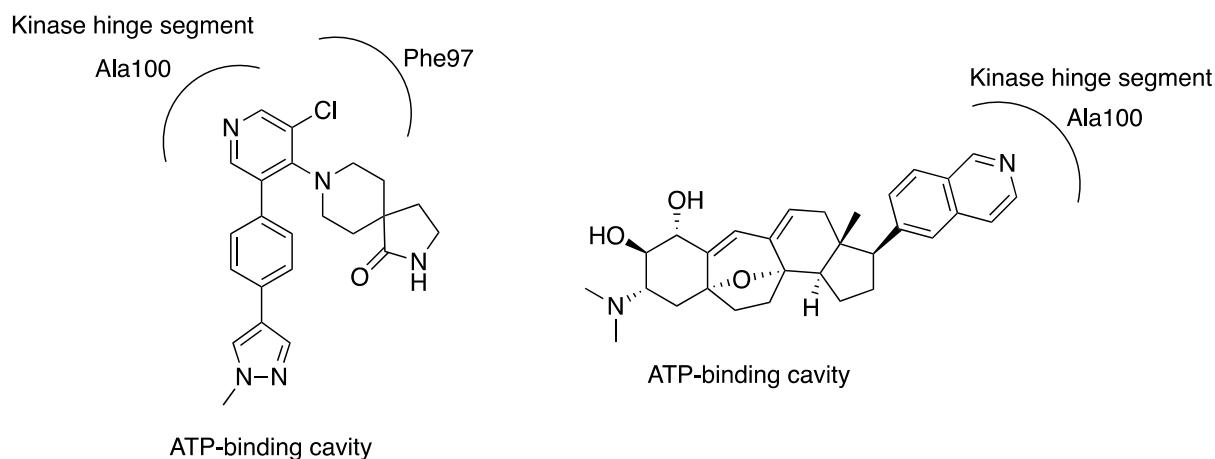
Figure 3: Binding modes for cortistatin A (**9**) and CCT251545 (**10**) adopted from references[12, 25].

Given the similarity between the core structure of cortistatin A, CCT251545, and steroids, the complex core can be replaced with a simpler steroid structure[24]. In this project, the aim is to combine and simplify the structures of cortistatin A and CCT251545 to retain and improve both the potency towards CDK8 as well as the durability by extending the A-ring in the steroid core and introducing a variety of *N*-containing heterocycles on the five-membered D-ring, see Scheme 2.
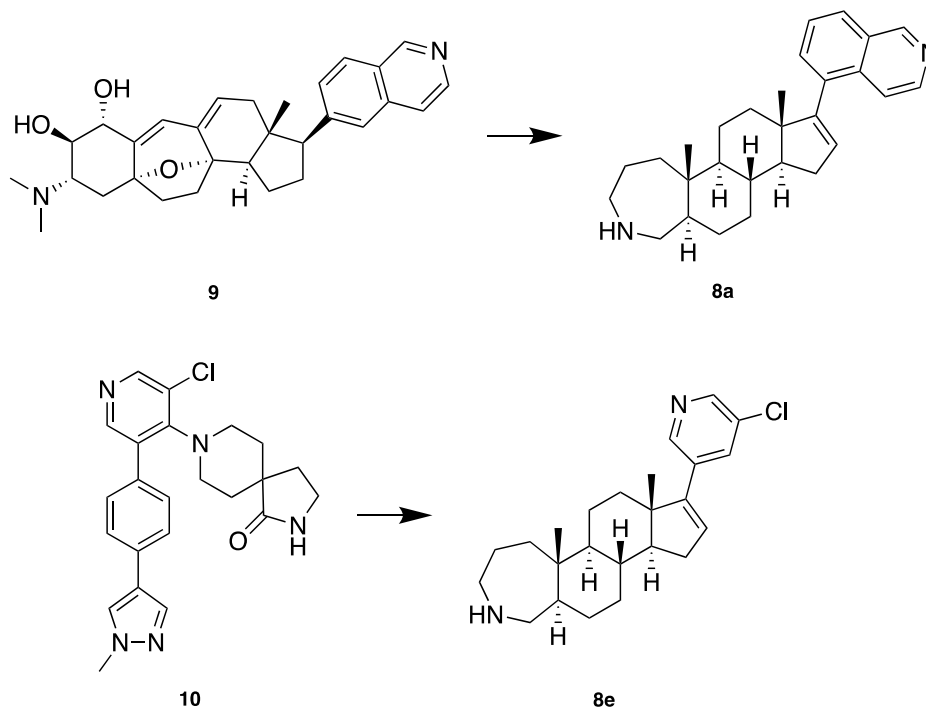
Scheme 2: Simplification of cortistatin A (**9**) and CCT251545 (**10**) to a steroidal core by extending the A-ring and adding 7-isoquinoline (**8c**) and 2-chloro-4-pyridine (**8e**) to the D-ring.

1.2.1 Steroids as lead compounds

Several steroids have been reported to reveal anti-cancer effects[27]. The steroidal core is influential for an array of different physiological effects. Their affinities for various types of nuclear receptors, and their safe pharmacological profile, have facilitated their wide application in drug discovery and development[28, 29]. An extensive focus on chemical modification of the steroidal structure has been seen over the recent years and has resulted in various important anti-cancer lead compounds. A structure of the steroid scaffold for the starting steroid with numbered positions is presented in Figure 4.
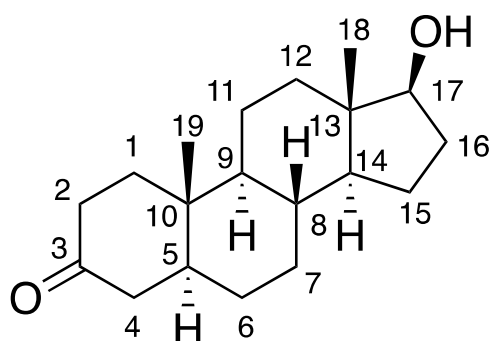
Figure 4: A presentation of the steroid scaffold with numbered positions for the starting steroid (**3**) in this thesis.

The biological activities of steroids often depend on the structures of the A- and D-ring[6]. This thesis aims to modify the steroid by expanding the A-ring in a Schmidt reaction. Relatively few approaches to *N*-containing steroid collections have been reported in recent years[29]. Previous studies have displayed limitations to afford only one of the two rearrangement products or achieve high selectivity at all[30, 31]. Aubé and Charaschanya have used stereochemically controlled ring expansion to effect regiochemical control in a complex molecular setting, thus permitting the directed introduction of a *N*-containing group in settings where no regiochemical control has previously been reported[29]. Introducing a heteroatom in a steroidal molecule affects the chemical properties and often results in alterations of the steroid´s biological activities[31]. A structure of the steroid scaffold with a ring expansion at the A-ring and numbered positions is presented in Figure 5.
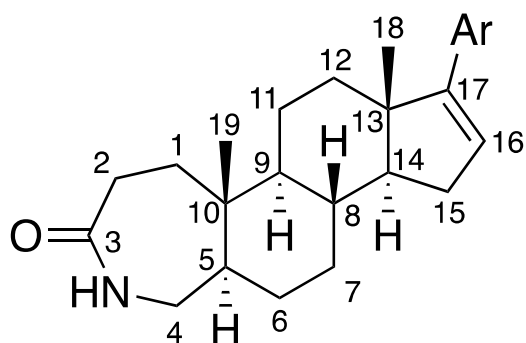
Figure 5: A presentation of the steroid scaffold with numbered positions for the products (**8**) in this thesis.

The nitrogen at the A-ring can potentially interact with the ATP-binding cavity like cortistatin A and CCT251545. Furthermore, a variety of *N*-containing heterocycles will be introduced at the 17-position. The amine at the aromatic rings can form a hydrogen bonding with Ala100 in CDK8. The chlorine at the pyridine-ring can possibly increase the affinity by interacting with Phe97. The target compounds (**8a-e**) are presented in Figure 6.
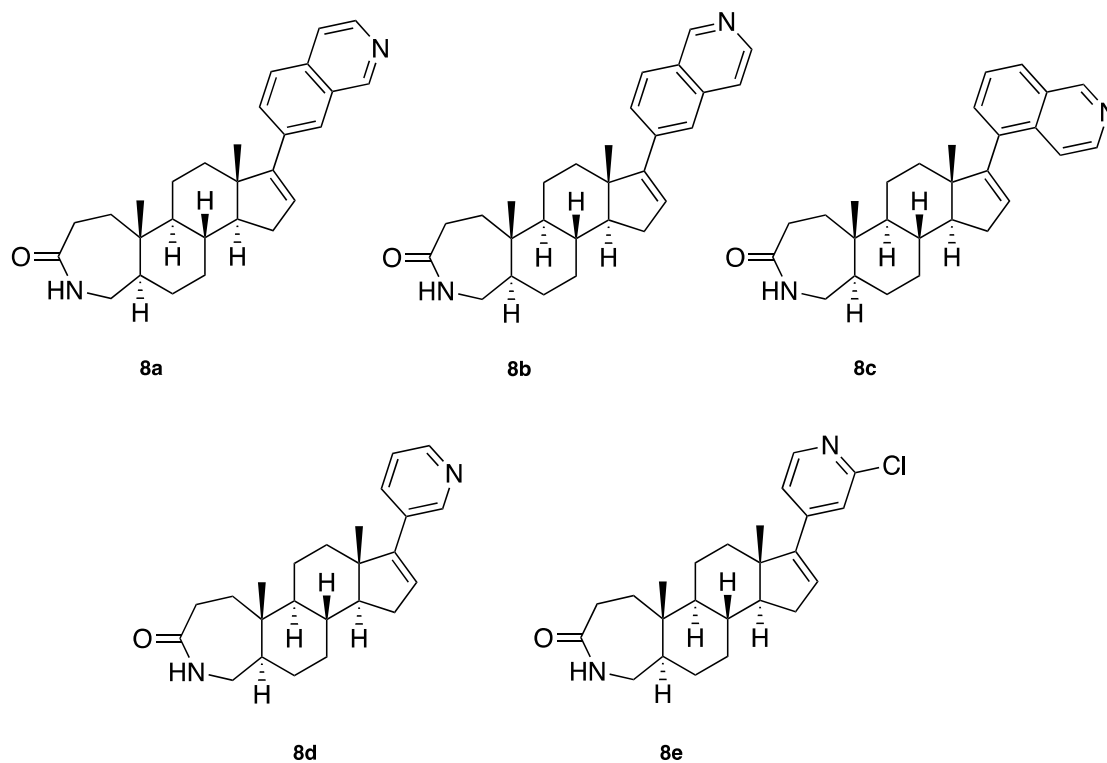
Figure 6: The target steroids (**8a-e**) in this master´s thesis.

1.2.2 Previous Work

The work performed in this thesis is a part of an ongoing study. Solum, Hansen, Aesoy and, Herfindal have been using steroids as lead compounds to develop new anti-cancer agents and synthesized a series of new synthetic steroids as potential CDK8 inhibitors. Like the steroids in this thesis, the 17-position on D-ring was added various aromatic heterocycles (**a-j**). The 3-position on A-ring contained a dimethylamino-group (**11**) and a hydroxyl-group (**12**). Some of the steroids are presented in Figure 7[6, 28].
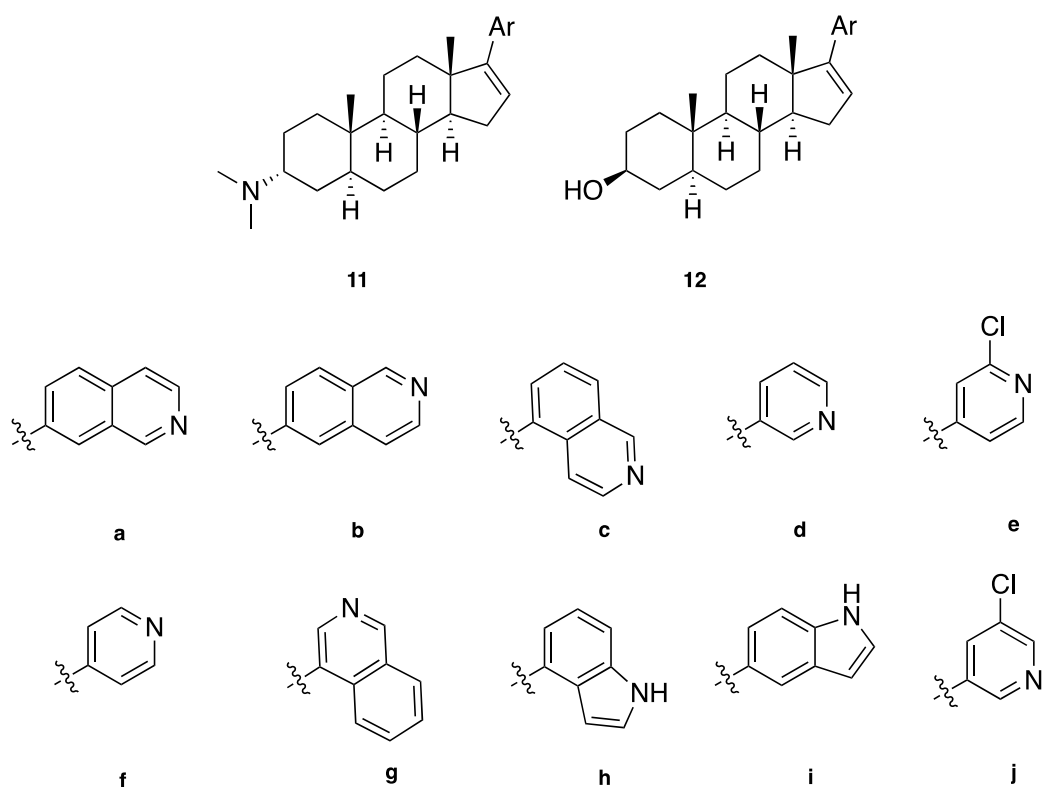
Figure 7: Earlier synthesised compounds by *Solum et al.* [6, 28]

The synthetic compounds were evaluated for their inhibitory properties towards CDK8. Compounds **11a-j** displayed inhibitory activity towards CDK8 at 50 nM concentration, except for **11i**. The three most potent inhibitors were proved to be **a, c** and **j**, in addition to **b** and **d**, which also showed promising results[6]. Later efforts proved **12a, b**, and **i** to be the most cytotoxic compounds. The most prominent CDK8 inhibitor was proved to be compound **12c**. Analogs with either a 7-isoquinoline (**a**), 6-isoquinoline (**b**) or 5-indole (**i**) side chain at the 17-position are revealed to have the most promising anti-proliferative agents[28].

1.3 Synthesis

The synthesis route in this master's thesis was based on reactions done by Aubé and Charaschanya and Solum *et al.*[6, 28, 29]. To achieve the wanted regioisomer of the steroid, it was necessary to synthesize an *(S)*-isomer of the auxiliary hydroxyalkyl azide (**2**). *(S)*-3-Azido-1-phenylpropanol was synthesized in a S_N2 reaction using *(S)*-3-chloro-1-phenylpropanol (**1**) mixed with NaN_3 and NaI in DMF, see Scheme 3.
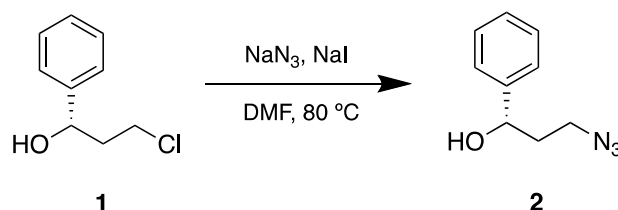
Scheme 3: Synthesis of the auxiliary hydroxyalkyl azide (**2**).

5α-Dihydrotestosterone (**3**) was used as a starting point in this synthesis. The aim was to expand the A-ring to a *N*-containing seven-membered ring in a Schmidt reaction using the hydroxyalkyl azide (**2**). The hydroxyl-groups in the steroid (**4**) were then oxidized using PCC mixed with celite in DCM to give a steroidal ketone (**5**). An amide (**6**) was then formed by a *β*-elimination using NaH dissolved in dry THF. To modify the D-ring, a triflate was added in an enolate formation using $PhN(SO_2CF_3)_2$ and NaHMDS in THF at -78 °C. The resulting enol triflate (**7**) was further reacted with different aromatic heterocycles in a Suzuki-Miyaura cross-coupling using different boronic acids mixed with Cs_2CO_3 in a mixture of THF and water (5:2) at 60 °C and $Pd(PPh_3)_4$ as a catalyst. The synthesis route in this thesis is given in Scheme 4.
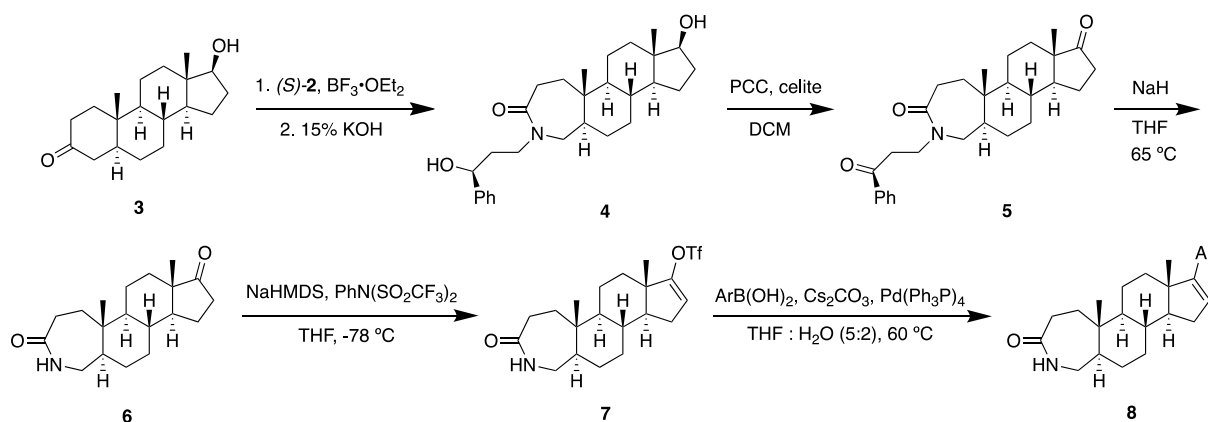
Scheme 4: Overview of the synthetic route to potential CDK8-inhibitors.

Five different analogs were prioritized as aromatic heterocycles to be introduced on the five-membered D-ring. Previous studies have shown that analogs with either a 7-isoquinoline (**a**) or 6-isoquinoline (**b**) side chain at the 17-position were revealed to have the most promising anti-proliferative agents and that 5-isoquinoline (**c**) and analogs with chlorine attached to the pyridinyl ring (**e**) were proved to be potent inhibitors of CDK8[6, 28]. The five analogs (**a-e**) are given in Figure 8.
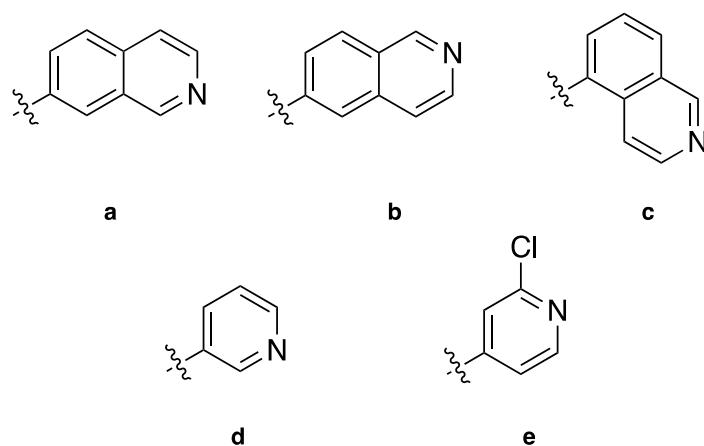
Figure 8: Five different heteroaromatics (**a-e**) introduced in the 17-position in a Suzuki-Miyaura cross-coupling.

2 Theory

2.1 Substitution reaction (S$_N$2)

Azides are useful intermediates for the synthesis of various *N*-containing compounds and are usually introduced by nucleophilic substitutions[32]. One of the most reliable procedures involves heating an appropriate halide with sodium azide in DMF[33]. The reaction conditions in this synthesis favor a S$_N$2 reaction. The S$_N$2 reaction of *(S)*-3-chloro-1-phenylpropanol (**1**) is given in Scheme 5.
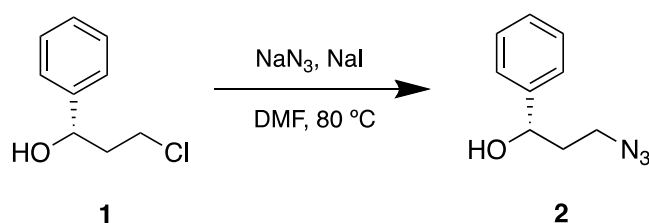
Scheme 5: *(S)*-3-Chloro-1-phenylpropanol (**1**) reacts with NaN$_3$ and NaI in DMF in a S$_N$2 reaction and results in *(S)*-3-azido-1-phenylpropanol (**2**).

2.1.1 Mechanism

Chloride is a weak base and acts as a good leaving group. A good leaving group is a weak base that is able to be stable after leaving. The group for the strongest corresponding acid and having low pK_a values being the best[34]. When adding NaI, an equilibrium between the amount iodide and chloride occurs. Given the above, iodide is a better leaving group than chloride.

In the first part of the mechanism, the azide attacks the carbon atom of the substrate through a backside pathway[35]. Neither azide nor iodide are fully bonded to carbon in the transition state, and they both bear a partial negative charge. Then a bond between the azide and carbon is formed, and the leaving group is displaced concurrently[36]. A polar aprotic solvent, like DMF, is favourable since it does not form interaction between substrate and nucleophile[37, 38]. A proposed mechanism for the synthesis of (**2**) is given in Scheme 6.
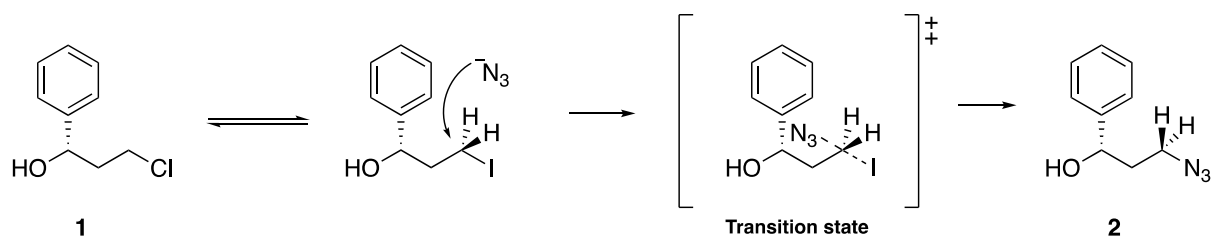
Scheme 6: A proposed S_N2 mechanism for the formation of the hydroxyalkyl azide (**2**)[35].

2.2 Schmidt reaction

The Schmidt reaction is a reaction between carbonyl compounds and hydrazoic acid or alkyl azide in the presence of a strong acid. The reaction offers a valuable method for the formation of amines from acids[39]. Gracias, Milligan & Aubé have developed a strategy that leads to asymmetric Schmidt reactions using chiral azido alcohols[40]. Later studies by Aubé have shown that reactions involving the rearrangement of alkyl azides with carbonyls are a powerful strategy for synthesizing various *N*-heterocycles under acidic conditions[41, 42]. Lewis acids, such as $BF_3 \cdot OEt_2$, are typically required to promote the reaction.

Ring expansion provides a powerful way of introducing a heteroatom substituent into a carbocyclic framework[42]. This synthesis aims to expand the A-ring to give a 7-membered ring in a Schmidt reaction using the concept of affecting the regiocontrol by using chiral reagents. The ring expansion of the A-ring in 5α-dihydrotestosterone (**3**) using *(S)*-3-azido-1-phenylpropanol (**2**) is given in Scheme 7.
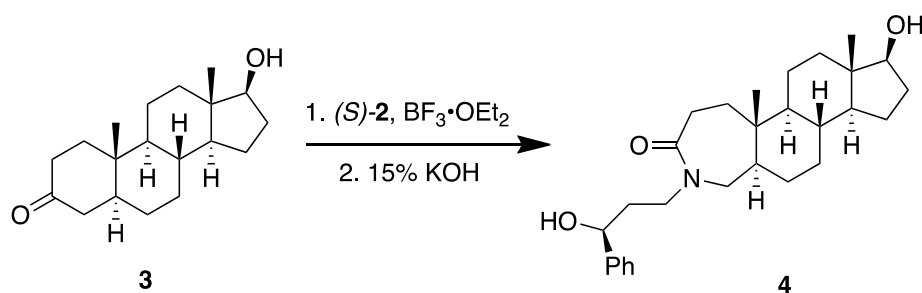
Scheme 7: Ring expansion of the A-ring in 5α-dihydrotestosterone (**3**) using *(S)*-3-azido-1-phenylpropanol (**2**) and $BF_3 \cdot OEt_2$ to form **4**.

2.2.1 General mechanism

In the first step of the Schmidt reaction, the alcohol attacks the ketone. The attack is followed by an elimination of water and results in a formation of an oxonium ion intermediate. A spirocyclic intermediate is formed after the azide attacks the oxonium ion. The intermediate undergoes a migration to give an iminium ether and reacts with a nucleophile to provide a *N*-substituted lactam product[29]. A general mechanism of a Schmidt reaction is shown in Scheme 8.
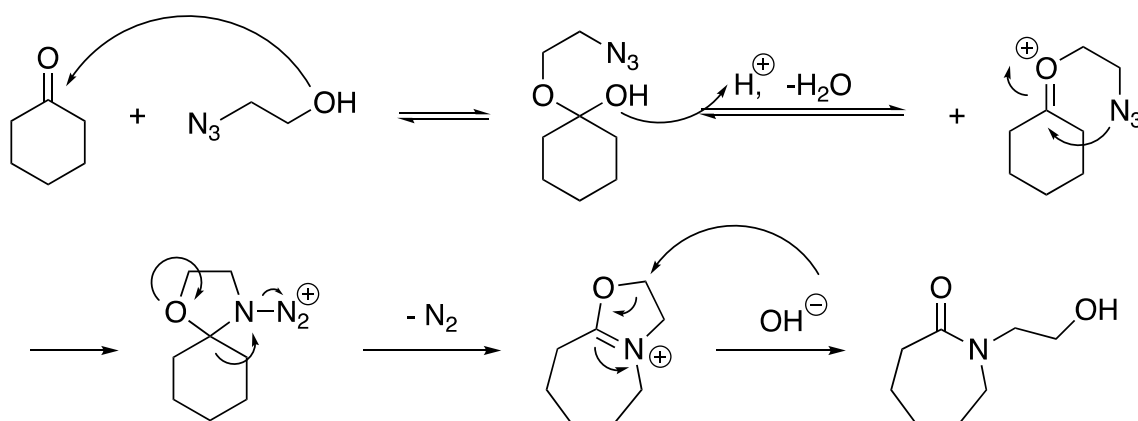
Scheme 8: A general mechanism of a ketone and hydroxyalkyl azide converted to a *N*-substituted lactam product in a Schmidt reaction[29].

Ring expansions are often limited by the tendency of a given substrate to provide only one rearrangement product or fail to achieve high selectivity. In an A-ring rearrangement, a problem occurs since the two methylene groups attached to the 3-oxysteroid are similarly substituted. Reported ring expansion reactions at this position is poorly selective[30, 43]. Aubé and Charaschanya have used a stereocontrolled ring expansion to influence the regioselectivity of the insertion of the *N*-side chain[29]. This gave a mixture of two regioisomers, see Scheme 9.
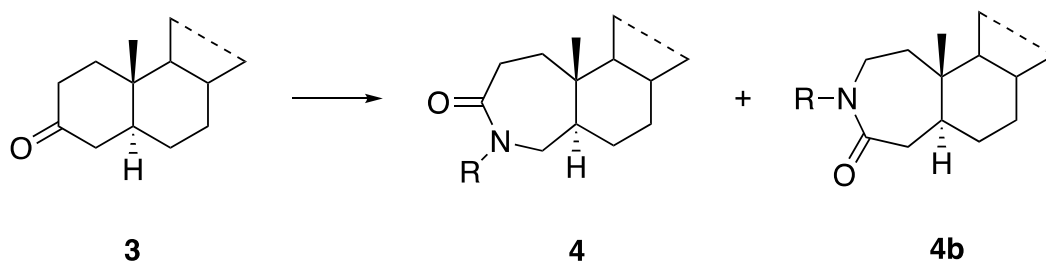
Scheme 9: A challenge associated with regioselectivity in 3-oxosteroid. The A-ring is poorly selective and gives a mixture of two regioisomers[29].

Enantiomerically pure isomers were then used to affect the regiocontrol. This resulted in high regiochemical control in each case. The method using either (*R*)- or (*S*)-azide in the reaction sequence has the advantage that two ketones regioselectivity can be converted into either desirable lactam in high yields[29]. An illustration of this is given in Scheme 10.
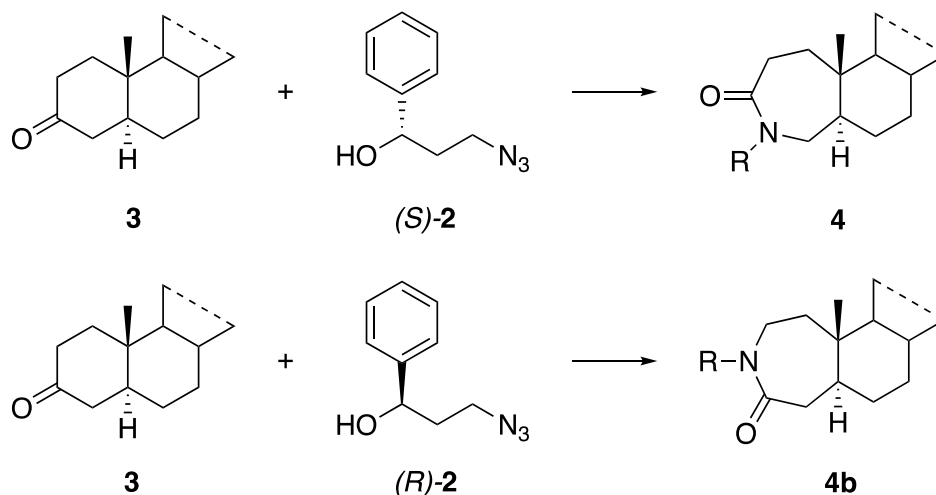
Scheme 10: Chiral hydroxyalkyl azides (**2**) in Schmidt reactions result in regioselectivity at the A-ring[29].

In later studies, Aubé and Charaschanya have investigated factors that determine the stereo- and regioselectivity in ring expansion using auxiliary hydroxyalkyl azides. The three determinants of stereo- or regioselectivity in ring expansion reaction mediated by chiral hydroxyalkyl azides are given in Section 2.2.2-2.2.4[29, 44].

2.2.2 Direction of azide attack onto ketone

One factor affecting the reaction regio- and stereochemistry in ring expansion reactions, is the direction of azide attack relative to pre-existing substitution on the ketone. Both thermodynamically and kinetically, the equatorial azide attack intermediate is preferred over the axial[45]. The stereoselectivity is related to the relative populations of the possible conformations of the starting ketone[29]. In cases with ketones of other ring sizes, the attack depends on steric accessibility. An illustration of the two intermediates as a result of equatorial and axial attack are given in Figure 9.
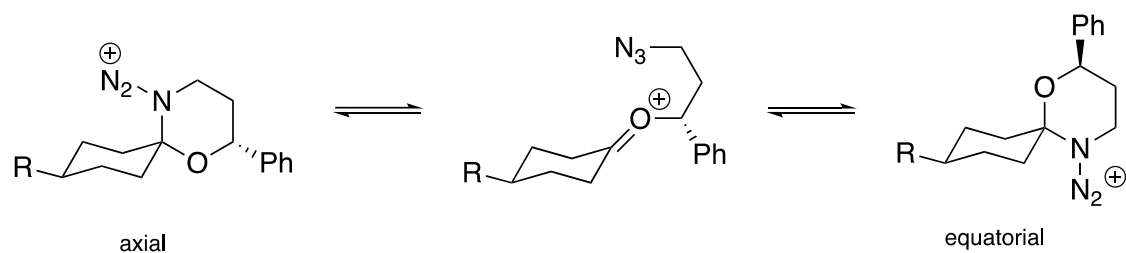
Figure 9: The equatorial intermediate is preferred over the axial intermediate[29].

2.2.3 Selective formation and reaction of the most stable heterocyclic ring

Selective formation and reaction of the most stable new heterocyclic ring (1,3-oxazinane) influence the regio- and stereochemistry. The 1,3-oxazinane ring is expected to adopt the most stable chair-like conformation[29]. The major product arises from spirocyclic 1,3-oxazinanes containing the carbon substituent in an equatorial orientation. The two possible conformations are given in Figure 10.
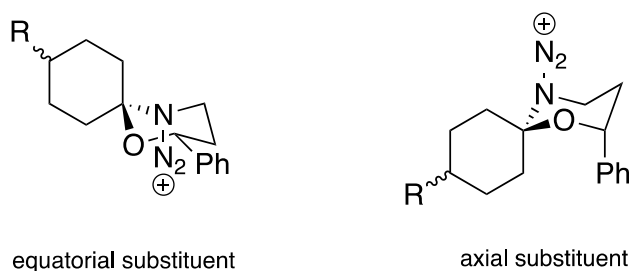
Figure 10: Equatorial substituents on the 1,3-oxazinane ring is more stable than substituents in an axial orientation[29].

2.2.4 Antiperiplanar migration

The last factor determining the reaction regio- and stereochemistry is the antiperiplanar C→N migration to afford the iminium ether product. All known C→N migrations involve antiperiplanar migration to the N_2^+ leaving group, see Figure 11. There are two antiperiplanar options; migration of the C-O bond or the C-C bond. The C-O bond is assumed to form a weak N-O bond and make it very unlikely to migrate[45]. The C-C bond leads to a cation unstabilized by a neighboring oxygen atom. Therefore, the reaction coordinate necessarily goes through an axial N_2^+ group[29].

antiperiplanar/axial N$_2^+$
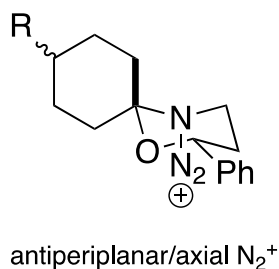
Figure 11: The reaction coordinate goes through an axial N$_2^+$ group[29].

2.2.5 Mechanism

In Schmidt reactions using enantiomerically pure ketones with chiral reagents, the three principles determine the outcome of the reaction. Excess of BF$_3$·OEt$_2$ is necessary to accommodate the disproportionation of the reagent into BF$_4^-$ [46]. The reaction starts with an equatorial attack of the azide (**2**). The attack establishes the stereogenicity of the spirocyclic carbon. A reaction between the 1,3-oxazinane conformer with the equatorial phenyl group occurs, and the carbon antiperiplanar to the departing axial N$_2^+$-group migrates[29]. Then aqueous KOH hydrolyse the intermediate iminium ether and results in the lactam product (**4**)[46]. The mechanism for the reaction of **4** is given in Scheme 11.
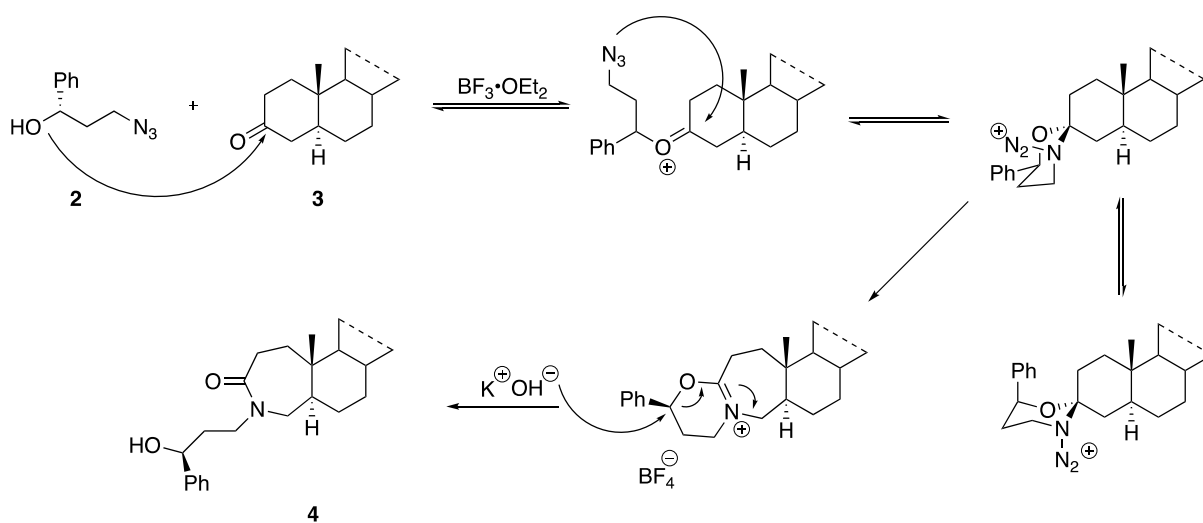
Scheme 11: A proposed mechanism of the ring expansion of the A-ring in the steroid (**3**) using hydroxyalkyl azide (**2**) to give **4**[29]. β/equatorial attack by the azide is preferred.

A consequence of these factors is the migration of one possible methylene group over the other. When the opposite enantiomer of the chiral azide is used, this changes. As a result, it is possible to regioselectively convert ketones to the desired lactam using *(S)*-hydroxyalkyl azide (**2**)[29].

2.3 Oxidation of alcohols

Before the elimination, it is necessary to convert the hydroxyl-group into a ketone. This could be done in an oxidation reaction. The oxidation of the secondary alcohols in the steroid (**4**) using PCC is given in Scheme 12.
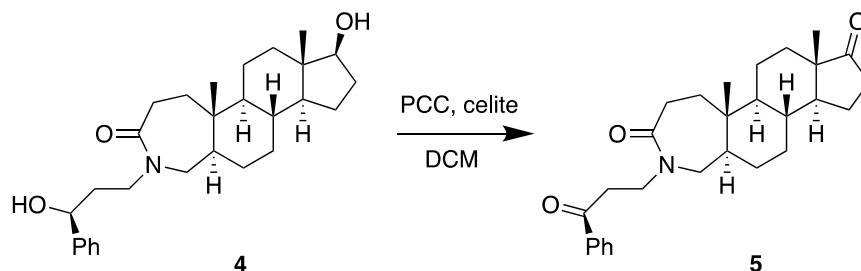
Scheme 12: PCC oxidizes the secondary alcohols in **4** to form ketones (**5**).

Cr(VI) is the most widely employed transition metal oxidant for alcohols. These species are powerful oxidants and are very versatile and efficient[32]. Some of the most common Cr(VI) reagents are chromium(VI) oxide (CrO$_3$), Pyridinium dichromate (PDC), and pyridinium chlorochromate (PCC) (see Figure 12). PCC and PDC are primarily used to oxidize alcohols to form carbonyls and are not strong enough to convert primary alcohol to carboxylic acid. They convert primary alcohols to aldehydes and secondary alcohols to ketones[47]. PDC is less acidic than PCC, which means PCC is more suitable when acid-sensitive substrates are oxidized[48]. Chromic acid is a stronger version and can also oxidize aldehydes to carboxylic acid. PCC is soluble in halogenated organic solvents and can be used without a strong acid present[49]. This makes PCC a more selective Cr(VI) oxidant.

chromium(VI) oxide   pyridinium dichromate   pyridinium chlorochromate
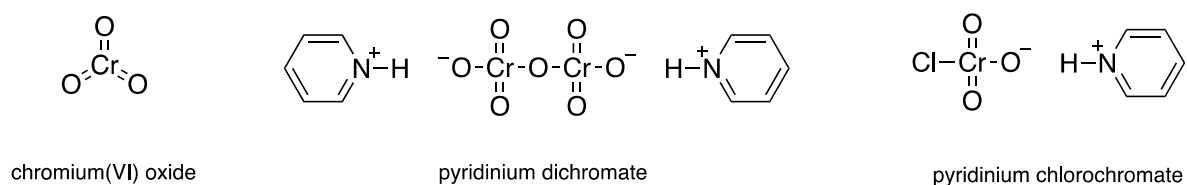
Figure 12: Example of three common Cr(VI) reagents; chromium(VI) oxide, PDC and PCC.

Oxidations reactions using PCC are normally performed in DCM at rt with 1.5 equiv. of PCC and are usually complete within 2 hours[50]. Celite is often used to simplify the work-up so that byproducts, like reduced chromium salt, are deposited onto solids. The solids could then be removed by filtration.

2.3.1 Mechanism

The oxidation-mechanism of alcohols involves a formation of a chromate ester and a rate-determining deprotonation[32]. In the first step, a formation of a Cr-O bond occurs by the attack of oxygen on the chromium. The next step involves a proton transfer. The proton on the hydroxyl-group is transferred onto the oxygen on the chromium. The chloride ion is displaced and then acts as a base, to form a chromate ester. Deprotonation occurs and the base forms the C=O bond. While the secondary alcohol is being oxidized to a ketone, the Cr(VI) is reduced to Cr(IV)[51]. The chromium attacks the oxygen near the phenyl first because it is more acidic than the hydroxyl-group at the D-ring. Then the same mechanism occurs at the 17-position. A proposed mechanism for the oxidation at the A-ring is shown in Scheme 13.
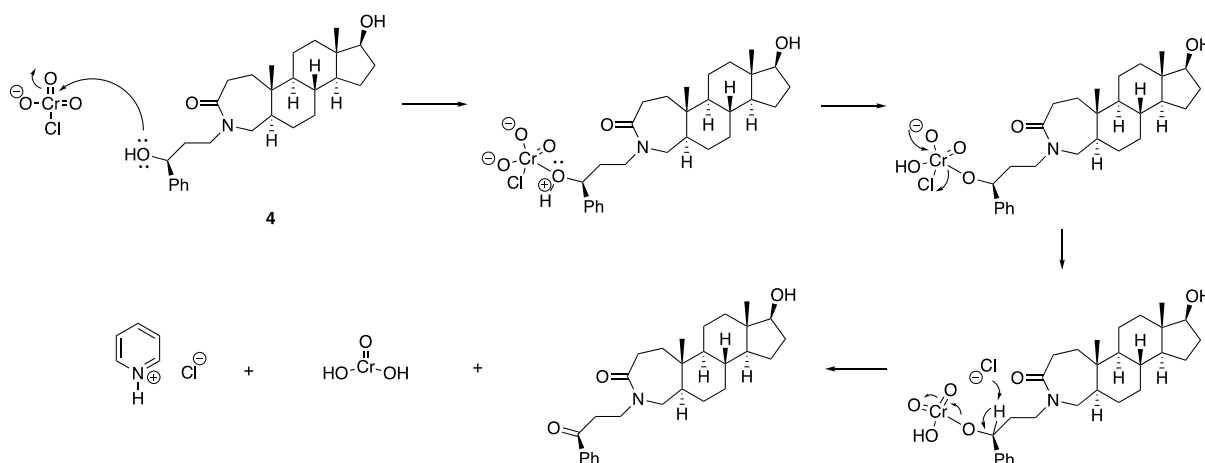
Scheme 13: A mechanism for the oxidation of the steroidal alcohol (**4**) by PCC to give a steroidal ketone[51].

2.4 β-elimination using NaH

To achieve the preferred A-ring, the aryl alkyl ketone is eliminated. The synthesis of **6** in a β-elimination of the steroid (**5**) using NaH dissolved in dry THF at 65 °C is given in Scheme 14.
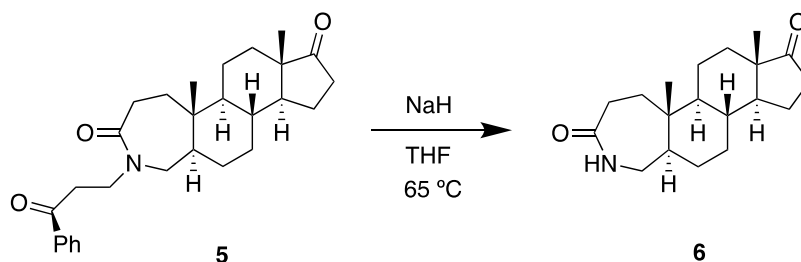
Scheme 14: The steroid (**5**) was mixed with NaH in THF and refluxed at 65 °C to give **6**.

A β-elimination involves a cleavage of a single bond and elimination of an atom or group from adjacent atoms. This results in a formation of a double bond[52]. NaH is a strong base that is used in the formation of enolates. Air-free techniques are required when using NaH. In many cases, NaH is used as a suspension in THF, which solvates many reactive compounds containing sodium and resist attach by strong bases.

2.4.1 Mechanism

The α-carbon of the ketone is acidic. Deprotonation occurs due to using NaH as a strong base. The deprotonation results in a formation of an enolate, and the β-hydride is eliminated. As a result, a double bond is formed and result in 1-phenyl-2-propen-1-one as a side-product and an elimination from the adjacent atom to give an intermediate. Addition of NH_4Cl results in the formation of the product (**6**) and hydrogen gas (H_2). A proposed mechanism is shown in Scheme 15.
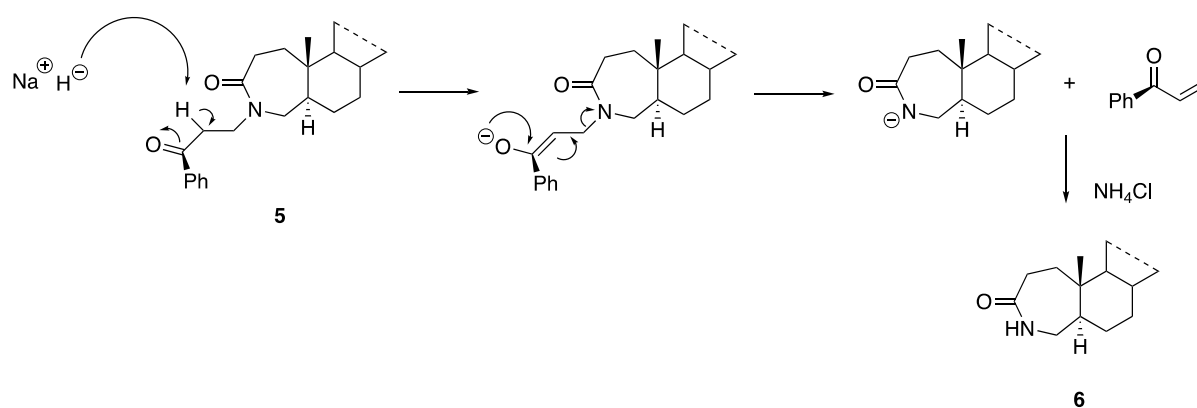
Scheme 15: A proposed mechanism for the β-elimination to form an amide (**6**) using NaH[53].

2.5 Triflate formation

The trifluoromethanesulfonate anion (triflate, TfO^-) is an excellent leaving group and is widely used in organic chemistry[54]. Triflates are often used in nucleophilic substitution, Suzuki cross-coupling and Heck reactions. A steroid triflate (**7**) can be synthesised in a reaction using *N*-phenyl-bis(trifluoromethanesulfonimide) (PhN(SO_2CF_3)_2) and sodium bis(trimethylsilyl)amide (NaHMDS) in THF at – 78 °C as shown in Scheme 16.
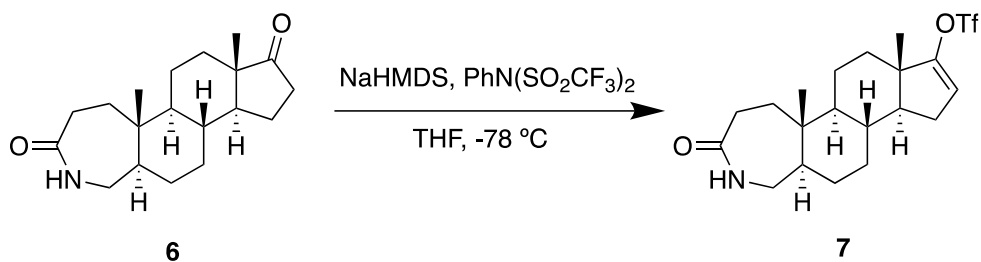
Scheme 16: The steroidal ketone **(6)** undergoes a triflation using NaHMDS and PhN(SO$_2$CF$_3$)$_2$ in THF at -78 °C to give a steroidal triflate **(7)**.

PhN(SO$_2$CF$_3$)$_2$ is a mild triflating reagent, and is used to synthesize triflates from the corresponding ketone enolate. Bases commonly used in the formation of enolates are anions of hexamethyldisilamine (HMDS)[32]. The lithium, sodium and potassium salts are abbreviated LiHMDS, NaHMDS and KHMDS (see Figure 13). HMDS is weakly basic due to its inherent α-silyl stabilization, and the disilylamides have a pK around 30[55, 56]. In most cases, NaHMDS and KHMDS are more reactive than LiHMDS. However, Li$^+$ is more oxophilic than Na$^+$ which might affect deprotonation facilitated by the directing effect of the oxygen atom[57]. The rate of the proton exchange can be reduced by Li$^+$ as a consequence of the tighter coordination at oxygen[32].
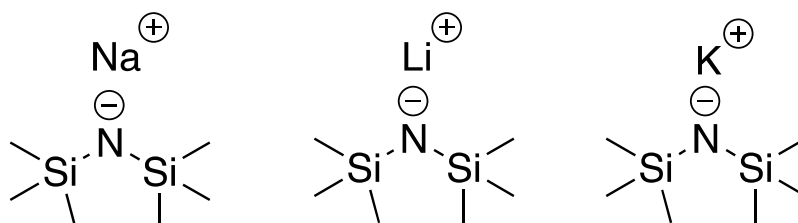
Figure 13: NaHMDS, LiHMDS and KHMDS are bulky bases commonly used in triflate formation.

2.5.1 Mechanism

NaHMDS is a typically strong, bulky base that converts ketones into its enolate form. The carbonyl group is strongly electron-withdrawing, and the enolate is produced when the carbonyl compound loses a α-proton and the acidic proton is replaced with Na$^+$. This results in two resonance structures[37]. The most stable enolate form is the resonance structure which places the negative charge on the oxygen. The greater electronegativity of the oxygen will better stabilize the negative charge. The two resonance structures are shown in Scheme 17.
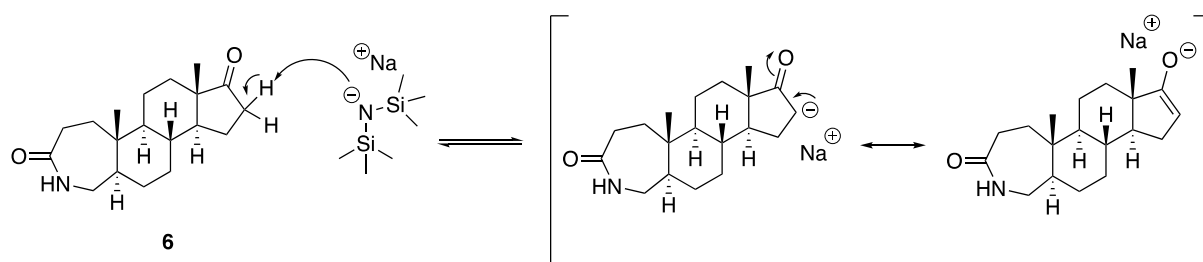
Scheme 17: Formation of the enolate by a base resulting in two resonance strucutres[32].

The obtained enolate then reacts with PhN(SO$_2$CF$_3$)$_2$ to form the triflate (**7**) , see Scheme 18[58].
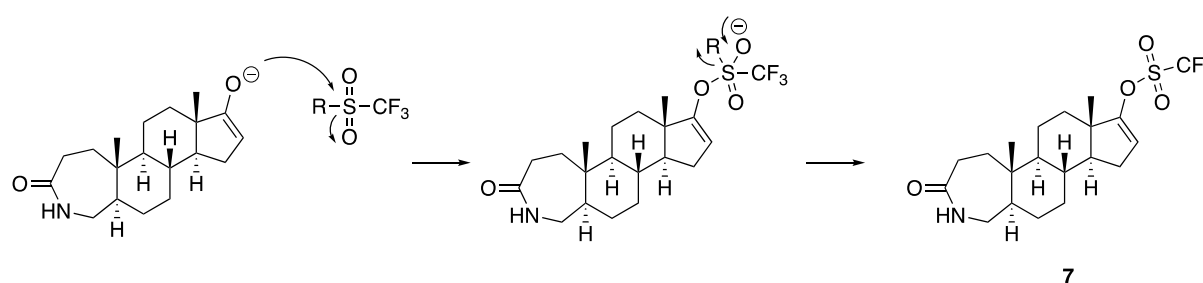
Scheme 18: Formation of the steroid triflate (**7**) form the enolate.

2.6 Suzuki-Miyaura cross-coupling

A variety of *N*-containing aromatics can be introduced in a Suzuki-Miyaura cross-coupling at the 17-position (Scheme 19) by mixing different boronic acids were with Cs$_2$CO$_3$ and Pd(PPh$_3$)$_4$ in THF:H$_2$O (5:2) at 60 °C.
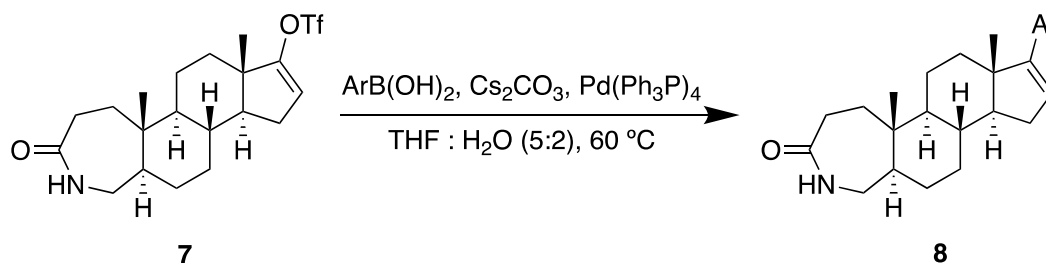
Scheme 19: The steroidal triflate (**7**) mixed with different boronic acids (**a-e**), Cs$_2$CO$_3$ and Pd(PPh$_3$)$_4$ in THF:H$_2$O (5:2) at 60 °C resulted in the product (**8a-e**) in a cross-coupling reaction.

The Suzuki-Miyaura cross-coupling reaction is used to couple organic halides or triflates with an organoborane compound in the presence of a palladium catalyst[49, 59]. One of the most commonly used catalysts is tetrakis(triphenylphosphine)-palladium(0) (Pd(PPh$_3$)$_4$), see Figure 14. The Suzuki reaction is suitable for a range of substrates due to the mild reaction conditions. The cross-coupling reaction involves forming a C–C bond between the organoboron nucleophile and the organohalide or -pseudohalide electrophile[60]. Many commercially available organoboron species exist, and provide the opportunity to synthesize several analogs[49]. Given the above, the cross-coupling presents a wide range of applications in the production of polymers, agrochemicals, pharmaceutical intermediates, and high-tech materials[10, 61].
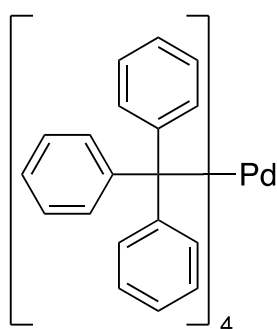
Tetrakis(triphenylphosphine)-palladium(0)

Figure 14: Pd(PPh$_3$)$_4$ is a common catalyst in Suzuki cross-couplings[37].

2.6.1 Mechanism

The mechanism of the Suzuki-Miyaura cross-coupling reaction involves four stages: oxidative addition of the organo halide or triflate to the transition metal catalyst followed by metathesis where the halide or triflate anion is exchanged by the base in the reaction. Then a transmetallation of the organoboron reagent occur before reductive elimination of the product, which contains a new bond between the carbon linked to the boron group in the nucleophile and the carbon linked to the halide or triflate in the electrophile[62]. A general catalytic cycle for the cross-coupling reaction is given in Scheme 20[62].

$$Pd(II)$$

$$Pd(0)$$

$$R_1-X$$

Oxidative addition

$$R_1-R_2$$

Reductive elimination

$$R_1-Pd(II)-R_2$$

$$R_1-Pd(II)-X$$

$$MOH$$

Metathesis

$$\begin{array}{c} HO \quad OH \\ B^- \quad M^+ \\ HO \quad OH \end{array}$$

Transmetallation

$$\begin{array}{c} R_1 \\ | \\ Pd(II) \\ | \\ OH \end{array}$$

$$MX$$

$$M = Li, Na, K$$

$$R_2-B(OH)_2 \xrightarrow{MOH} \begin{array}{c} HO \quad OH \\ R_2-B^- \quad M^+ \\ OH \end{array}$$
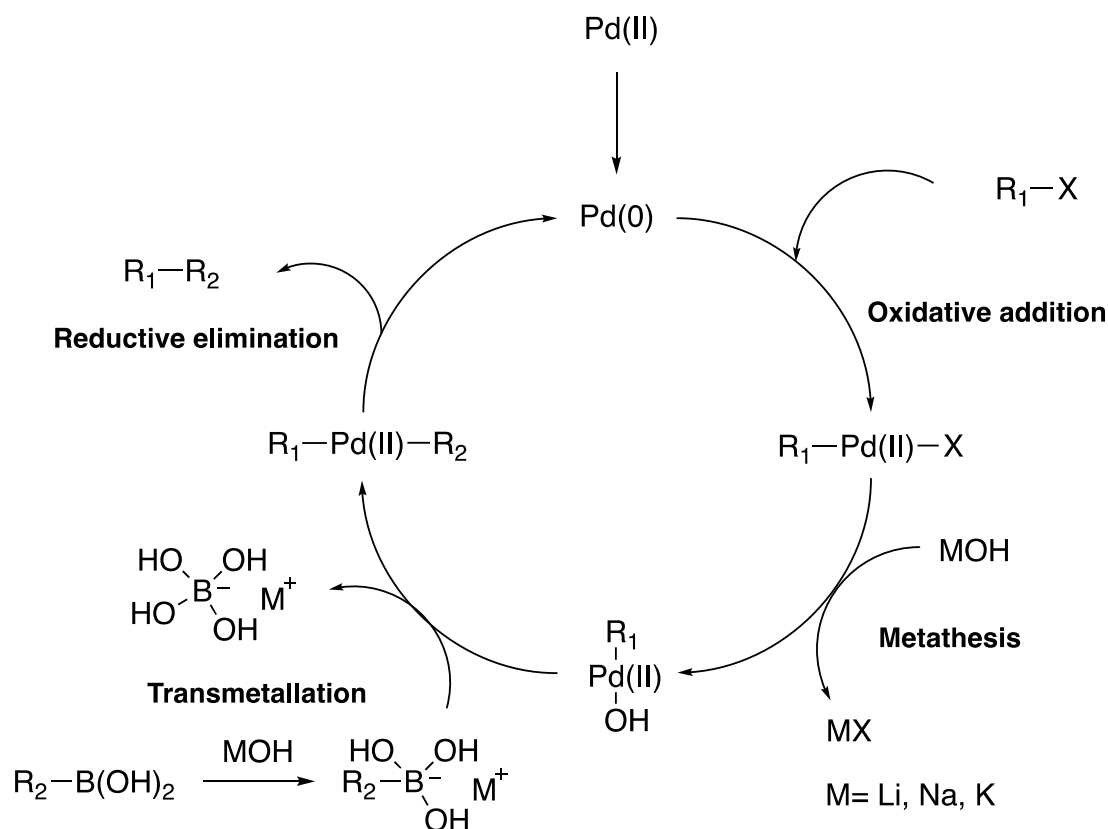
Scheme 20: A general catalytic cycle mechanism for the cross-coupling of organometallic reagents with organic halides or -pseudohalide electrophiles[63].

2.6.1.1 Oxidative addition

As the name indicates, both oxidation and addition take place in this step. The oxidative addition is catalysed by electron-rich ligands linked to the metal catalyst, like $Pd(PPh_3)_4$. Oxidative addition is often the rate-determining step. The relative reactivity of leaving groups typically follows: $I^- > OTf^- > Br^- \gg Cl^-$ [64]. In this step, the bond between carbon in the steroid-core and triflate breaks. The palladium catalyst Pd(0) is oxidized to Pd(II). Pd(II) gets coupled to the R_1-group and the triflate and makes an organopalladium complex[65].

2.6.1.2 Metathesis

In the next step of the cycle, the triflate anion is exchanged by the base in the reaction. This results in a more reactive intermediate that undergoes a transmetallation[66]. The rate of the metathesis could be increased by changing to a stronger base. As a result, the formation of side reactions could be prevented.

2.6.1.3 Transmetallation

The transmetallation is the most characteristic step. In this step, ligands are transferred from one species to another. The boronic acid serves as the source of the N-containing aromatic ring to be introduced at the 17-position. First, the boronic acid has to be activated in a base catalysis for the transmetallation to form the desired product. Organic groups held by boron are weakly nucleophilic, and the reactivity are low. Nucleophilicity can be increased by the coordination of a negatively charged base to the boron atom[32]. The boronate species interact with the Pd centre and then transmetallate[10]. R_2 is bound to an electropositive group and then transferred to the palladium catalyst[63].

Transmetallation is initiated with the base since organoboron compounds do not undergo transmetallation in the absence of base. The reactivity varies with solvent. Electron withdrawing substituents increase the reactivity of the borane. General trend of borane reactivity is: $ArBF_3$ > $RB(OH)_2$ > $RB(OR)_2$ >> R_3B[67]. Examples of bases are Cs_2CO_3, NaOH, NaOEt, K_2CO_3 and K_3PO_4, and they are necessary to give a nucleophilic boronate anion.

2.6.1.4 Reductive elimination

In the final step of the cross-coupling, a reduction and elimination take place. Pd(II) gets eliminated as Pd(0). This results in a C-C bond to form the desired compound (**8**), while the palladium gets regenerated. The relative rate of reductive elimination from Pd(II) complexes follows: aryl-aryl > alkyl-aryl > n-propyl-n-propyl > ethyl-ethyl > methyl-methyl[68].

A specific mechanism for the synthesis of **8** in Suzuki-Miyaura cross-coupling cycle, including the four steps, is given in Scheme 21.
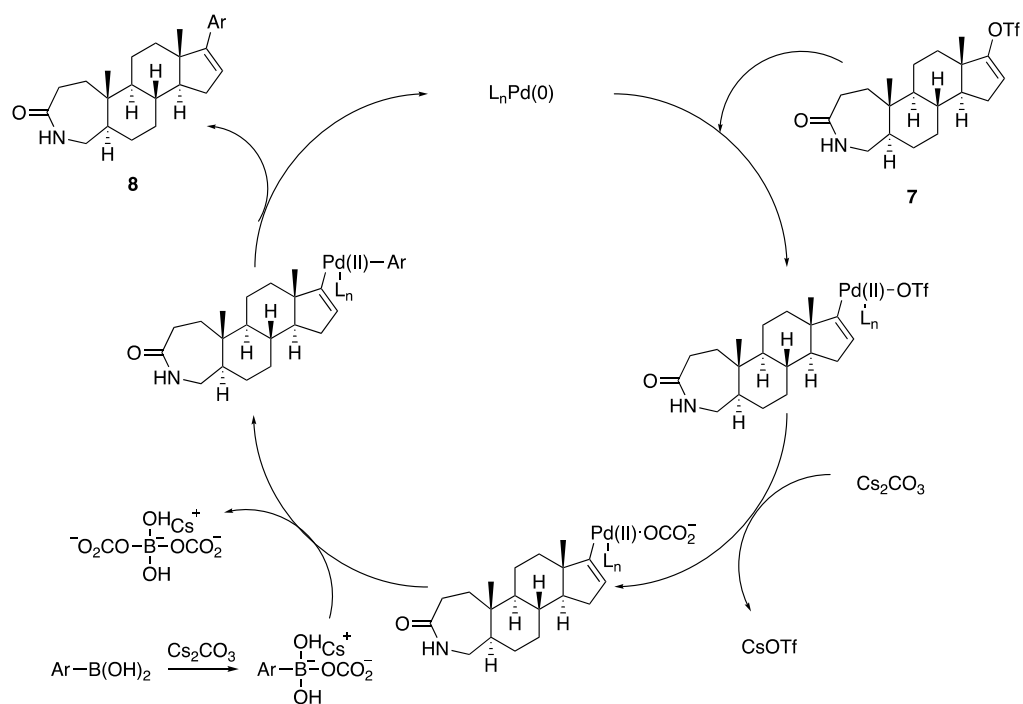
Scheme 21: A specific proposed Suzuki-Miyaura cross-coupling using a steroidal triflate (**7**) to add aromatic heterocycles at the 17-position resulting in **8**.

2.6.2 Side reactions

In addition to the main Suzuki reactions, two other main reaction pathways have been observed. The two important side reactions are homocoupling and hydrolytic deboronation of the two competing boronic acids, see Scheme 22[69]. The side reactions occur in the transmetallation step. This step is not entirely understood, but it strongly depends on the reaction conditions[69].
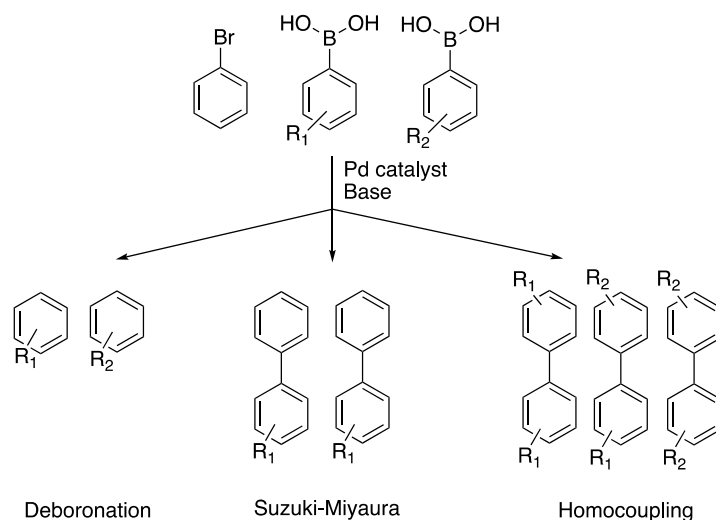
Scheme 22: The three reactions pathways in a Suzuki-Miyaura cross-coupling, including deboronation and homocoupling[69].

Another problem could be polymerization of chlorinated boronic acid. Some trouble occurred in the reaction with the chlorinated analogs in the Suzuki-Miyaura reaction performed by Solum *et al.,* and the polymeric material was hard to remove during work-up. Decent yields were achieved by slowly adding a solution of the boronic acid in THF to the stirred reaction mixture. This resulted in a smaller amount of polymeric material[28].

The side reactions affect the yield in the reaction and could result in challenging product purification. Side reactions are more susceptible to occur in slow reactions[70]. To minimize the number of by-products in the Suzuki-Miyaura cross-couplings, an option could be to shorten the reaction time[71]. It has been developed "ligand-free" conditions, using $Pd(OAc)_2$ in the cross-couplings[72, 73]. An advantage of using this condition is those side reactions associated with phosphine ligands, like the formation of phosphonium salt aryl-aryl exchange between substrate and phosphine, could be avoided[74].

3 Results and discussion

The aim of this master´s thesis was to synthesize several previously unknown steroid analogs to be evaluated as potential CDK8-inhibitors. The design of the new compounds is based on a steroid scaffold simplified of cortistatin A and CCT251545. Different heteroaromatic rings were added to the D-ring. Previous results from the research group showed that similar analogs with either a 7- or 6-isoquinoline (**a** and **b**) side chain at the 17-position are revealed to have the most promising anti-proliferative agents[6, 28]. A presentation of a general structure for the target compounds is given in Figure 15.

8
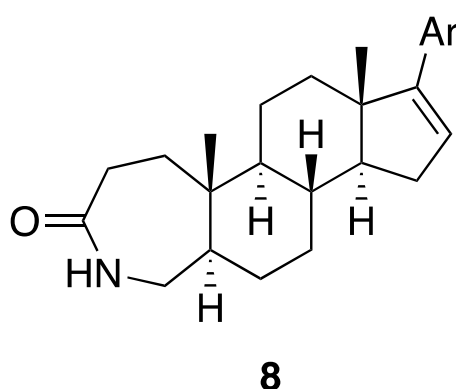
Figure 15: The general structure of the target compound.

The results and discussion are divided into three sections. Section 3.1 is based on modifying the A-ring and presents the synthesis of the hydroxyalkyl azide in a S_N2 reaction, the ring expansion of the A-ring in a Schmidt reaction, oxidation using PCC, and β-elimination using NaH as a base. Section 3.2 focuses on the modification of the D-ring and covers the formation of the triflate and the Suzuki-Miyaura cross-coupling with different boronic acids. Assigned chemical shifts (^{1}H and ^{13}C) for the compounds synthesized in this thesis are presented in Section 3.3

3.1 Modification on the A-ring

3.1.1 Hydroxyalkyl azide

Aubé and Charaschanya have earlier received yields up to 89% in the synthesis of *(S)*-3-azido-1-phenylpropanol (**2**)[29]. *(S)*-3-Chloro-1-phenylpropanol (**1**) was mixed with NaN_3 and NaI in anhydrous DMF at 80 °C. The synthesis is illustrated in Scheme 23.
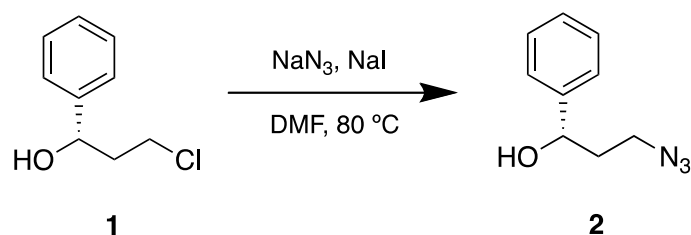
Scheme 23: Conditions for the synthesis of **2** as described by Aubé and Charaschanya[29].

The strong nucleophile and the polar aprotic solvent favour the S_N2 reaction. After adding all the reactants and heating the solution, the solution had a light grey colour. During the night, the solution had turned yellow. The TLC-plate showed full conversion after refluxing in 24 hours. The extraction with Et_2O and water effectively removed the impurities, and ^1H NMR and ^{13}C NMR showed full conversion, and purification was not needed. *(S)*-3-Azido-1-phenylpropanol (**2**) appeared as a colourless oil, and the reaction gave satisfying yields of 80-86%. A summary of some of the achieved results from the reactions is given in Table 1.

Table 1: Results achieved from the S_N2 synthesis of compound **2**.

Scale [g]	Reaction time [h]	State and colour	Yield [%]
1.12	25	Colourless oil	80
0.95	24	Colourless oil	86

3.1.2 Schmidt reaction

A Schmidt reaction was performed to expand the A-ring in the steroid core. The steroid (**3**) and hydroxyalkyl azide (**2**) were dissolved in anhydrous DCM under N_2-atmosphere at 0 °C, and added $BF_3 \cdot OEt_2$. Aubé and Charaschanya have earlier achieved yield up to 88% following this procedure[29]. The synthesis is illustrated in Scheme 24.

Scheme 24: Conditions for the synthesis of **4** as described by Aubé and Charaschanya[29].

The first entry was executed with a ratio of 1:2 between the steroid (**3**) and hydroxyalkyl azide (**2**), following the procedure developed by Aubé and Charaschanya[29]. Excess of $BF_3 \cdot OEt_2$ was necessary to assist the disproportionation of the reagent into BF_4^- [46]. The mixture was stirred for 16 hours, and after being concentrated under reduced pressure, it appeared as a thick, orange oil. This is a result of the addition of $BF_3 \cdot OEt_2$. Aqueous KOH was then needed to hydrolyse the intermediate iminium ether to the lactam product (**4**). The first entry followed the procedure by adding $MgSO_4$ to remove the water phase under the extraction. This was challenging due to the large scale and a large amount of $MgSO_4$ was needed to remove the water, and may have reduced the yield. This resulted in a yield of 74%. In the second entry, the water phase was extracted, washed with brine, and dried over $MgSO_4$. This resulted in a higher yield of 92%. In both cases, the crude product had a light yellow colour. Purifying the product in a flash column chromatography using 20% EtOAc/*n*-pentane and 2% MeOH/DCM resulted in a pure product.

The last entry was performed with a ratio of 1:1 between the hydroxyalkyl azide (**2**) and steroid (**3**). The crude product was observed as a white solid compared to a yellow crude product in the other entries. After purifying the solid using flash column chromatography, the yield was 81%. It should be noted that the overall yield was higher in this case, despite the fact that the yield in percent was lower. In retro perspective, all the entries should have been executed with a ratio of 1:1. In total, this step was successful and performed without any trouble. A summary of some of the achieved results from the reactions is given in Table 2

Table 2: Results from the Schmidt reaction of compound **4.**

Scale [g]	Ratio[a]	Reaction time [h]	State and colour	Yield [%]
0.76	1:2	16 + 24	Light yellow solid	74
0.69	1:2	16 + 24	Light yellow solid	92
1.47	1:1	16 + 24	White solid	81

[a] The ratio between 5α-dihydrotestosterone (**3**) and hydroxyalkyl azide (**2**) calculated in mmol.

The ^{1}H NMR spectrum for compound **4** was compared to earlier studies to investigate if *(S)*-**2** affected the regiocontrol. Prior research by Aubé and Charaschanya suggests that the regioisomers have different signals around 2.50-3.00 ppm in the ^{1}H NMR spectra[29]. A doublet of a doublet at 2.37 ppm is observed in the spectrum for **4a**, while a multiplet is observed at 3.02 ppm for **4b**. Figure 16 illustrates the obtained shifts in the 4.09-1.98 ppm region for the regioisomers [29].
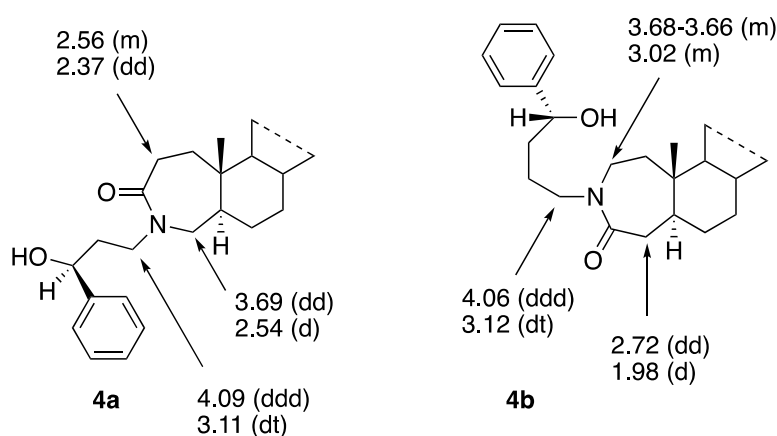
Figure 16: A summary of the ^{1}H NMR data from the article showing some of the shifts at the A-ring for the regioisomers **4a** and **4b**[29].

The ^{1}H NMR spectra for **4a** and **4b** in the article were compared to the spectrum for compound (**4**) in this thesis. Signals around 4.15-4.03 (m), 3.15-11 (dt), 2.62-2.53 (m) and 2.10-2.03 (m) are observed in all three spectra[29]. In the ^{1}H NMR spectrum for compound **4**, a doublet of a doublet at 2.39-2.33 ppm is observed. These results are in line with the spectra for compound **4a**. A multiplet at 3.02 ppm is not observed like in the spectra for **4b**[29]. Under certain assumptions, this can be construed as regioselectivity was obtained. To conclude with this,

several two-dimensional spectra should have been run. A fragment of the ^{1}H NMR spectrum for **4** showing shifts around 4.30-2.03 is given in Figure 17.
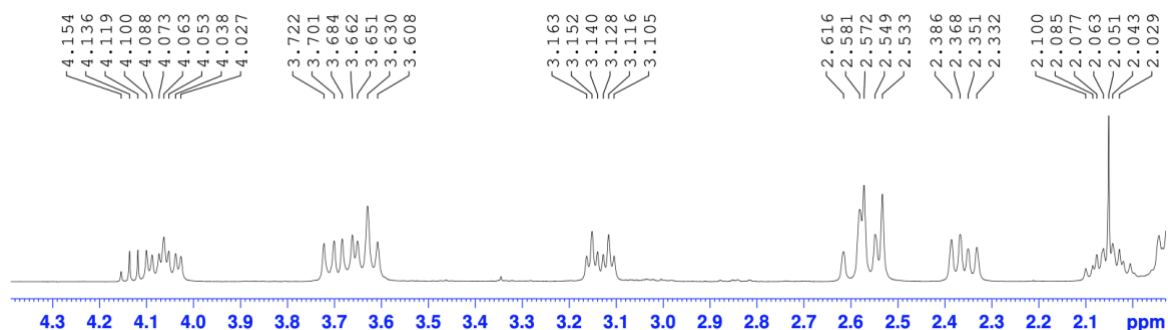
Figure 17: The ^{1}H NMR spectrum for **4** shows a shift at 2.39-2.33 ppm in accordance with the spectrum for compound **4a** from earlier studies by Aubé and Charaschanya[29].

3.1.3 Oxidation of alcohols using PCC

Aubé and Charaschanya have earlier received yields up to 72% in the synthesis of **5**[29]. PCC, celite, and the steroid (**4**) were stirred in a solution of DCM under N_2-atmosphere. The solution got a dark brown colour, and the reaction mixture was stirred overnight. The reaction is illustrated in Scheme 25.

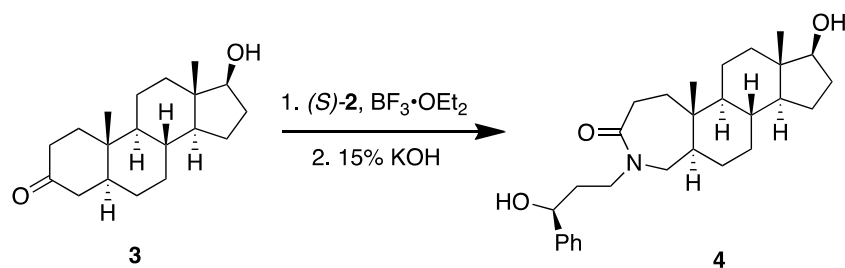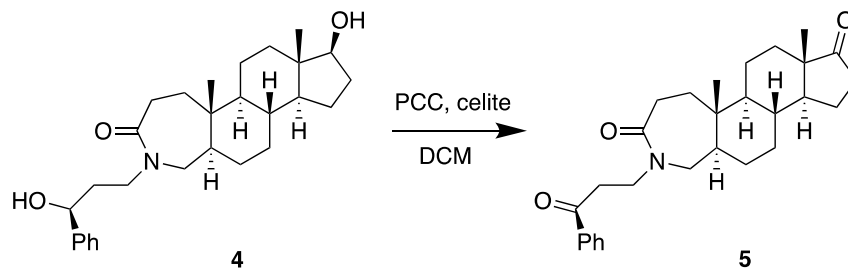**Scheme 25:** Conditions for the synthesis of **5** as described by Aubé and Charaschanya[29].

Some problems occurred during the oxidation reaction using PCC. The brown crude product was purified in flash column chromatography using 90% EtOAc/*n*-pentane as an eluent. The purification resulted in a low yield of 30% as a white solid. In the second entry, the reaction time was reduced, and the reaction was monitored by TLC every hour. The TLC-plate showed full conversion after 5.5 hours. After performing a flash column chromatography, the yield was still 30%. In the third entry, the amount of PCC was increased from 4 equiv. to 6 equiv. Some problems occurred during flash column chromatography with separating the product from the

larger amount of PCC. In the first column, the pyridinium-ring and some steroid-derivates were separated from the product. To separate the product from PCC, the product was purified by flash chromatography twice. The product was observed as a light brown solid, and the yield was 40%. Only signals from the steroid (**5**) were observed in the ^{1}H NMR spectrum, thus the impurities were likely inorganic Cr(IV) which also the brown colour indicate.

This reaction was generally troublesome due to problems with purification. Flash column chromatography using 75% EtOAc/*n*-pentane was implemented, and the by-product and product in the mixture seemed to elude from the column at the same time. A larger amount celite was added to the reaction mixture hoping to increase the yield. Addition of celite can simplify the work-up due to by-products are deposited onto these solids, which later can be removed by filtration. Column chromatography was prepared by packing an even longer column than in earlier attempts. In addition, the column chromatography was performed without applying pressure. This resulted in a pure product as a white solid in 50% yield. After following this procedure a couple of times, yields up to 67% was achieved. A summary of some of the achieved results from the reactions is given in Table 3.

Table 3: Results from the oxidation of compound **5**. Different reaction parameters were tested.

Scale [g]	PCC [equiv.]	Reaction time [h]	State and colour	Yield [%]
0.20	3	16	White solid	30
0.28	3	5.5	White solid	27
0.23	6	5.5	Light brown solid	37
0.49	6	5.5	Light brown solid	50
0.65	6	5.5	White solid	67

3.1.4 *β*-elimination using NaH

The steroid (**5**) and NaH were refluxed in anhydrous THF for 2 hours under N$_2$-atmosphere. Since NaH is strongly water-reactive, dry solvents and conditions were used to prevent unwanted reactions between water and NaH. Aubé and Charaschanya have earlier synthesized **6** in yields up to 76%[29]. The reaction is illustrated in Scheme 26.
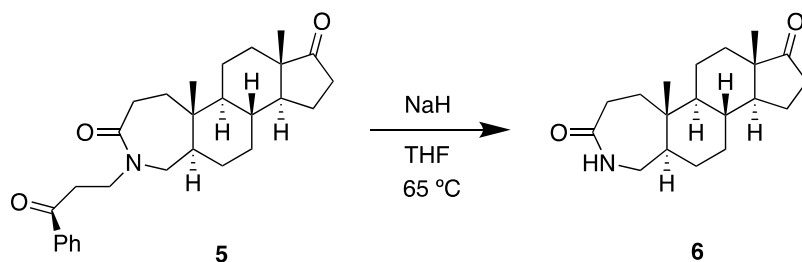
Scheme 26: Conditions for the synthesis of **6** as described by Aubé and Charaschanya[29].

It was observed that the solution had a grey colour at the beginning of the reaction. After a few minutes, the solution turned yellow. At the end of the reaction time, the solution had an orange colour. The TLC-plate was checked after 2 hours, and the plate showed full conversion and some UV-active by-products. The reaction mixture was quenched with NH_4Cl dropwise due to the formation of hydrogen gas. Under extraction, emulsions occurred and large amounts of solvents were used during the extraction process.

In the first entries, the reaction resulted in low yields between 34-40%. The poorer yields might partially be due to insufficient extractions. Some of the product vanished under the column chromatography. This could be due to the formation of hydrogen bonding between the amide and hydrogen in silica. ^1H NMR showed similarities between the shift in the by-products and starting steroid (**5**), as well as derivates with sign of the phenyl-ring. A larger amount of NaH was added, hoping to increase the yield. The purification using flash column chromatography was performed by packing a short column trying to reduce the loss of product in the purification process. Increasing the equivalents NaH resulted in higher yields (70-82%). A summary of some of the achieved results from the reactions is given in Table 4.

Table 4: Results from the synthesis of compound **6**.

Scale [g]	NaH [equiv.]	Reaction time [h]	State and colour	Yield [%]
0.23	5	2	White solid	34
0.31	8	2	White solid	70
0.27	8	2	White solid	82

3.2 Modification on the D-ring

3.2.1 Formation of triflate

The steroid (**7**) had not previously been synthesized using these reaction conditions. Solum *et al.* have earlier performed the same procedure on several different steroids. The reactions were stirred between 4 and 10 hours, and yielded up to 89%[6,28]. The steroidal ketone (**6**) and PhN(SO$_2$CF$_3$)$_2$ were dissolved in anhydrous THF at -78 °C. NaHMDS was added dropwise, and the solution was stirred between 10 and 16 hours. The reaction is illustrated in Scheme 27.
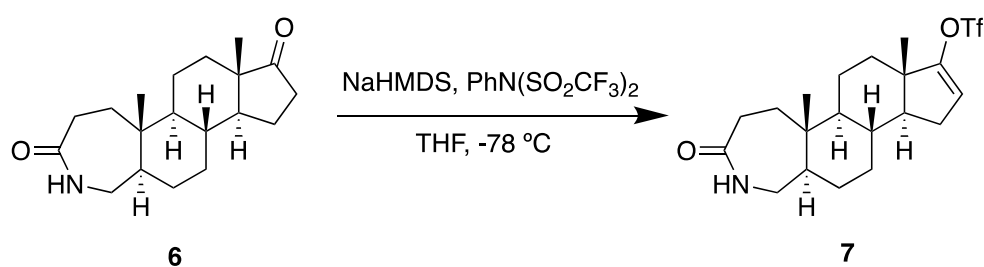
Scheme 27: Conditions for the synthesis of **7** as described by Solum *et al.*[6,28].

The first attempt was performed with 2 equiv. base like earlier performed in the articles. The reaction mixture was monitored by TLC every hour. No differences were noted after 10 hours, and then the reaction mixture was terminated. The ^{1}H NMR spectrum of the crude product showed signs of PhN(SO$_2$CF$_3$)$_2$, NaHMDS and, steroid (**6**). A weak new signal was observed as a double of doublets around 5 ppm in the ^{1}H NMR spectrum for the product (**7**). However, a flash column was not performed due to the small amount of product. The reaction was performed again with an increased amount of base (3.5 equiv.). After 14 hours, it seemed as if some conversion occurred and the reaction was ended even though TLC showed the remaining starting material. ^{1}H NMR and ^{13}C NMR of the crude product showed signs of product, and a flash column chromatography was performed. Due to several spots on the TLC and challenges separating the spots at the TLC-plates, the eluents used in the purification were 90% EtOAc/*n*-pentane and 2% MeOH/DCM. Separating the triflate from the product in a flash column chromatography was unsuccessful after changing the eluent too early. As a result, the product was not separated from the side-products. The flash column chromatography was repeated to give the pure product. This resulted in a yield of 15%. In addition, a large amount of starting material was achieved. The ratio between product and starting material was 1:2, and the reaction was not successful.

To improve the conversion of the starting material and increase the yield of the product (**7**), the reaction time was increased to 16 hours. The TLC plate showed that some conversion had occurred, but it was still difficult to decide when to terminate the reaction. After purifying the crude product, the yield was calculated to 10%. The ratio between product (**7**) and starting material (**6**) was estimated to 3:5, and increasing the reaction time was not successful to fully convert all the starting material (**6**). In the next attempt, the equivalents of NaHMDS were increased to 4.5 equiv. The reaction mixture was stirred in 14 hours, and the yield was still only 10% after the purification. The ratio between product (**7**) and starting material (**6**) was 3:5. In the last entry, the reaction time was decreased to 12.5 hours. The reaction was performed with 3.5 equiv. of NaHMDS. The flash column was performed without any problems, and this resulted in a yield of 22%. The ratio was estimated to 7:3 between the product (**7**) and starting material (**6**). Neither of the attempts gave satisfying yields and the reaction was unsuccessful in converting all the starting material (**6**) to the steroidal triflate (**7**). A summary of some of the achieved results from the reactions is given in Table 5.

Table 5: Results from the synthesis of compound **7**. Different reaction parameters were tested.

Scale [mg]	NaHMDS [equiv.]	Reaction time [h]	State and colour	Yield [%]	Ratio [a]
40.0	2.0	10	White solid	-	-
100.4	3.5	14	White solid	15	1:2
141.1	3.5	16	White solid	10	3:5
100.1	4.5	14	White solid	10	3:5
117.8	3.5	12.5	White solid	22	7:3

[a] The ratio between steroid triflate (**7**) and starting material (**6**) estimated in mmol.

The overall results of the reaction were disappointing, and this is an issue for future research to explore. As mentioned, Solum *et al.* have earlier synthesized a steroidal triflate from a steroidal ketone in a similar reaction using $PhN(SO_2CF_3)_2$ in the presence of KHMDS at -78 °C and have afforded yield up to 89%[6,28]. The reaction was performed with steroids consisting of a six-membered A-ring and not a seven-membered heterocycle. Another difference is the amide at the A-ring. The product (**7**) has been synthesized earlier by Chu, Wand, and Ye[75]. The synthesis was performed with different reaction conditions, and the attempts resulted in low yields (15%). The solution of a regioisomer mixture of the steroid (**6-6a**) in DCM was treated dropwise with

trifluoromethanesulfonic anhydride (Tf$_2$O) at 0 °C. The mixture was added triethylamine (Et$_3$N) and stirred overnight at room temperature, see Scheme 28.
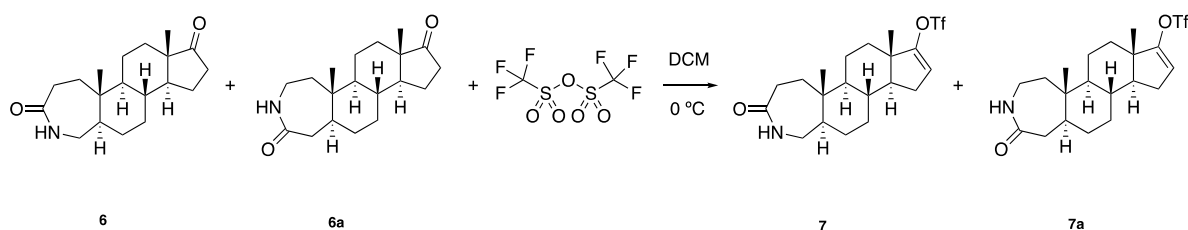
Scheme 28: An alternative synthesis route of a mixture of **7** and regioisomer **7a** by adding Tf$_2$O in DCM at 0 °C. This resulted in 15% yield[75].

The best achieved yield in this thesis was 22% and higher than the synthesis performed by Ye *et al.* above. The low yields seem to depend on the expanded *N*-containing A-ring. The yield might have been higher with some adjustments, but it was difficult to interpret the TLC plate, making it challenging to decide when to stop the reaction. Next time an option could be to use ^{1}H NMR to monitor the conversion. It seemed like the reaction should be terminated somewhere between 10 and 13 hours. In retro perspective, it could also be wise to try using another base like KHMDS or LiHMDS. KHMDS is more reactive than LiHMDS, but Li$^+$ might affect deprotonation facilitated by the directing effect of the oxygen[32]. Due to time and a small amount of starting material (**6**) left, there was too little time to improve the synthesis step further. To achieve higher yields, an option could be to reduce the amide to amine before the formation of the triflate. If the reduction does not result in a higher yield, this step can alternatively be replaced by using a different synthesis pathway, and perform a Wittig reaction followed by a Heck reaction.

3.2.2 Suzuki-Miyaura cross-coupling

The procedure for this experiment and all the following Suzuki coupling reactions were based on previous work by *Solum et al.,* who have achieved high yields of 64-85%[6]. The target compounds (**8a-e**) had not previously been synthesized and could be potential CDK8 inhibitors. Compared to Solum *et al.* the equivalents in these reactions were doubled, except for the steroid triflate (**7**).   Five different boronic acids were used as coupling partners. Tetrakis(triphenylphosphine)palladium and cesium carbonate in THF:H$_2$O (5:2) enabled the preparation of compounds **8a–e**. The general synthesis is illustrated in Scheme 29.
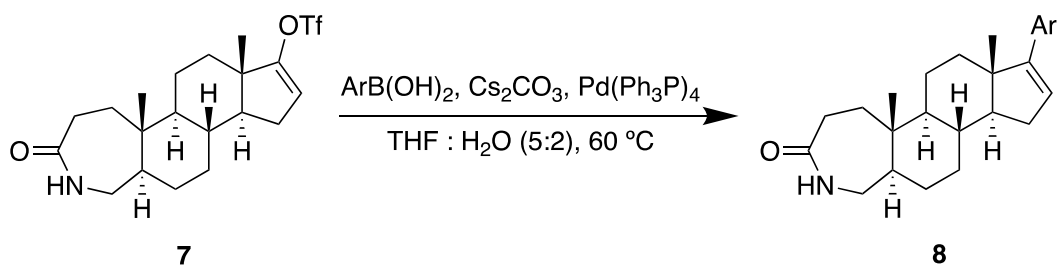
Scheme 29: Conditions for the synthesis of **8** as described by Solum *et al.*[6,28]

Before this step, the total yield of steroid triflate (**7**) was calculated to 120 mg. The steroid was divided into five equal parts to give different analogs (**8a-e**). Each reaction was performed with 24 mg steroid triflate reacting with different boronic acids (**a-e**), and each reaction is described in separated parts below.

3.2.2.1 Isoquinoline-7-boronic acid

The steroid (**7**), isoquinoline-7-boronic acid (**a**), and the other reactants were mixed and stirred for 18 hours. The TLC-analysis at the beginning at the reaction showed seven spots. Overnight the mixture got a black colour. TLC still showed seven different spots after 12 hours and 18 hours. It is possible the reaction could have been terminated earlier, but the procedure was performed like Solum *et al.* which prior had achieved high yields when stirring the mixture between 18 and 22 hours. After the extraction with EtOAc, the TLC plate showed five spots. The crude product in this reaction had a yellow colour and a sand-like appearance. Purification turned out to be difficult due to overlapping spots at the TLC plate. It was challenging separating the spots at the TLC plate and finding a suitable eluent for performing a flash column chromatography. A flash column chromatography was performed using gradient elution from 0-5% MeOH/DCM. After the attempt to purify the product, the product still showed minor signs of by-products by the fact that the integrals in the ^{1}H NMR spectrum were too high (see Appendix H). The signals of the by-products were located close to the signals of the steroid core. This might be due to derivates of the wanted product (**8a**).

3.2.2.2 Isoquinoline-6-boronic acid

The steroid (**7**), isoquinoline-6-boronic acid (**b**), and the other reactants were mixed and stirred for 18 hours. The reaction mixture got a dark brown colour after 8 hours due to the palladium. The crude product was observed as a brown oil with signs of some white solid. The TLC-plate

showed three spots after the extraction. This indicates the formation of water-soluble by-products removed during work-up. A flash column chromatography was performed, and in this entry, a gradient elution from 0-5% MeOH/DCM was used. This time the ^{1}H NMR showed more impurities. The second product was slightly less pure than the product (**8a**) obtained in the first cross-coupling. Some impurities were located around the 7 ppm region and resonate to aromatics. Other impurities could be observed in the steroid-core region. This indicates that the by-product is a derivate of the wanted product (**8b**). A second flash column chromatography was performed using 90% EtOAc/*n*-pentane and 5% MeOH/DCM as eluents. A significant amount of material disappeared in the column as a possible consequence of hydrogen bonding between the amide and silica. The yield was only 11% of pure product (**8b**). Spectroscopic data are given in Appendix I.

3.2.2.3 Isoquinoline-5-boronic acid

The steroid (**7**), isoquinoline-5-boronic acid (**c**), and the other reactants were mixed and stirred for 18 hours. The reaction mixture got a black colour after 4 hours. The TLC-plate showed the same spots at the start of the reaction as the TLC-analysis performed after 4 hours and 18 hours. After the extraction with EtOAc, fewer spots were noted at the TLC plate, indicating some by-products were removed. The crude product was observed as a brown oil with signs of a white solid. Due to not obtaining the pure product in the other Suzuki cross-couplings, flash column chromatography was performed with 90% EtOAc/*n*-pentane and 5% MeOH/DCM as eluents. The first fractions had an orange colour and ^{1}H NMR showed signals similar to the boronic acid (**c**). This could be a result of homocoupling or deboronation. The spectroscopic data showed a pure product (**8c**) in 27% yield, see Appendix J.

3.2.2.4 Pyridine-3-boronic acid

The steroid (**7**), pyridine-3-boronic acid (**d**), and the other reactants were mixed and stirred for 18 hours. The reaction mixture got a brown colour after 4 hours. Compared to the other cross-couplings, fewer spots were observed at the TLC-plate. The crude product was observed as a brown solid. In the first fractions, 90% EtOAc/*n*-pentane was used before switching to gradient elution from 0-5% MeOH/DCM. When changing eluents, a couple of orange fractions was

observed. These fractions contained aromatic by-products. The purified product (**8d**) was yielded 59%. Spectroscopic data are given in Appendix K.

3.2.2.5 2-Chloro-pyridine-4-boronic acid

The steroid (**7**), 2-chloro-pyridine-4-boronic acid (**e**), and the other reactants were mixed and stirred for 18 hours. A solution of the boronic acid (**e**) in THF was added to the reaction mixture to prevent polymerization of the chlorinated boronic acid earlier experienced by Solum *et al.*[28]. Several spots were observed at the TLC-plate. The crude product had a dark brown colour as a solid. A flash column was performed using 90% EtOAc/*n*-pentane before changing eluent to a gradient elution from 0-5% MeOH/DCM. The flash column was troublesome. When changing the eluent to MeOH/DCM it was observed some yellow fractions containing the product (**8e**). Spectroscopic data show impurities due to high integrals in the ^{1}H NMR spectrum (Appendix L)

3.2.3 Summary of Suzuki-Miyaura cross-coupling reactions

The Suzuki-Miyaura cross-coupling reactions were performed like earlier by Solum *et al*. using five boronic acids (**a-e**), see Figure 18. The reaction time could possibly be shortened due to the change in colour after stirring for 4 hours. Purification using column chromatography was troublesome due to overlapping spots at the TLC-plate, and therefore challenging to find a suitable eluent. Using 90% EtOAc/*n*-pentane as eluent before changing to 5% MeOH/DCM gave satisfying purification. Higher yields could have been achieved by upscaling the reaction. There were formed several by-products in all the reactions, and this lowered the yield. The ^{1}H NMR spectra showed that some of the by-products had similar shifts as the products. This could indicate that the formed by-products were derivatives of the wanted product, including the starting boronic acid or boronation or homocoupling of the boronic acid. A summary of the achieved results from the reactions is given in Table 6.
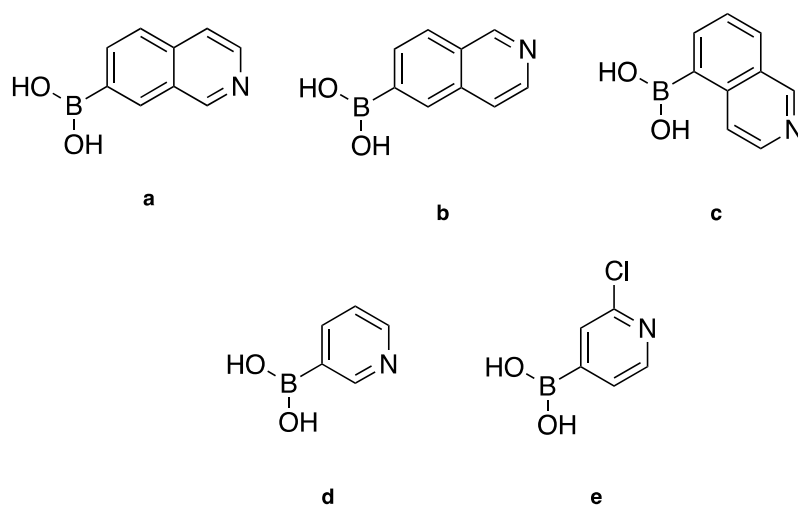
Figure 18: The different boronic acids (**a-e**) used in the Suzuki-Miyaura cross-coupling.

Table 6: Results from the Suzuki-Miyaura cross-coupling reactions using different boronic acids (**a-e**).

| Boronic acid	Scale [mg]	Reaction time [h]	Crude product [mg]	Yield [%]
a	24	20	25.0	44
b	24	20	22.1	11
c	24	20	23.1	27
d	24	20	28.1	59
e	24	20	35.2	73

3.3 Structural elucidation

The synthesized compounds have been characterized by using ^{1}H and ^{13}C NMR. Data reported by Fulmer *et al.* have been used to determine chemical shifts of common solvents and impurities[76]. General trends were observed in the ^{1}H NMR and ^{13}C NMR spectra for the steroidal core, and the shifts are fairly constant, respectively, 0.9-3.0 ppm and 10.0-60.0 ppm. This section focus on the modifications on the A-ring and D-ring due to the impact of different substituents. The spectra were used to determine that the reactions had taken place. Since no two-dimensional spectra were taken (COSY, HSQC, HMBC), it was challenging to characterize the compounds. Hence the characterization of the compounds is presented with some uncertainty. Several of the compounds synthesized in this master´s thesis are synthesized earlier by Aubé and Charaschanya, thus previous spectroscopic data were compared to the spectra for compounds **2-6** in this thesis. In addition, ChemDraw software was used as assisting sources in the structural elucidation. Other analyses used in this thesis were IR-analyses to confirm if the reactions had occurred, and optical rotation. Additionally, the new steroids have been analysed by MS.

3.3.1 Structural elucidation of the hydroxyalkyl azide
Compound 1 and 2

^{1}H NMR and ^{13}C NMR spectra for compound **1** and **2** can be found in Appendix A and B. The structures of the compounds with numbered positions are given in Figure 19, and the chemical shifts are presented in Table 7.

The shifts of aromatic protons are typically higher than those of alkenes due to deshielding, and the phenyl-ring are observed between 8-7 ppm in both spectra[49]. A change in the shift is observed for the proton at the 4 position. Protons on oxygen typically have a wide range of expected chemical shifts. Often they appear as broad peaks due to these protons being acidic and therefore exchangeable[49]. In the spectrum for **2**, the hydroxyl-group is observed at 3.54 ppm, compared to around 2 ppm in prior studies[29]. The protons in position 1 are adjacent to a heteroatom in both **1** and **2**. Electronegative elements cause increased shift. The degree of the shifts correlates roughly with electronegativity. Chlorine is more electronegative than nitrogen, thus the shifts are higher for compound **1**. The NMR data for these compounds are found in literature and are consistent with previously reported data[29]. The suggested structure elucidation for compound **1** and **2** are given in Figure 19.
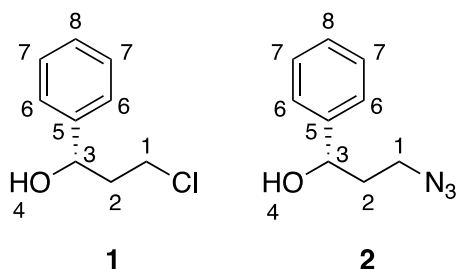
Figure 19: Structures of **1** and **2** with numbered positions correlating to NMR-shifts in Table **7**.

Table 7: ^{1}H and ^{13}C NMR chemical shifts for compound **1** and **2** in CDCl$_3$.

Position	^{1}H NMR [ppm]		^{13}C NMR [ppm]	
	1	**2**	**1**	**2**
1	3.71	1.95	41.1	48.2
2	2.05	3.43	42.0	37.8
3	4.92	4.80	71.3	71.5
4	2.25	3.54	-	-
5	-	-	143.7	143.9
6	7.37	7.49	127.9	127.9
7	7.30	7.48	128.7	128.7
8	7.30	7.48	125.8	125.9

IR-spectra was useful to get a confirmation on the presence of the functional groups in the compounds, and were used to determine if a S$_N$2 reaction had occurred. Both IR-spectra show broad peaks around 3300 cm^{-1} that correspond to the hydroxyl-group. The characteristic range can be observed between 3500-3000 cm^{-1} and a C-O stretching around 1300-1000 cm^{-1} [49]. Furthermore, both the spectra contain a phenyl ring, and around 3150-3000 cm^{-1} aromatic C-H stretching is observed as weak peaks. In both spectra, the aromatic C=C stretching modes appeared between 1600-1400 cm^{-1}. The IR-spectrum to the starting material (**1**) gave strong absorptions at 800-700 cm^{-1} that resonate with the Cl-group. However, a strong signal at 2094 cm^{-1} is observed in the spectrum for the product (**2**). The signal corresponds to N=N=N stretching,due to azides absorbing in the 2500-1900 cm^{-1} region[49]. The present findings confirm that a S$_N$2 reaction occurred.

Optical rotation to (*S*)-3-azido-1-phenylpropanol (**2**) was measured to $[\alpha]_D^{20}$ = -38.4 (c 1.20, CHCl₃). The results from optical rotation show accordance with findings reported by Aubé and Charaschanya that obtained $[\alpha]_D^{23}$ = -35.9 (c 1.09, CHCl₃)[29].

3.3.2 Structural elucidation of the A-ring

Compound 3-6

The A-ring in these four compounds has been compared. ¹H NMR and ¹³C NMR spectra for compounds **3**, **4**, **5** and **6** can be found in Appendix C-F, and chemical shifts are presented in Table 8.

One of the differences in the ¹H NMR spectra for all the compounds (**3-6**) are the shifts around 7 ppm which resonates with the phenyl rings. The phenyl ring can be observed in the spectra for **4** and **5**. The shifts from the OH-groups (**4**) at 3.15 ppm and 4.72 ppm are not observed in the spectrum for the steroidal ketone (**5**). Moreover, the ¹³C NMR spectrum shows a high shift at 190.11 ppm characterizing the ketone. After the *β*-elimination the signals at 7.99-7.45 vanished for compound **6**. However, a new signal at 6.65 ppm has appeared. Broad signals in the 5-9 ppm region resonate amides[49]. This suggests that the phenyl-group and alkane-chain are eliminated and resulted in a formation of the amide (**6**). ¹H NMR and ¹³C NMR data for the compounds are found in literature. The obtained data are consistent with previously reported data. The suggested structure elucidation for compounds **3**, **4, 5** and **6** are given in Figure 20.
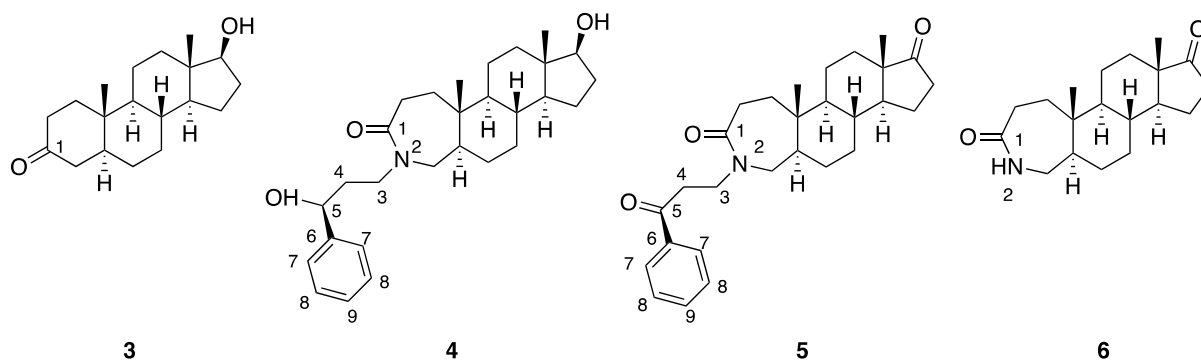
Figure 20: Structures of **3**, **4**, **5** and **6** with numbered positions correlating to NMR-shifts in Table 8.

Table 8: ^{1}H and ^{13}C NMR chemical shifts for the A-ring in compound **3**, **4**, **5** and **6** in CDCl$_3$.

Position	^{1}H NMR [ppm]				^{13}C NMR [ppm]			
	3	**4**	**5**	**6**	**3**	**4**	**5**	**6**
1	-	-	-	-	212.2	176.9	175.4	178.9
2	-	-	-	6.65	-	-	-	-
3	-	3.15	nd	-	-	-	nd	-
4	-	nd^a	nd	-	-	-	nd	-
5	-	4.72	-	-	-	70.0	190.1	-
6	-	-	-	-	-	144.2	136.7	-
7	-	7.36	7.99	-	-	127.0	128.7	-
8	-	7.27	7.45	-	-	128.3	128.8	-
9	-	7.27	7.59	-	-	125.5	133.4	-

^{a} nd = not determined (in the alkane region between 50-0 ppm).

Common in three of the IR-spectra (**4-6**) are the two signals around 2940 cm^{-1} and 2849 cm^{-1}, indicating the amide in the A-ring. The spectrum for compound **3** gave an absorption around 1700 cm^{-1} that corresponds to the C=O stretching from the ketone. After the ring expansion of the A-ring, the IR-spectrum for compound **4** show a strong peak at 1625 cm^{-1} that indicates an aromatic C=C bending. Additionally, it can be observed strong absorptions at 732 cm^{-1} and 700 cm^{-1} that could resonate to an aromatic C-H bending. Similar signals can be observed for compound **5**, but the broad absorption at 3366 cm^{-1} has vanished. Instead, a new strong peak is observed at 1736 cm^{-1} that indicate a formation of the ketones. The findings from the IR-spectra confirm that oxidation had occurred.

After the β-elimination, the spectrum for compound **6** shows strong absorptions at 3185 cm^{-1} and 3073 cm^{-1}. N-H bonds and O-H bonds often occur in the same region. Usually, the N-H absorption is less intense since the bonds do not participate in hydrogen bonding as readily as O-H bonds. This results in sharper peaks as seen in the spectrum for compound **6**[49]. Moreover, amides are accompanied by a strong C=O band between 1730 and 1680 cm^{-1} and be observed at 1678 cm^{-1}. The overall observations from the IR-spectra are consistent with results from NMR.

3.3.3 Structural elucidation of the D-ring

Compound 6 and 7

The D-ring in compounds **6** and **7** have been compared. ^{1}H NMR and ^{13}C NMR spectra for the compounds can be found in Appendix F and G, and chemical shifts are presented in Table 9.

In the ^{1}H NMR spectrum for the steroidal triflate (**7**), a double of doublets is observed at 5.57 ppm. A similar shift was obtained in the formation of steroidal triflates in research by Solum *et al.*[28]. Substitution by unsaturated groups causes increases shifts[49]. This can be noted at the 16-position. The shift increases from 2.64 ppm to 5.57 ppm in the ^{1}H NMR spectra. The carbon at the 16-position in the spectrum for compound (**6**) is not determined due to being in the alkane-region (0-50 ppm), but the shift increased to 114.5 ppm in the spectrum for the steroidal triflate (**7**). When observing the ^{13}C NMR spectra, the ketone in compound **6** has a signal at 220.9 ppm. In addition, a new signal at 120.2 ppm is observed in the spectrum for compound **7**. The suggested structure elucidation for compounds **6** and **7** is given in Figure 21.
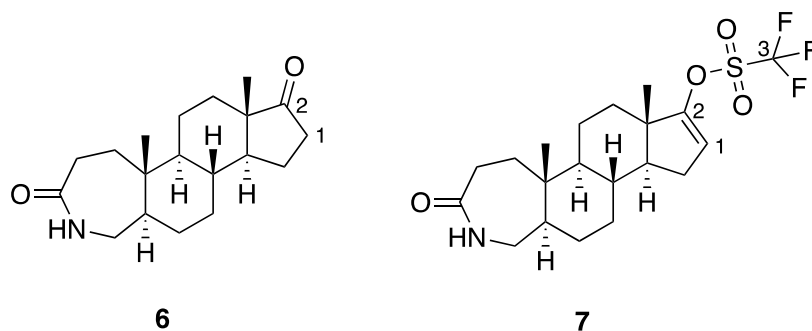
Figure 21: Structures of **6** and **7** with numbered positions correlating to NMR-shifts in Table 9.

Table 9: ^{1}H and ^{13}C NMR chemical shifts for the D-ring in compound **6** and **7** in $CDCl_3$.

	^{1}H NMR [ppm]		**^{13}C NMR [ppm]**	
Position	**6**	**7**	**6**	**7**
1	2.6	5.57	nd[a]	114.5
2	-	-	220.9	178.6
3	-	-	-	120.2

[a] not determined (in the alkane region between 50-0 ppm)

The strong absorption at 1737 cm^{-1} observed in the IR-spectrum for the steroidal ketone (**6**) has vanished in the spectrum for the steroidal triflate (**7**). Strong absorption at the 1850-1650 cm^{-1} region indicates C=O stretching. The IR-spectrum for the steroid triflate (**7**), shows strong absorptions at 1354 cm^{-1} and 1135 cm^{-1} that correspond to S=O streching[49]. The C-F stretching is observed as a sharp peak at 1089 cm^{-1}.

High resolution mass spectroscopy gave *m/z* 436.1775 [M+H]$^+$ for compound **7**. The calculated value was 436.1769 from the molecular formula $C_{20}H_{29}NO_4SF_3$. The accuracy was confirmed to 1.4 ppm.

3.3.4   Structural elucidation of the A-ring

Compound 8a-e

The spectra for the potential CDK8-inhibitors have been compared. ^{1}H NMR and ^{13}C NMR spectra for the compounds can be found in Appendix H-L.

Compounds **8a-c** contain an isoquinoline substituent at the 17-position. The group affecst the ^{1}H and ^{13}C NMR spectra for the three compounds in a similar way. The isoquinoline substituent is observed in the aromatic region, respectively, from 9-7 ppm and 160-110 ppm. Protons adjacent to nitrogen resonance to high shifts and shift rapidly decreasing intensity to more distant protons[49]. The suggested structure elucidation for compound **8a-c** is given in Figure 23 and Table 10.
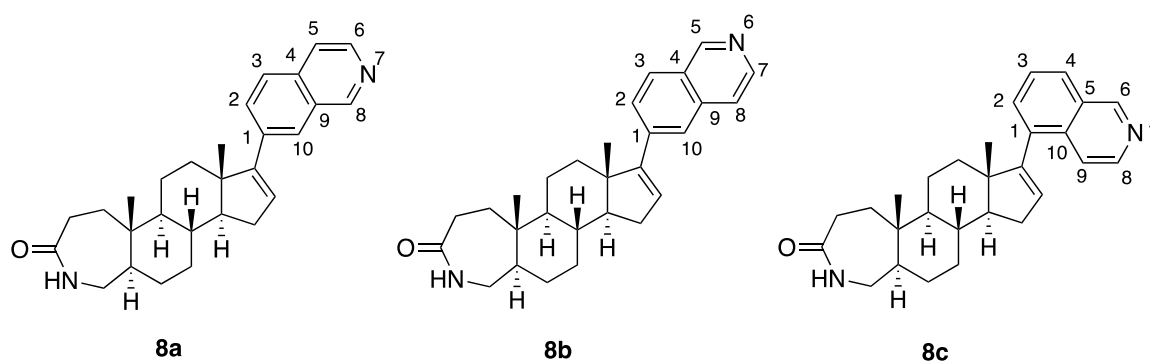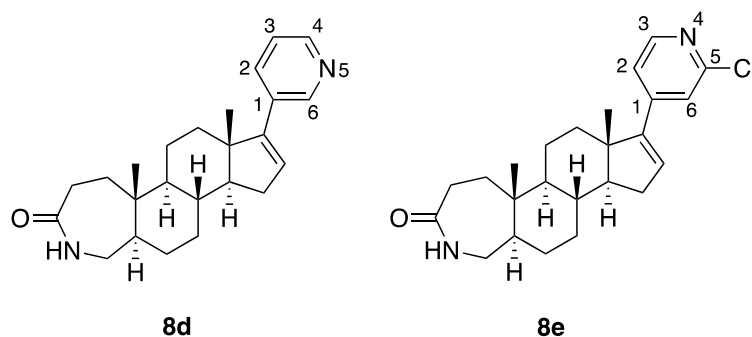

Figure 22: Structures of **8a, 8b** and **8c** with numbered positions correlating to NMR-shifts in Table 10.

Table 10: ^{1}H and ^{13}C NMR chemical shifts for the D-ring in compound **8a-c** in CDCl$_3$.

Position	^{1}H NMR [ppm]			^{13}C NMR [ppm]		
	8a	8b	8c	8a	8b	8c
1	-	-	-	130.6	139.2	135.4
2	7.67	7.62	7.56	127.4	122.9	129.0
3	8.02	7.82	7.49	126.5	127.6	126.6
4	-	.	7.92	135.9	130.2	129.5
5	7.75	9.21	-	114.5	152.0	130.8
6	8.56	-	9.25	142.6	-	152.6
7	-	8.51	-	-	143.1	-
8	9.31	7.76	8.51	159.1	no[a]	142.9
9	-	-	7.85	120.8	136.0	119.2
10	7.87	7.76	-	120.7	127.1	134.9

[a] not observed in the ^{13}C NMR spectrum.

Compounds **8d** and **8e** contain a pyridine substituent at the 17-position. In addition, **8e** contain chlorine. Both spectra have similar patterns. The spectrum for compound **8d** shows two high shifts around 8 ppm due to nitrogen, while the spectra for **8e** consist of one less hydrogen. The suggested structure elucidation for compounds **8a-d** and **8e** are given in Figure 23 and Table 11.

Figure 23: Structures of **8d** and **8e** with numbered positions correlating to NMR-shifts in Table 11.

Table 11: ^{1}H and ^{13}C NMR chemical shifts for the D-ring in compound 8d and 8e in CDCl$_3$.

Position	^{1}H NMR [ppm]		^{13}C NMR [ppm]	
	8d	8e	8d	8e
1	-	-	132.9	151.4
2	7.66	7.70	no[a]	118.9
3	7.23	8.18	132.0	149.4
4	8.48	-	147.9	-
5	-	-	-	151.7
6	8.26	7.18	151.6	121.3

[a] not observed in the ^{13}C NMR spectrum.

A similarity in the spectra for the target compounds (**8a-e**) are the signals at 3200-2800 cm^{-1} that correspond to the amide at the A-ring. A strong signal at 1680 cm^{-1} is observed that typically resonating to a C=O stretching for a secondary amide. Usually, the IR-spectra for aromatic amines show a strong peak around 1342-1266 cm^{-1}. The aromatic amines can be observed as a medium peak in the spectra in this thesis. C=N has a frequency between 1700-1620 cm^{-1} and can be observed as a strong signal. This corresponds to the heterocyclic rings at the 17-position. The signal around 850-730 cm^{-1} indicates an aromatic C-H or N-H. Compound **8e** holding a chlorine display absorption due to C-Cl stretching at 730 cm^{-1}.

High resolution mass spectroscopy gave *m/z* 415.2756 [M+H]$^+$ for compound **8c**. The calculated value was 415.2649 from the molecular formula C$_{28}$H$_{35}$N$_2$O. The accuracy was confirmed to 1.7 ppm.

High resolution mass spectroscopy gave *m/z* 365.2597 [M+H]$^+$ for compound **8d**. The calculated value was 365.2593 from the molecular formula C$_{24}$H$_{33}$N$_2$O. The accuracy was confirmed to 1.1 ppm.

High resolution mass spectroscopy gave *m/z* 399.2210 [M+H]$^+$ for compound **8e**. The calculated value was 399.2203 from the molecular formula C$_{24}$H$_{32}$N$_2$OCl. The accuracy was confirmed to 1.8 ppm.

MS of compounds **8a** and **8b** were not performed due to the small amount of product left.

4 Conclusion

For this master´s thesis, potential CDK8 inhibitors have been synthesized. All of the compounds were based on the steroid scaffold with an extended A-ring and with different aromatic heterocycles in the 17-position on the D-ring.

First, an auxiliary hydroxyalkyl azide (**2**) was synthesized in a S_N2 reaction that gave 86% yield. The following reactions focused on modifications on the A-ring. A ring expansion was performed in a Schmidt reaction using *(S)*-**2** and a steroid (**3**), resulting in 81% yield. The oxidation reaction using PCC was troublesome due to work-up, but an acceptable yield of 67% was obtained after increasing the addition of PCC and celite. The *β*-elimination using NaH gave varying yields (30-82%) due to insufficient extraction and problems with purification in the flash column chromatography in the first entries. The two last steps focused on modifications on the D-ring. The step involving the triflate formation resulted in low yields (10-22%) after several attempts to change the reaction parameters. Suzuki-Miyaura cross-couplings were performed to add heteroaromatic substituents on the D-ring. Pd(PPh3)4 was used as a catalyst and, the reaction was performed with five boronic acids (**a-e**). This gave varying yields (11-73%). Overall, the aim to synthesize potential CDK8 inhibitors was successful, and compounds (**8b-e**) can be biological evaluated. A summary of the synthesis and yields is given in Scheme 30.
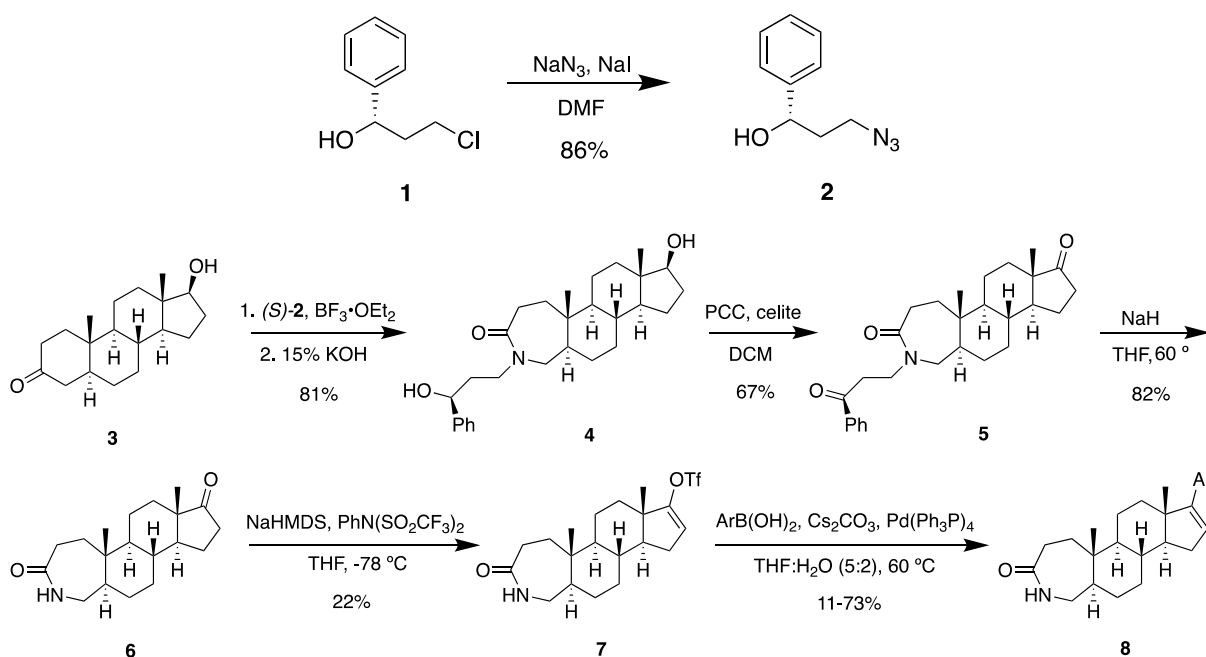

**Scheme 30:** The total synthesis in this master´s thesis involving the best achieved results.

5   Future work

Initially, the aim was to synthesize steroid analogs with an amine at the A-ring, but due to time and a small amount of steroid left, compounds **8a-e** were synthesized. In future work, an opportunity is to use a larger amount of starting material and reduce the products (**8a-e**) by using lithium aluminum hydride (LiAlH$_4$) in THF, see Scheme 31. Compound **13a-e** can further be tested as potential CDK8 inhibitors by evaluating their biological effect (Figure 24).
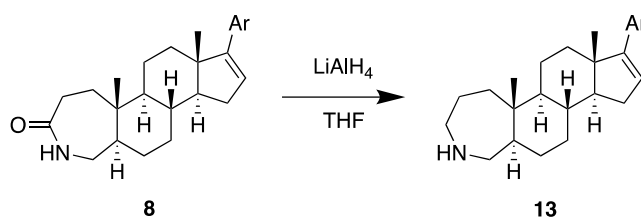

Scheme 31: Reduction of **8** using LiAlH$_4$ in THF to give a steroidal amine (**13**).
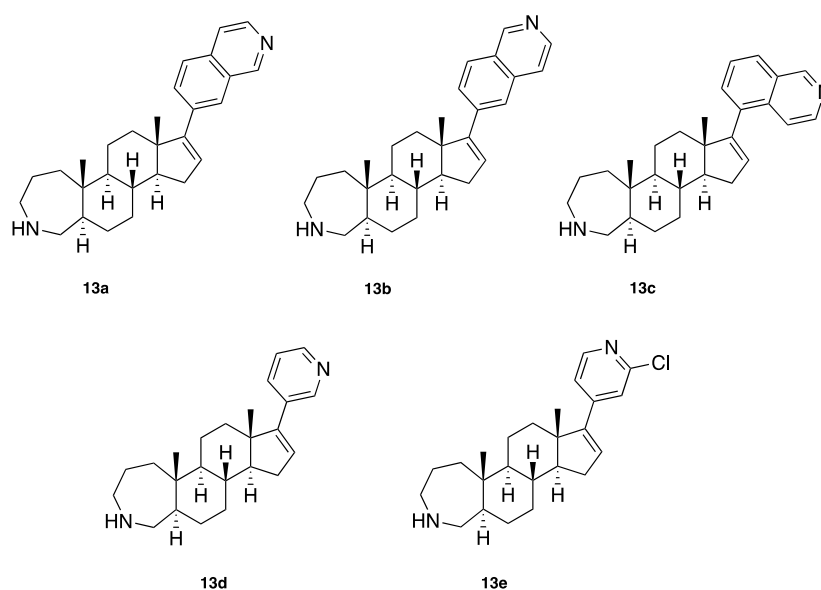

Figure 24: Potential steroid analogs (**13a-e**) containing an amine in the A-ring.

As mentioned, there were some issues involving the formation of triflate (**7**). In future work, improving this step might be desirable. Alternatively, a different synthesis pathway could be done by reducing the amide to an amine earlier in the synthesis pathway. In that case, it is necessary to protect the ketone at the D-ring by forming a ketal (**14**). This could be done by mixing the steroid with *p*-toluenesulfonic acid (*p*-TsOH) and ethylene glycol in toluene. After the reduction, the ketal could be removed by adding hydrochloric acid (HCl) and acetone. The alternative synthesis is given in Scheme 32.
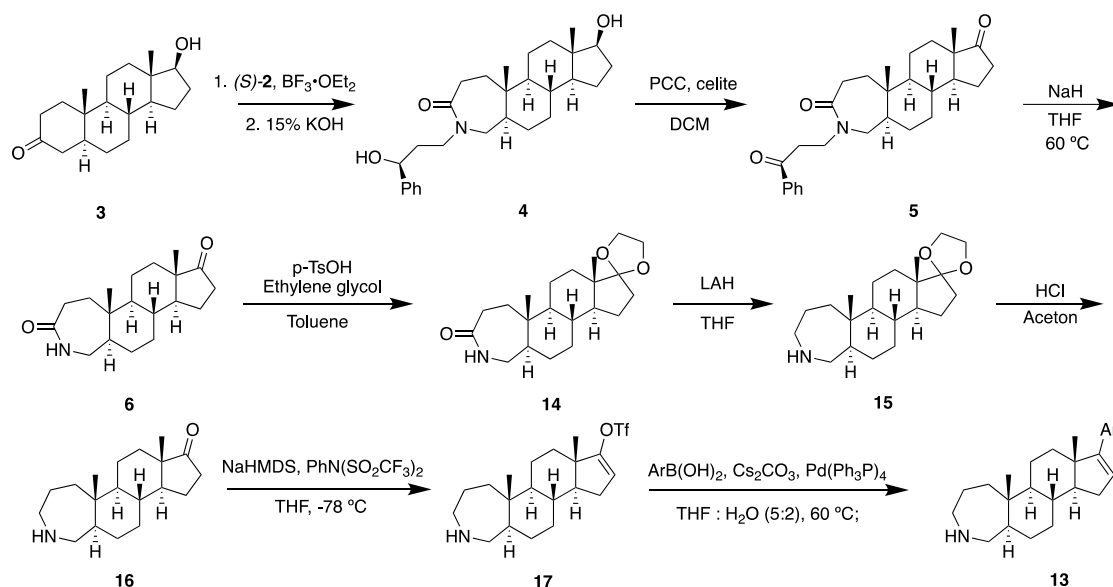
Scheme 32: One potential synthesis route to give **13**[49, 68].

If there is still a problem with the formation of the steroid triflate, the synthesis pathway could be changed. After the *β*-elimination using NaH, one alternative is to perform a Wittig reaction and a Heck reaction. The Wittig reaction converts the ketone to an alkene (**18**) using the ylide generated from a phosphonium salt. The alkene (**18**) can react in a Heck reaction with aryl halides in the presence of a palladium catalyst. This results in a substituted alkene (**19**). Then the amide could be reduced by using LiAlH₄. The altering of the steroid´s 17-position (**20**) could possibly affect the interaction with the kinase hinge segment. A proposed alternative synthesis route is given in Scheme 33.
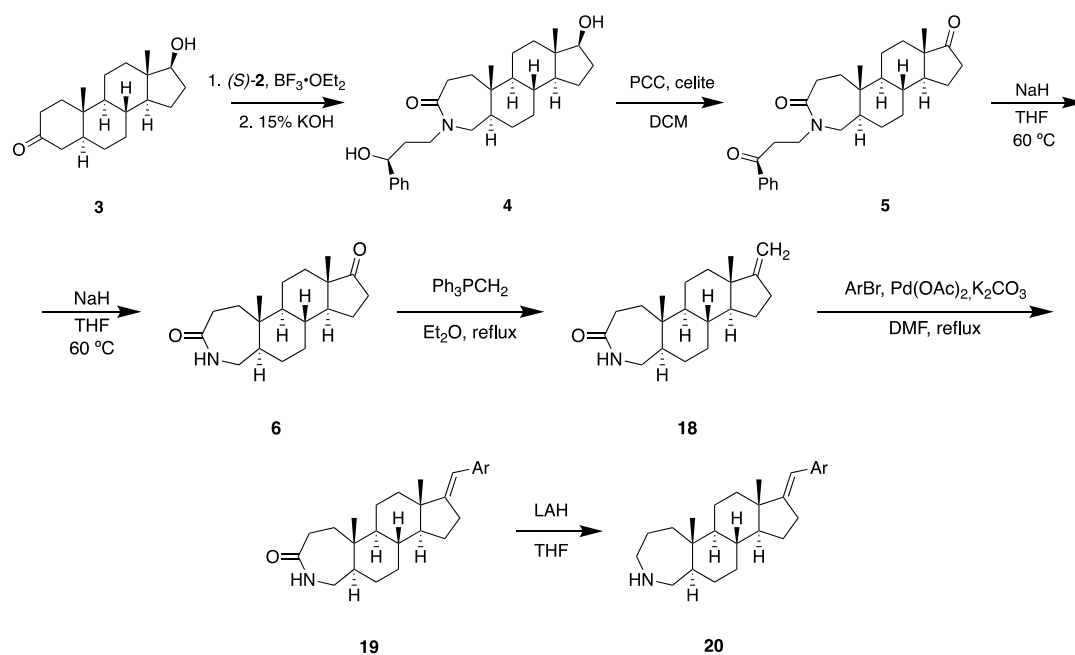
Scheme 33: An alternative synthesis route by performing Wittig and Heck reactions[77, 78].

Regardless, future studies should continue to explore several analogs of **8**. Solum *et al.* have earlier performed Suzuki-Miyaura cross-coupling with other boronic acids giving promising results. If promising results in biological testing of analogs (**8a-e)** as potential CDK8 inhibitors, future research should include Suzuki reactions using several other boronic acids. Some potential heterocycles (**f-j**) that could be introduced to the D-ring are shown in Figure 25.
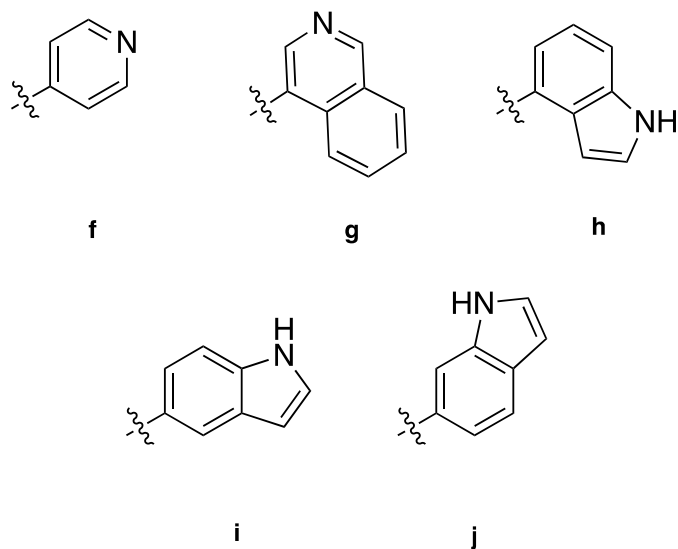
Figure 25: Potential heterocycles to be introduced at the D-ring.

6   Experimental

6.1   General methods - Chemistry

All reagents and solvents were used as purchased without further purification unless stated otherwise. Analytical TLC was performed using silica gel 60 F_{254} aluminium plates (Merck). For plate visualization, UV-light was used (wavelength 254 nm and 365 nm) for visualizing aromatics and conjugated systems. Potassium permanganate ($KMnO_4$) was used for visualizing alkenes and oxidizable groups, while Cerium ammonium molybdate (CaM) was used as a universal stain. Flash column chromatography was performed on silica gel (40-63 mesh, 60 Å) produced by Merck.

6.1.1   Nuclear magnetic resonance spectroscopy (NMR)

NMR spectra were recorded on a Bruker Advance DPX-400 MHz spectrometer for ^1H NMR and ^{13}C NMR. Peaks are described according to their multiplicity: s (singlet), d (doublet), t (triplet), and m (multiplet). Coupling constants (J) are reported in hertz, and chemical shifts are reported in parts per million relative to $CDCl_3$ (7.26 ppm for ^1H and 77.0 ppm for ^{13}C)[79].

6.1.2   Infrared spectroscopy (IR)

IR was performed with an Alpha FTIR spectrometer. The frequencies are reported in the range 4000-500 cm^{-1}. Peaks are described as w (weak), m (medium), s (strong) and br (broad).

6.1.3   Optical rotation

Optical rotation was recorded on an AA10 Polarimeter, Optical Activity, LTD, with a 10 mm sample cell and a 2.5 mm sample cell for the products (**8a-e**). The samples were dissolved in CH_3Cl in room temperature. The light had a wavelength of 579 nm.

6.1.4   Mass spectroscopy (MS)

Accurate mass determination in positive and negative mode was performed on a "Synapt G2-S" Q-TOF instrument from Water TM. Samples were ionized by the use of ASAP probe (APCI) or ESI probe. No chromatographic separation was used previous to the mass analysis. Calculated exact mass and spectra processing was done by Waters TM Software Masslynx V4.1 SCN871.

6.2 *(S)*-3-Azido-1-phenylpropanol, *(S)*-2

A mixture of *(S)*-3-chloro-1-phenylpropanol (**1**) (0.95 g, 5.6 mmol), NaN_3 (1.11 g, 16.7 mmol, 3.0 equiv.), NaI (1.28 g, 8.4 mmol, 1.5 equiv.) in anhydrous DMF (55 mL) was heated to 80 °C for 24 h. The reaction mixture was partitioned between Et_2O (25 mL) and H_2O (25 mL), then washed with Et_2O (3 x 20 mL) and water (3 x 20 mL). The combined organic layer was washed with brine (20 mL), dried over anhydrous $MgSO_4$, filtered and concentrated *in vacuo*. This resulted in a colourless oil (**2**) (0.85 mg, 4.8 mmol, 86% yield). Rf = 0.15 (15% EtOAc/*n*-pentane); IR (neat) 3396 (br w), 2094 cm^{-1}; $[\alpha]_D^{20}$ = -38.4 (c 1.20, $CHCl_3$); ^{1}H NMR (400 MHz $CDCl_3$) δ 7.49-7.40 (m, 5H), 4.82-4.79 (dd, J= 7.86, 5.16, 1H), 3.55 (s, 1H), 3.50-3.33 (m, 2H), 2.09-1.92 (m, 2H); ^{13}C NMR (100 MHz, $CDCl_3$) δ 143.9, 128.7, 127.9, 125.9, 71.5, 48.2, 37.8.
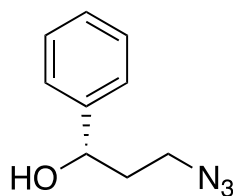

2

6.3 (5a*R*,5b*S*,7a*S*,8*S*,10a*S*,10b*R*,12a*R*)-8-hydroxy-2-((*S*)-3-hydroxy-3-phenylpropyl)-5a,7a-dimethylhexadecahydrocyclopenta[5,6]naphtho[2,1-*c*]azepin-3(2*H*)-one (4)

5α-Dihydrotestosterone (**3**) (1.47 g, 5.01 mmol, 1.0 equiv.) and the hydroxyalkyl azide (**2**) (0.90 g, 5.01 mmol, 1.0 equiv.) was dissolved in anhydrous DCM (0.4 M) and put under N_2-atmosphere at 0 °C. The stirring solution was added $BF_3 \cdot OEt_2$ (3.6 mL, 5.0 equiv.) dropwise. The reaction mixture was stirred at rt for 16 h. The solvent was concentrated in vacuo and the residual iminium was treated with an aqueous solution of KOH (15%, 100 mL) and THF (20 mL). The biphasic mixture was stirred vigorously at rt for 24 h. The reaction mixture was diluted with DCM (100 mL), and was washed with water (2 x 20 mL) and brine (20 mL). The organic layer was dried over anhydrous $MgSO_4$ and filtered, and the resulting solution was concentrated in vacuo. The crude product was purified by flash chromatography column using 20% EtOAc/*n*-pentane and 2% MeOH/DCM. This resulted in white solid (**4**) (1.77 g, 4.05 mmol, 81% yield). Rf = 0.27 (2% MeOH/DCM); IR (neat) 3365 (w br), 2932 (s), 2851 (m), 1625 (s), 1447 (m), 732 (s) cm^{-1}; $[\alpha]_D^{20}$ = +7.0 (c 1.00, $CHCl_3$); ^{1}H NMR (400 MHz $CDCl_3$) δ

7.36-7.35 (m, 4H), 7.28-7.26 (m, 1H), 4.73-4.62 (d, J = 9.18, 3.06, 1H), 4.10-4.02 (ddd, J = 14.69, 10.42, 4.57, 1H), 3.72-3.61 (m, 1H), 3.17-3.11 (dt, J = 4.61, 9.22, 14.32, 1 H), 2.62-2.53 (m, 2H), 2.39-2.33 (m, 1H), 2.10-2.01 (m, 1H), 1.94-1.73 (complex, 6H), 1.66-1.55 (complex, 2H), 1.50-1.19 (complex, 8H), 1.09-1.02 (m, 1H), 0.98-0.86 (complex, 5H), 0.74-0.68 (complex, 4H); ^{13}C NMR (100 MHz, CDCl$_3$) δ 178.9, 144.2, 128.3 (2C), 127.0, 125.5 (2C), 81.6, 69.9, 54.3, 52.3, 50.9, 49.5, 45.8, 42.8, 38.3, 37.9, 36.6, 36.0, 35.0, 32.0, 31.6, 30.4, 28.2, 23.3, 20.6, 12.1, 11.2.


4
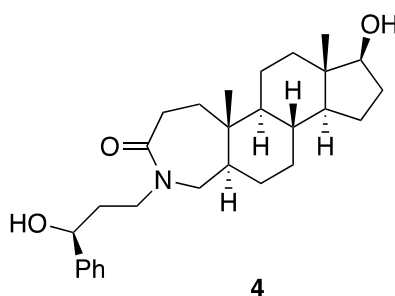
6.4   (5a*R*,5b*S*,7a*S*,10a*S*,10b*R*,12a*R*)-5a,7a-dimethyl-2-(3-oxo-3-phenylpropyl)   hexadecahydrocyclopenta[5,6]naphtho[2,1-*c*]azepine-3,8-dione (5)

PCC (1.90 g, 8.84 mmol, 6 equiv.) and celite was added a solution of steroid **4** (0.65 g, 1.47 mmol) in anhydrous DCM (75 mL) at 0 °C under N$_2$-atmosphere. The brown mixture was allowed to rt and stirred for 5.5 h. The reaction mixture was diluted with DCM and filtered over Celite. The resulting solution was concentrated *in vacuo*. The crude product was purified by flash chromatography column using 75% EtOAc/*n*-pentane. This resulted in a white solid (**5**) (0.43 g, 0.98 mmol, 67 % yield). R$_f$ = 0.28 (75% EtOAc/*n*-pentane); IR (neat) 2932 (m), 2856 (w), 1736 (s), 1643 (s), 731 (m) cm^{-1}. $[\alpha]_D^{20}$ = +62.1 (c 1.03, CHCl$_3$); ^{1}H NMR (400 MHz CDCl$_3$) δ 7.99-9.97 (d, 2H), 7.57-7.55 (m, 1H), 7.49-7.45 (m, 2H), 3.82-3.80 (dt, J= 13.37, 6.95, 1H), 3.73-3.65 (m, 2H), 3.29-3.24 (m, 2H), 2.82-2.79 (d, J= 15.59, 1H), 2.64-2.57 (t, J = 13.90, 1H), 2.47-2.40 (m, 1H), 2.34-2.29 (m, 1H), 2.11-2.01 (m, 1H), 1.95-1.77 (complex, 4H), 1.71-1.64 (m, 1H), 1.54-1.45 (complex, 3H), 1.38-1.18 (complex, 7H), 0.97-0.96 (complex, 4H), 0.89-0.84 (s, 3H), 0.71-0.65 (complex, 1H); ^{13}C NMR (100 MHz, CDCl$_3$) δ 220.8, 199.1, 175.5, 136.7, 133.4, 128.7 (2C), 128.2 (2C), 53.9, 52.9, 51.3, 48.9, 47.5, 45.3, 38.2, 37.7, 35.8, 35.7, 34.5, 32.3, 31.4, 30.6, 27.9, 21.7, 20.2, 13.8, 12.1.

5
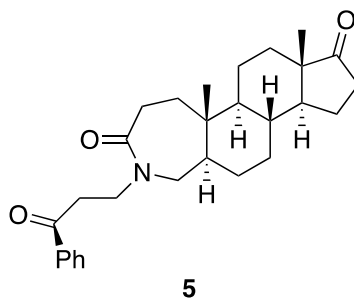
6.5 (5a*R*,5b*S*,7a*S*,10a*S*,10b*R*,12a*R*)-5a,7a-dimethylhexadecahydrocyclopenta[5,6]naphtho[2,1-*c*]azepine-3,8-dione (6)

A solution of steroid (**5**) (270.0 mg, 0.62 mmol) and sodium hydride (60% dispersion in mineral oil, 0.12 mg, 4.94 mmol, 4.8 equiv.) was dissolved in anhydrous THF (60 mL). The orange solution was refluxed at 65 °C for 2 h under N_2-atmosphere. The reaction was cooled to rt and quenched with a saturated solution of NH_4Cl (20 mL). The reaction mixture was diluted with DCM and was washed with a saturated solution of NH_4Cl (2 x 15 mL), water (15 mL) and brine (15 mL). The combined organic layer was dried over anhydrous $MgSO_4$ and filtered. The resulting solution was concentrated *in vacuo*. The crude product was purified by flash chromatography column using 75% EtOAc/*n*-pentane and 2% MeOH/DCM. This resulted in a white solid (**6**) (154.7 mg, 0.51 mmol, 82 % yield). R_f = 0.14 (4% MeOH/DCM); IR (neat) 3185 (w), 2932 (s), 1736 (s), 1682 (s), 1643 (m) cm^{-1}; $[\alpha]_D^{20}$ = +33.66 (c 1.00, CHCl$_3$); ^{1}H NMR (400 MHz CDCl$_3$) δ 6.8 (br s, 1H), 3.38-3.34 (m, 1H), 2.64-2.55 (m, 2H), 2.48-2.41 (m, 1H), 2.28-2.22 (m, 1H), 2.12-2.03 (m, 1H), 1.96-1.25 (complex, 18H), 1.03-0.79 (complex, 5H); ^{13}C NMR (100 MHz, CDCl$_3$) δ 220.9, 178.9, 53.9, 51.3, 49.5, 47.5, 44.3, 38.8, 35.8, 35.2, 34.6, 31.5, 31.4, 30.5, 27.4, 21.7, 20.3, 13.8, 12.1.

6
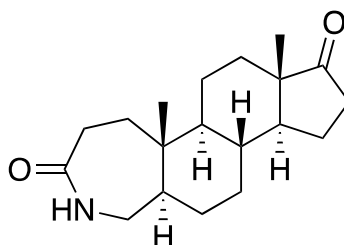
6.6 (5a*R*,5b*S*,7a*S*,10a*S*,10b*R*,12a*R*)-5a,7a-dimethyl-3-oxo-1,2,3,4,5,5a,5b,6,7,7a,10,10a,10b,11,12,12a-hexadecahydrocyclopenta[5,6]naphtho[2,1-*c*]azepin-8-yl trifluoromethanesulfonate (7)

The steroid (**6**) (117.8 mg, 0.38 mmol) and *N*-phenylbis(trifluoromethanesulfonimide) (207.4 g, 0.58 mmol, 1.5 equiv.) were dissolved in anhydrous THF (25 mL) and cooled to -78 °C. NaHMDS (1.36 mL, 1.0 M in THF, 1.36 mmol, 3.5 equiv.), was added dropwise at -78 °C, and the solution was stirred for 12.5 h under N_2-atmosphere. The reaction mixture was brought to rt and then quenched by addition of saturated aqueous NH_4Cl (5 mL). The mixture was extracted with DCM(4 x 10 mL). The combined organic layer was washed with water (10 mL) and brine (10 mL), dried over anhydrous $MgSO_4$ and filtered. The resulting solution was concentrated *in vacuo.* The crude product was purified by flash chromatography column using 90% EtOAc/*n*-pentane and 2% MeOH/DCM. This resulted in a white solid (**7**) (38.5 mg, 0.09 mmol, 22% yield). R_f = 0.18 (2% MeOH/DCM); IR (neat) 3183 (w), 3069 (w), 2919 (m), 1679 (s), 1421 (s), 1207 (s), 612 (m) cm^{-1}. $[\alpha]_D^{20}$ = -4.00 (c 1.00, CHCl$_3$); ^{1}H NMR (400 MHz CDCl$_3$) δ 6.61 (br s, 1H), 5.57 (dd, J =1.83, 4.24, 1H), 3.41-3.34 (m, 1H), 2.65-2.55 (m, 2H), 2.30-2.20 (m, 2H), 2.06-1.32 (complex, 12H), 0.95-0.89 (complex, 9H); ^{13}C NMR (100 MHz, CDCl$_3$) δ 178.6, 159.1, 120.2, 114.5, 54.1, 54.2, 49.8, 44.6, 44.4, 38.9, 35.0, 33.0, 32.7, 31.3, 30.5, 28.5, 27.4, 20.4, 15.2, 11.9; HRMS (EI, m/z): Detected 436.1775, calculated for C$_{20}$H$_{28}$F$_3$NO$_4$S [M + H]$^+$ 436.1769.
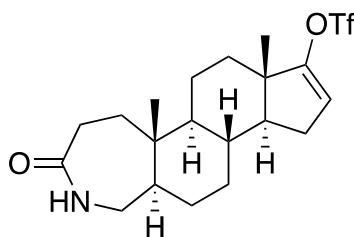

7

6.7 General procedure for the Suzuki cross-coupling (8a–e)

The steroid (**7**) (0.06 mmol), cesium carbonate (4 equiv.) and the boronic acid (2.1 equiv.) were put under N_2-atmosphere. Water and THF (2:5) were degassed by flushing with N_2 while under ultrasonication for 30 min before added to dry reagents. Pd(PPh$_3$)$_4$ (5% mol) was added and the reaction mixture was stirred at rt (18-20 h). The reaction mixture was poured into brine (15 mL) and extracted with EtOAc (4 x 10 mL). The combined organic extracts were dried over

anhydrous MgSO4 and filtered. The resulting solution was concentrated *in vacuo*. The crude product was purified by flash chromatography column using 90% EtOAc/*n*-pentane and gradient elution from 0-5% MeOH/DCM.
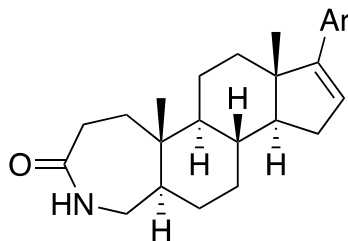
8

6.7.1 (5aR,5bS,7aS,10aS,10bR,12aR)-8-(isoquinolin-7-yl)-5a,7a-dimethyl-1,4,5,5a,5b,6,7,7a,10,10a,10b,11,12,12a-tetradecahydrocyclopenta[5,6]naphtho[2,1-c]azepin-3(2H)-one (8a)
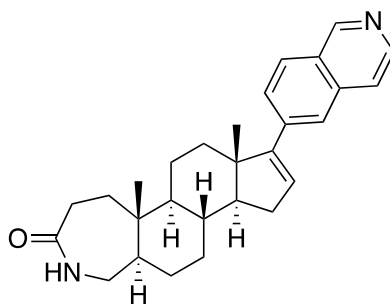
The compound was prepared following the general procedure described. This resulted in impure product as a brown solid (10.1 mg, 0.02 mmol, 44% yield). R_f = 0.38 (5% MeOH/DCM); IR (neat) 3184 (w), 2922 (s), 1681 (s), 1137 (s), 616 (w) cm^{-1}; ^{1}H NMR (400 MHz CDCl$_3$) δ 9.30 (s, 1H), 8.56-8.54 (d, 1H), 8.03-8.01 (d, 1H), 7.87-7.85 (d, 1H), 7.76-7.64 (m, 2H), 6.85 (2, 1H), 5.58-5.58 (dd, J = 3.09, 1.66, 1H), 3.42-3.35 (m, 1H), 2.66-2.57 (m, 2H), 2.36-2.21 (complex, 2H), 2.09-1.96 (complex, 1H), 1.91-1.86 (complex, 2H), 1.77-1.73 (complex, 2H), 1.67-1.63 (complex, 3H), 1.57-1.55 (complex, 2H), 1.49-1.42 (complex, 3H), 1.41-1.36 (complex, 2H), 1.33-1.27 (complex, 2H), 1.03-0.87 (complex, 6H); ^{13}C NMR (100 MHz, CDCl$_3$) δ 179.2, 159.1, 152.3, 142.6, 135.9, 130.6, 128.7, 127.8, 127.4, 126.5, 120.7, 114.5, 54.1, 49.6, 44.6, 44.4, 38.9, 34.9, 33.0, 32.69, 31.2, 30.5, 29.7, 28.5, 27.4, 20.4, 15.3, 12.0.
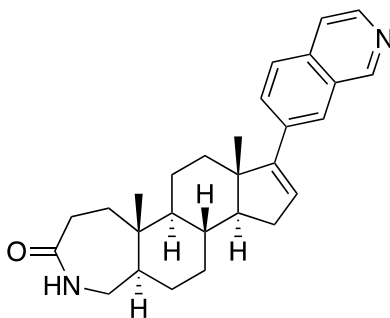
8a

6.7.2 (5aR,5bS,7aS,10aS,10bR,12aR)-8-(isoquinolin-6-yl)-5a,7a-dimethyl-1,4,5,5a,5b,6,7,7a,10,10a,10b,11,12,12a-tetradecahydrocyclopenta[5,6]naphtho[2,1-c]azepin-3(2H)-one (8b)

The compound was prepared following the general procedure described. This resulted in a light brown solid (2.1 mg, 0.01 mmol, 11% yield). R_f = 0.38 (5% MeOH/DCM); IR (neat) 3189 (w), 2924 (s), 1680 (s), 1138 (w), 800 (w) cm^{-1}; ^{1}H NMR (400 MHz CDCl$_3$) δ 9.21 (s, 1H), 8.51 (s, 1H), 7.91-7.89 (d, 1H), 7.77 (s, 1H), 7.68-7.65 (dd, J = 8.58, 1.46, 1H), 7.64-7.62 (d, 1H), 6.17-6.16 (dd, 2.99, 1.75, 1H), 6.07 (s, 1H), 3.46-3.40 (m, 1H), 2.68-2.56 (m, 2H), 2.34-2.28 (complex, 2H), 2.21-2.19 (complex, 1H), 2.12-2.07 (complex, 2H), 1.96-1.81 (complex, 2H), 1.71-1.63 (complex, 3H), 1.55-1.49 (complex, 2H), 1.42-1.35 (complex, 3H), 1.32-1.26 (complex, 2H), 1.12-0.94 (complex, 6H); ^{13}C NMR (100 MHz, CDCl$_3$) δ 179.2, 159.1, 152.3, 142.6, 135.9, 130.6, 128.7, 127.8, 127.4, 126.5, 120.7, 114.5, 54.1, 49.6, 44.6, 44.4, 38.9, 34.9, 33.0, 32.7. 31.2, 30.5, 29.7, 28.5, 27.4, 20.4, 15.3, 12.0.
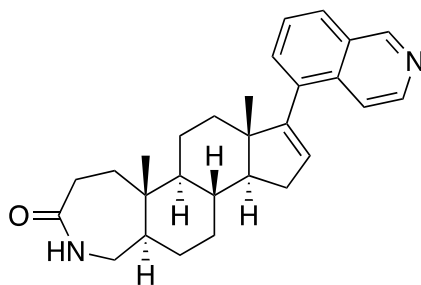

8b

6.7.3 (5aR,5bS,7aS,10aS,10bR,12aR)-8-(isoquinolin-5-yl)-5a,7a-dimethyl-1,4,5,5a,5b,6,7,7a,10,10a,10b,11,12,12a-tetradecahydrocyclopenta[5,6]naphtho[2,1-c]azepin-3(2H)-one (8c)

The compound was prepared following the general procedure described. This resulted in **8c** (6.1 mg, 0.02 mmol, 27% yield). R_f = 0.30 (5% MeOH/DCM); IR (neat) 3212 (br w), 2919 (s), 1668 (s), 1212 (m) cm^{-1}. $[\alpha]_D^{20}$ = +8.00 (c 1.00, CHCl$_3$); ^{1}H NMR (400 MHz CDCl$_3$) δ 9.25 (s, 1H), 8.51-8.50 (d, 1H), 7.91-7.85 (m, 2H), 7.60-7.49 (m, 2H), 6.11 (br s, 1H), 5.81-5.80 (dd, J = 3.02, 1.61 , 1H), 3.45-3.39 (m, 1H), 2.66-2.57 (complex, 2H), 2.41-2.39 (complex, 1H), 2.31-2.18 (complex, 2H), 2.10-1.88 (complex, 2H), 1.77-1.74 (complex, 2H), 1.70-1.66 (complex, 3H), 1.51-1.45 (complex, 2H), 1.41-1.32 (complex, 3H), 1.27-1.14 (complex, 2H), 0.98-0.97 (d, 6H); ^{13}C NMR (100 MHz, CDCl$_3$) δ 178.6, 152.6, 151.0, 142.9, 135.4, 134.9, 130.8, 129.5, 129.0, 126.6, 126.3, 119.2, 57.2, 54.2, 49.9, 49.4, 44.5, 38.9, 35.2, 35.1, 34.0, 32.2, 31.7, 31.3,

27.7, 21.0, 16.4, 12.1; HRMS (EI, m/z): Detected 415.2756, calculated for $C_{28}H_{34}N_2O$ [M + H]$^+$ 415.2749.

8c

6.7.4 (5aR,5bS,7aS,10aS,10bR,12aR)-5a,7a-dimethyl-8-(pyridin-3-yl)-1,4,5,5a,5b,6,7,7a,10,10a,10b,11,12,12a-tetradecahydrocyclopenta[5,6]naphtho[2,1-c]azepin-3(2H)-one (8d)

The compound was prepared following the general procedure described. This resulted in **8d** as a white solid (11.8 mg, 0.03 mmol, 59% yield). R_f = 0.34 (5% MeOH/DCM); IR (neat) 3185 (br w), 2916 (m), 1678 (s), 800 (m), 712 (m) cm^{-1}; $[\alpha]_D^{20}$ = +4.00 (c 1.00, CHCl$_3$); ^{1}H NMR (400 MHz CDCl$_3$) δ 8.82 (d, 1H), 8.48-8.47 (dd, J = 4.76, 1.53, 1H), 7.66-7.63 (dt, J = 8.00, 3.80, 1.79, 1H), 7.39-7.35 (complex, 1H), 7.25-7.21 (complex, 1H), 6.24 (br s, 1H), 5.99-5.98 (dd, J = 3.00, 1.65, 1H) , 3.45-3.38 (m, 1H), 3.10 (s, 1H), 2.67-2.56 (complex, 2H), 2.32-2.23 (complex, 2H), 2.08-2.02 (complex, 2H), 1.94-1.89 (complex, 1H), 1.82-1.72 (complex, 3H), 1.58-1.49 (complex, 2H), 1.42-1.38 (complex, 3H), 1.35-1.27 (complex, 2H), 1.07-0.91 (complex, 6H); ^{13}C NMR (100 MHz, CDCl$_3$) δ 178.4, 151.6, 147.9, 133.7, 132.9, 129.1, 123.0, 57.3, 54.02, 49.84, 47.3, 44.5, 38.9, 35.4, 35.1, 33.6, 31.7, 31.5, 31.3, 27.7. 21.0, 16.7, 12.1; HRMS (EI, m/z): Detected 365.2597, calculated for $C_{24}H_{32}N_2O$ [M + H]$^+$ 365.2593.
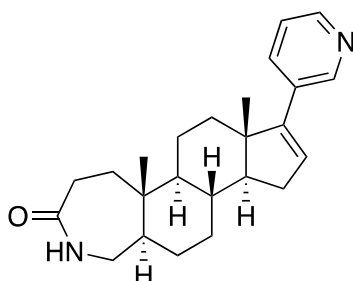
8d

6.7.5 **(5aR,5bS,7aS,10aS,10bR,12aR)-8-(2-chloropyridin-4-yl)-5a,7a-dimethyl 1,4,5,5a,5b,6,7,7a,10,10a,10b,11,12,12a- tetradecahydrocyclopenta[5,6]naphtho[2,1-c]azepin-3(2H)-one (8e)**

The compound was prepared following the general procedure described. This resulted in a light brown solid (16.0 mg, 0.04 mmol, 73% yield). Rf = 0.17 (5% MeOH/DCM); IR (neat) 3226 (br w), 2921 (s), 1737 (m), 1666 (s), 915 (w), 730 (m) cm^{-1}. $[\alpha]_D^{20}$ = +7.55 (c 1.06, CHCl$_3$); ^{1}H NMR (400 MHz CDCl$_3$) δ 8.18-8.13 (d, 1H), 7.70-7.47 (complex, 2H), 7.18-7.17 (dd, J = 5.34, 1.34, 1H), 6.50 (br s, 1H), 6.21-6.20 (dd, J = 3.06, 1.62, 1H), 3.42-3.36 (m, 2H), 2.65-2.56 (complex, 5H), 2.48-2.41 (dd, J= 19.08, 8.98, 2H), 2.30-2.24 (complex, 4H), 2.18-2.03 (complex, 5H), 1.94-1.17 (complex, 15H), 1.56 (complex, 6H), 1.37-1.28 (complex, 17H), 1.03-0.95 (complex, 9H), 0.87-0.81 (complex, 9H); ^{13}C NMR (100 MHz, CDCl$_3$) δ; HRMS (EI, m/z): Detected 399.2210, calculated for C$_{24}$H$_{31}$N$_2$OCl [M + H]$^+$ 399.2203.

8e
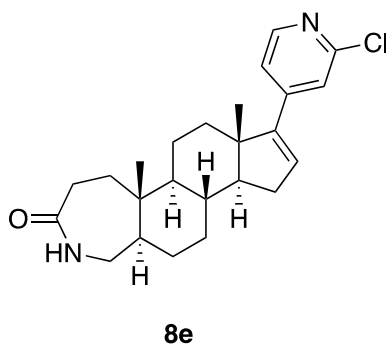
References

1.   Wang, H.; Naghavi, M.; Allen, C.; Barber, R. M.; Bhutta, Z. A.; Carter, A.; Casey, D. C.; Charlson, F. J.; Chen, A. Z.; Coates, M. M., Global, regional, and national life expectancy, all-cause mortality, and cause-specific mortality for 249 causes of death, 1980–2015: a systematic analysis for the Global Burden of Disease Study 2015. *The Lancet* **2016,** *388* (10053), 1459-1544.

2.   Yu, J.; Jiang, P. Y. Z.; Sun, H.; Zhang, X.; Jiang, Z.; Li, Y.; Song, Y., Advances in targeted therapy for acute myeloid leukemia. *Biomark. Res.* **2020,** *8* (1), 17.

3.   Carter, J. L.; Hege, K.; Yang, J.; Kalpage, H. A.; Su, Y.; Edwards, H.; Hüttemann, M.; Taub, J. W.; Ge, Y., Targeting multiple signaling pathways: the new approach to acute myeloid leukemia therapy. *Signal Transduct. Target. Ther.* **2020,** *5* (1), 288.

4.   Perl, A. E., The role of targeted therapy in the management of patients with AML. *Am. Soc. Hematol. Educ. Program.* **2017,** *2017* (1), 54-65.

5.   Daver, N.; Wei, A. H.; Pollyea, D. A.; Fathi, A. T.; Vyas, P.; DiNardo, C. D., New directions for emerging therapies in acute myeloid leukemia: the next chapter. *Blood Cancer J.* **2020,** *10* (10), 107.

6.   Solum, E.; Hansen, T. V.; Aesoy, R.; Herfindal, L., New CDK8 inhibitors as potential anti-leukemic agents–Design, synthesis and biological evaluation. *Bioorg. Med. Chem.* **2020,** *28* (10), 115461.

7.   Patrick, G. L., *An introduction to medicinal chemistry*. Oxford university press: 2013.

8.   Xu, W.; Ji, J.-Y., Dysregulation of CDK8 and Cyclin C in tumorigenesis. *J. Genet. Genom* **2011,** *38* (10), 439-452.

9.   Xu, W.; Amire-Brahimi, B.; Xie, X.-J.; Huang, L.; Ji, J.-Y., All-atomic molecular dynamic studies of human CDK8: insight into the A-loop, point mutations and binding with its partner CycC. *Comput. Biol. Chem.* **2014,** *51*, 1-11.

10.   Martin, R.; Buchwald, S. L., Palladium-Catalyzed Suzuki−Miyaura Cross-Coupling Reactions Employing Dialkylbiaryl Phosphine Ligands. *Acc. Chem. Res.* **2008,** *41* (11), 1461-1473.

11.   Roninson, I. B.; Győrffy, B.; Mack, Z. T.; Shtil, A. A.; Shtutman, M. S.; Chen, M.; Broude, E. V., Identifying Cancers Impacted by CDK8/19. *Cells* **2019,** *8* (8), 821.

12.   Bergeron, P.; Koehler, M. F.; Blackwood, E. M.; Bowman, K.; Clark, K.; Firestein, R.; Kiefer, J. R.; Maskos, K.; McCleland, M. L.; Orren, L., Design and development of a series of potent and selective type II inhibitors of CDK8. *ACS Med. Chem. Lett.* **2016,** *7* (6), 595-600.

13.   Villarino, A. V.; Kanno, Y.; Ferdinand, J. R.; O'Shea, J. J., Mechanisms of Jak/STAT signaling in immunity and disease. *J. Immunol.* **2015,** *194* (1), 21-27.

14.   Stark, George R.; Darnell, James E., The JAK-STAT Pathway at Twenty. *Immunity* **2012,** *36* (4), 503-514.

15.   Lycke, E.; Norrby, E., Textbook of medical virology. **2014**, 369.

16.   Grafone, T.; Palmisano, M.; Nicci, C.; Storti, S., An overview on the role of FLT3-tyrosine kinase receptor in acute myeloid leukemia: Biology and treatment. *Oncol. Rev.* **2012,** *6*, 8.

17.   Soos, J. M.; Szente, B. E., CHAPTER 23 - Type I interferons: [IFNα, β, δ, K, ω, ι, IL-28A (IFNλ2) IL-28B (IFNλ3) and IL-29 (IFNλl)]. In *The Cytokine Handbook (Fourth Edition)*, Thomson, A. W.; Lotze, M. T., Eds. Academic Press: London, 2003; pp 549-566b.

18.   Bancerek, J.; Poss, Z. C.; Steinparzer, I.; Sedlyarov, V.; Pfaffenwimmer, T.; Mikulic, I.; Dölken, L.; Strobl, B.; Müller, M.; Taatjes, D. J.; Kovarik, P., CDK8 kinase phosphorylates transcription factor STAT1 to selectively regulate the interferon response. *Immunity* **2013,** *38* (2), 250-262.

19.	Li, J.; Liang, J.; Wang, L.; Broude, E.; Roninson, I.; Chen, M., Abstract 89: Role of CDK8 and CDK19 in STAT1 phosphorylation at serine 727. *Cancer Res.* **2020,** *80* (16 Supplement), 89.

20.	Levy, D. E.; Darnell, J. E., STATs: transcriptional control and biological impact. *Nat. Rev. Mol. Cell Biol.* **2002,** *3* (9), 651-662.

21.	Rzymski, T.; Mikula, M.; Żyłkiewicz, E.; Dreas, A.; Wiklik, K.; Gołas, A.; Wójcik, K.; Masiejczyk, M.; Wróbel, A.; Dolata, I.; Kitlińska, A.; Statkiewicz, M.; Kuklinska, U.; Goryca, K.; Sapała, Ł.; Grochowska, A.; Cabaj, A.; Szajewska-Skuta, M.; Gabor-Worwa, E.; Kucwaj, K.; Białas, A.; Radzimierski, A.; Combik, M.; Woyciechowski, J.; Mikulski, M.; Windak, R.; Ostrowski, J.; Brzózka, K., SEL120-34A is a novel CDK8 inhibitor active in AML cells with high levels of serine phosphorylation of STAT1 and STAT5 transactivation domains. *Oncotarget* **2017,** *8* (20), 33779-33795.

22.	Pelish, H. E.; Liau, B. B.; Nitulescu, II; Tangpeerachaikul, A.; Poss, Z. C.; Da Silva, D. H.; Caruso, B. T.; Arefolov, A.; Fadeyi, O.; Christie, A. L.; Du, K.; Banka, D.; Schneider, E. V.; Jestel, A.; Zou, G.; Si, C.; Ebmeier, C. C.; Bronson, R. T.; Krivtsov, A. V.; Myers, A. G.; Kohl, N. E.; Kung, A. L.; Armstrong, S. A.; Lemieux, M. E.; Taatjes, D. J.; Shair, M. D., Mediator kinase inhibition further activates super-enhancer-associated genes in AML. *Nature* **2015,** *526* (7572), 273-276.

23.	Nitulescu, I. I.; Meyer, S. C.; Wen, Q. J.; Crispino, J. D.; Lemieux, M. E.; Levine, R. L.; Pelish, H. E.; Shair, M. D., Mediator Kinase Phosphorylation of STAT1 S727 Promotes Growth of Neoplasms With JAK-STAT Activation. *EBioMedicine* **2017,** *26*, 112-125.

24.	Hatcher, J. M.; Wang, E. S.; Johannessen, L.; Kwiatkowski, N.; Sim, T.; Gray, N. S., Development of highly potent and selective steroidal inhibitors and degraders of CDK8. *ACS Med. Chem. Lett.* **2018,** *9* (6), 540-545.

25.	Dale, T.; Clarke, P. A.; Esdar, C.; Waalboer, D.; Adeniji-Popoola, O.; Ortiz-Ruiz, M.-J.; Mallinger, A.; Samant, R. S.; Czodrowski, P.; Musil, D.; Schwarz, D.; Schneider, K.; Stubbs, M.; Ewan, K.; Fraser, E.; TePoele, R.; Court, W.; Box, G.; Valenti, M.; de Haven Brandon, A.; Gowan, S.; Rohdich, F.; Raynaud, F.; Schneider, R.; Poeschke, O.; Blaukat, A.; Workman, P.; Schiemann, K.; Eccles, S. A.; Wienke, D.; Blagg, J., A selective chemical probe for exploring the role of CDK8 and CDK19 in human disease. *Nat. Chem. Biol.* **2015,** *11* (12), 973-980.

26.	Aoki, S.; Watanabe, Y.; Sanagawa, M.; Setiawan, A.; Kotoku, N.; Kobayashi, M., Cortistatins A, B, C, and D, Anti-angiogenic Steroidal Alkaloids, from the Marine Sponge Corticium simplex. *J. Am. Chem. Soc.* **2006,** *128* (10), 3148-3149.

27.	Gupta, G.; Chaitanya, R.; Golla, M.; Karnati, R., Allethrin toxicity on human corneal epithelial cells involves mitochondrial pathway mediated apoptosis. *Toxicol. In Vitro* **2013,** *27* (8), 2242-2248.

28.	J Solum, E.; Liekens, S.; Hansen, T. V., Synthesis and Biological Evaluation of Analogs of Didehydroepiandrosterone as Potential New Anticancer Agents. *Molecules* **2020,** *25* (13), 3052.

29.	Charaschanya, M.; Aubé, J., Reagent-controlled regiodivergent ring expansions of steroids. *Nat. Commun.* **2018,** *9* (1), 1-8.

30.	Doorenbos, N.; Wu, M., Steroids. III. Synthesis of Some 3-Aza-A-homocholestanes by the Beckmann and Schmidt Rearrangements in Polyphosphoric Acid. *J. Org. Chem.* **1961,** *26* (7), 2548-2549.

31.	Huang, Y.; Cui, J.; Chen, S.; Gan, C.; Zhou, A., Synthesis and antiproliferative activity of some steroidal lactams. *Steroids* **2011,** *76* (12), 1346-1350.

32.	Carey, F. A.; Sundberg, R. J., *Advanced organic chemistry: part B: reaction and synthesis*. Springer Science & Business Media: 2007; p 1321.

33.   Reist, E.; Spencer, R.; Baker, B.; Goodman, L., Potential Anticancer Agents. 83. Sodium Szide in Dimethylformamide for the Preparation of Amino-Sugars. SOC Chemical Industry 14 Belgrave Square , London SW1X 8PS, England 1962; pp 1794-1795.

34.   Janice Gorzynski Smith, D., *Organic Chemistry*. McGraw-Hill Education: 2013.

35.   Ouellette, R.; Rawn, J. D., 10-nucleophilic substitution and elimination reactions. Elsevier Boston: 2014; pp 333-356.

36.   Jug, U.; Pregeljc, D.; Mavri, J.; Vianello, R.; Stare, J., Elementary SN2 reaction revisited. Effects of solvent and alkyl chain length on kinetics of halogen exchange in haloalkanes elucidated by Empirical Valence Bond simulation. *Comput. Theor. Chem.* **2017,** *1116*, 96-101.

37.   Solomons, G.; Fryhle, C.; Snyder, S., *Organic chemistry - International Student Version*. 11th ed.; John Wiley & Sons Singapore Pte. Ltd: Asia, 2014; p 1208.

38.   Ouellette, R. J.; Rawn, J. D., 9 - Haloalkanes and alcohols Nucleophilic Substitution and Elimination Reactions. In *Organic Chemistry (Second Edition)*, Ouellette, R. J.; Rawn, J. D., Eds. Academic Press: 2018; pp 255-298.

39.   Wolff, H., The S chmidt Reaction. *Org. React.* **2004,** *3*, 307-336.

40.   Gracias, V.; Milligan, G. L.; Aube, J., Efficient Nitrogen Ring-Expansion Process Facilitated by in Situ Hemiketal Formation. An Asymmetric Schmidt Reaction. *J. Am. Chem. Soc.* **1995,** *117* (30), 8047-8048.

41.   Wrobleski, A.; Coombs, T. C.; Huh, C. W.; Li, S. W.; Aubé, J., The Schmidt reaction. *Org. React.* **2004,** *78*, 1-320.

42.   Aube, J.; Milligan, G. L., Intramolecular Schmidt reaction of alkyl azides. *J. Am. Chem. Soc.* **1991,** *113* (23), 8965-8966.

43.   Smith, B. T.; Gracias, V.; Aubé, J., Regiochemical studies of the ring expansion reactions of hydroxy azides with cyclic ketones. *J. Org. Chem.* **2000,** *65* (12), 3771-3774.

44.   Katz, C. E.; Aubé, J., Unusual Tethering Effects in the Schmidt Reaction of Hydroxyalkyl Azides with Ketones: Cation−π and Steric Stabilization of a Pseudoaxial Phenyl Group. *J. Am. Chem. Soc.* **2003,** *125* (46), 13948-13949.

45.   Hewlett, N. D.; Aubé, J.; Radkiewicz-Poutsma, J. L., Ab initio approach to understanding the stereoselectivity of reactions between hydroxyalkyl azides and ketones. *J. Org. Chem.* **2004,** *69* (10), 3439-3446.

46.   Sahasrabudhe, K.; Gracias, V.; Furness, K.; Smith, B. T.; Katz, C. E.; Reddy, D. S.; Aubé, J., Asymmetric Schmidt reaction of hydroxyalkyl azides with ketones. *J. Am. Chem. Soc.* **2003,** *125* (26), 7914-7922.

47.   Hunsen, M., Pyridinium chlorochromate catalyzed oxidation of alcohols to aldehydes and ketones with periodic acid. *Tetrahedron Lett.* **2005,** *46* (10), 1651-1653.

48.   Tojo, G.; Fernández, M., Oxidation of primary alcohols to carboxylic acids. *A Guide to Current Common Practice* **2007**, 132.

49.   Cranwell, P. B.; Harwood, L. M.; Moody, C. J., *Experimental organic chemistry*. John Wiley & Sons: 2017; p 671.

50.   Ley, S. V.; Madin, A., 2.7 - Oxidation Adjacent to Oxygen of Alcohols by Chromium Reagents. In *Comprehensive Organic Synthesis*, Trost, B. M.; Fleming, I., Eds. Pergamon: Oxford, 1991; pp 251-289.

51.   Corey, E. J.; Suggs, J. W., Pyridinium chlorochromate. An efficient reagent for oxidation of primary and secondary alcohols to carbonyl compounds. *Tetrahedron Lett.* **1975,** *16* (31), 2647-2650.

52.   Reddy, H.; Duffy, A.; Holtzman, N. G.; Emadi, A., The role of β-elimination for the clinical activity of hypomethylating agents and cyclophosphamide analogues. *Am. J. Cancer ther. Pharmacol.* **2016,** *3* (1), 1-8.

53. Ribelin, T. P.; Aubé, J., Synthesis of enantiomerically enriched (R)-5-tert-butylazepan-2-one using a hydroxyalkyl azide mediated ring-expansion reaction. *Nat. Protoc.* **2008,** *3* (1), 137-143.

54. Dhakal, B.; Bohé, L.; Crich, D., Trifluoromethanesulfonate Anion as Nucleophile in Organic Chemistry. *J. Org. Chem.* **2017,** *82* (18), 9263-9269.

55. Fraser, R. R.; Mansour, T. S., Acidity measurements with lithiated amines: steric reduction and electronic enhancement of acidity. *J. Org. Chem.* **1984,** *49* (18), 3442-3443.

56. Ojeda-Amador, A. I.; Martínez-Martínez, A. J.; Robertson, G. M.; Robertson, S. D.; Kennedy, A. R.; O'Hara, C. T., Exploring the solid state and solution structural chemistry of the utility amide potassium hexamethyldisilazide (KHMDS). *Dalton Trans.* **2017,** *46* (19), 6392-6403.

57. Javorskis, T.; Karpavičienė, I.; Jurys, A.; Snarskis, G.; Bukšnaitienė, R.; Orentas, E., An Enolate-Structure-Enabled Anionic Cascade Cyclization Reaction: Easy Access to Complex Scaffolds with Contiguous Six-, Five-, and Four-Membered Rings. *Angew. Chem.* **2020,** *132* (45), 20295-20303.

58. Nan, Z.; Zhang, S., *Theory and Problems for Chemistry Olympiad: Challenging Concepts in Chemistry.* World Scientific: 2019; p 450.

59. Blakemore, D., *Suzuki–Miyaura Coupling.* The Royal Society of Chemistry: 2015; Vol. 1.

60. Jójárt, R.; Ali, H.; Horváth, G.; Kele, Z.; Zupkó, I.; Mernyák, E., Pd-catalyzed Suzuki–Miyaura couplings and evaluation of 13α-estrone derivatives as potential anticancer agents. *Steroids* **2020,** *164*, 108731.

61. Sun, B.; Ning, L.; Zeng, H. C., Confirmation of Suzuki–Miyaura cross-coupling reaction mechanism through synthetic architecture of nanocatalysts. *J. Am. Chem. Soc.* **2020,** *142* (32), 13823-13832.

62. Miyaura, N., Cross-coupling reaction of organoboron compounds via base-assisted transmetalation to palladium (II) complexes. *J. Organomet. Chem.* **2002,** *653* (1-2), 54-57.

63. García-Melchor, M.; Braga, A. A. C.; Lledós, A.; Ujaque, G.; Maseras, F., Computational Perspective on Pd-Catalyzed C–C Cross-Coupling Reaction Mechanisms. *Acc. Chem. Res* **2013,** *46* (11), 2626-2634.

64. Bajo, S.; Laidlaw, G.; Kennedy, A. R.; Sproules, S.; Nelson, D. J., Oxidative Addition of Aryl Electrophiles to a Prototypical Nickel(0) Complex: Mechanism and Structure/Reactivity Relationships. *Organometallics* **2017,** *36* (8), 1662-1672.

65. Kotha, S.; Lahiri, K.; Dhurke, K., Recent applications of the Suzuki–Miyaura cross-coupling reaction in organic synthesis. *Tetrahedron* **2002,** *58*, 9633-9695.

66. Molloy, J. J.; Seath, C. P.; West, M. J.; McLaughlin, C.; Fazakerley, N. J.; Kennedy, A. R.; Nelson, D. J.; Watson, A. J., Interrogating Pd (II) anion metathesis using a bifunctional chemical probe: A transmetalation switch. *J. Am. Chem. Soc.* **2018,** *140* (1), 126-130.

67. Dziedzic, R. M.; Spokoyny, A. M., Metal-catalyzed cross-coupling chemistry with polyhedral boranes. *Chem. Commun. (Cambridge, England)* **2019,** *55* (4), 430-442.

68. Wolf, W. J.; Winston, M. S.; Toste, F. D., Exceptionally fast carbon-carbon bond reductive elimination from gold(III). *Nat. Chem.* **2014,** *6* (2), 159-164.

69. Lima, C. F.; Rodrigues, A. S.; Silva, V. L.; Silva, A. M.; Santos, L. M., Role of the Base and Control of Selectivity in the Suzuki–Miyaura Cross-Coupling Reaction. *Chem. Cat. Chem.* **2014,** *6* (5), 1291-1302.

70. Blakemore, D., Chapter 1 Suzuki–Miyaura Coupling. In *Synthetic Methods in Drug Discovery: Volume 1*, The Royal Society of Chemistry: 2016; Vol. 1, pp 1-69.

71. Hall, D. G., *Structure, properties, and preparation of boronic acid derivatives. Overview of their reactions and applications.* 2005; Vol. 1, p 133.

72.   Liu, C.; Ni, Q.; Hu, P.; Qiu, J., Oxygen-promoted PdCl2-catalyzed ligand-free Suzuki reaction in aqueous media. *Org. Biomol. Chem.* **2011,** *9* (4), 1054-1060.

73.   Leadbeater, N. E.; Marco, M., Ligand-Free Palladium Catalysis of the Suzuki Reaction in Water Using Microwave Heating. *Org. Lett.* **2002,** *4* (17), 2973-2976.

74.   Goodson, F. E.; Wallow, T. I.; Novak, B. M., Mechanistic studies on the Aryl− Aryl interchange reaction of ArPdL2I (L= triarylphosphine) complexes. *J. Am. Chem. Soc.* **1997,** *119* (51), 12441-12453.

75.   Chu, D. W., Bing; Ye, Tao Preparation of steroid derivatives as CYP17 inhibitors for the treatment of cancer. 2011.

76.   Fulmer, G. R.; Miller, A. J.; Sherden, N. H.; Gottlieb, H. E.; Nudelman, A.; Stoltz, B. M.; Bercaw, J. E.; Goldberg, K. I., NMR chemical shifts of trace impurities: common laboratory solvents, organics, and gases in deuterated solvents relevant to the organometallic chemist. *Organometallics* **2010,** *29* (9), 2176-2179.

77.   Byrne, P. A.; Gilheany, D. G., The modern interpretation of the Wittig reaction mechanism. *Chem. Soc. Rev.* **2013,** *42* (16), 6670-6696.

78.   Heck, R. F., Palladium-catalyzed vinylation of organic halides. *Org. React.* **2004,** *27*, 345-390.

79.   Gottlieb, H. E.; Kotlyar, V.; Nudelman, A., NMR chemical shifts of common laboratory solvents as trace impurities. *J. Org. Chem.* **1997,** *62* (21), 7512-7515.

Appendix

A   Spectroscopic data for compound 1
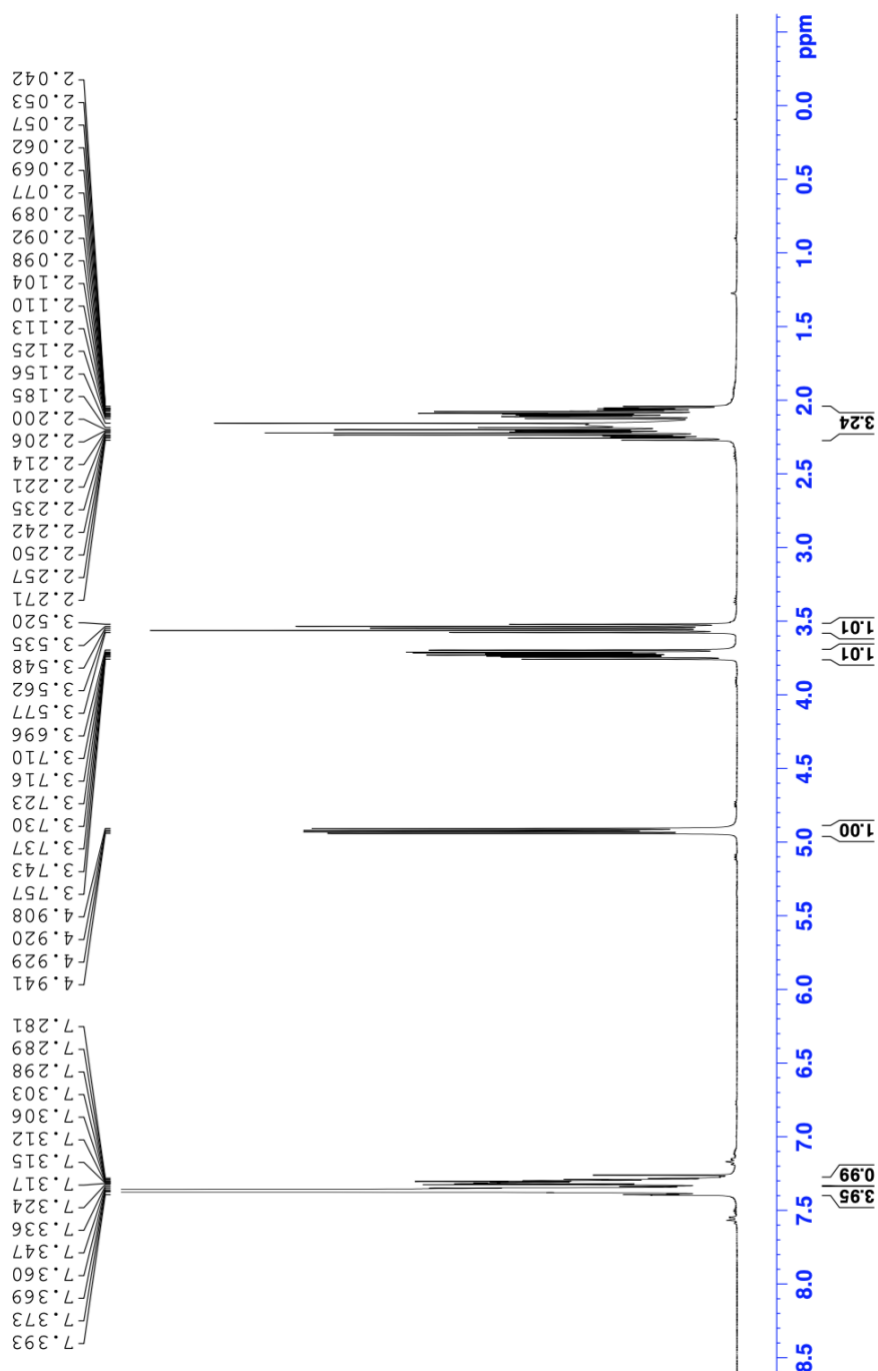
Supplementary Figure 1: ¹H NMR spectrum in CDCl₃, 400 MHz of *(S)*-3-chloro-1-phenylpropanol (**1**).
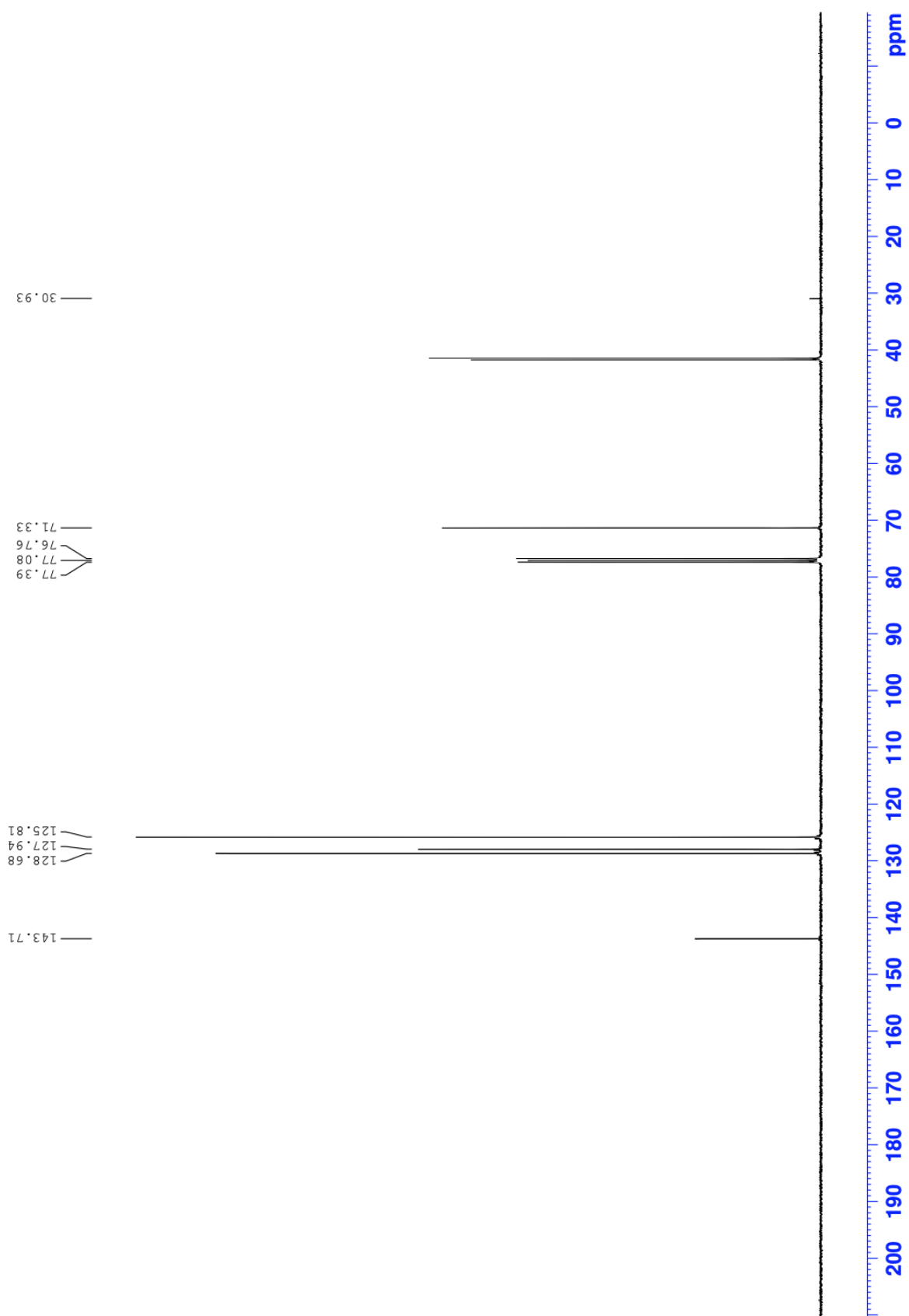
Supplementary Figure 2: ^{13}C NMR spectrum in CDCl$_3$, 100 MHz of **1**.

Peaks labeled: 30.93, 71.33, 76.76, 77.08, 77.39, 125.81, 127.94, 128.68, 143.71
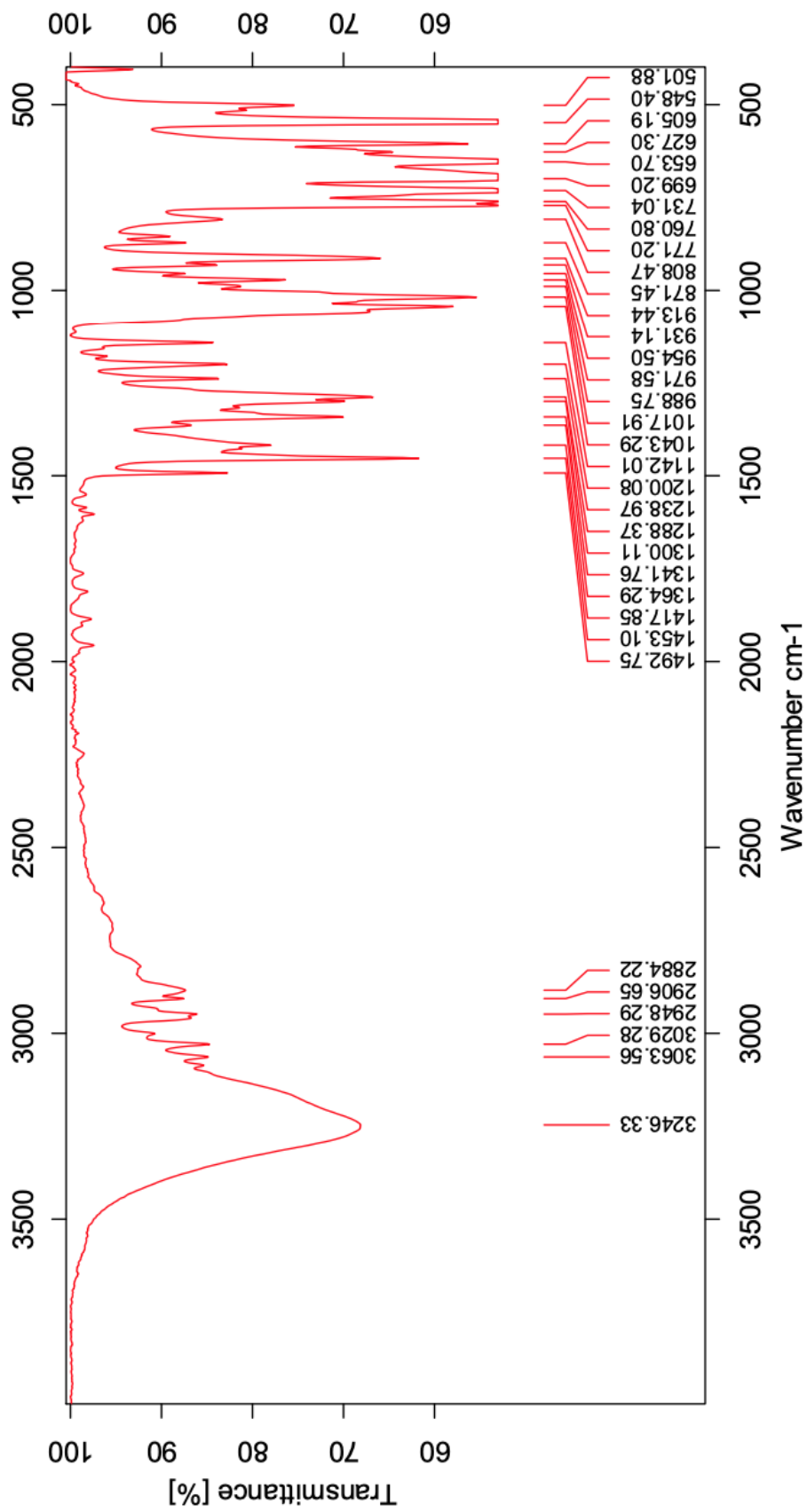
Supplementary Figure 3: IR spectrum of **1**.

B   Spectroscopic data for compound 2
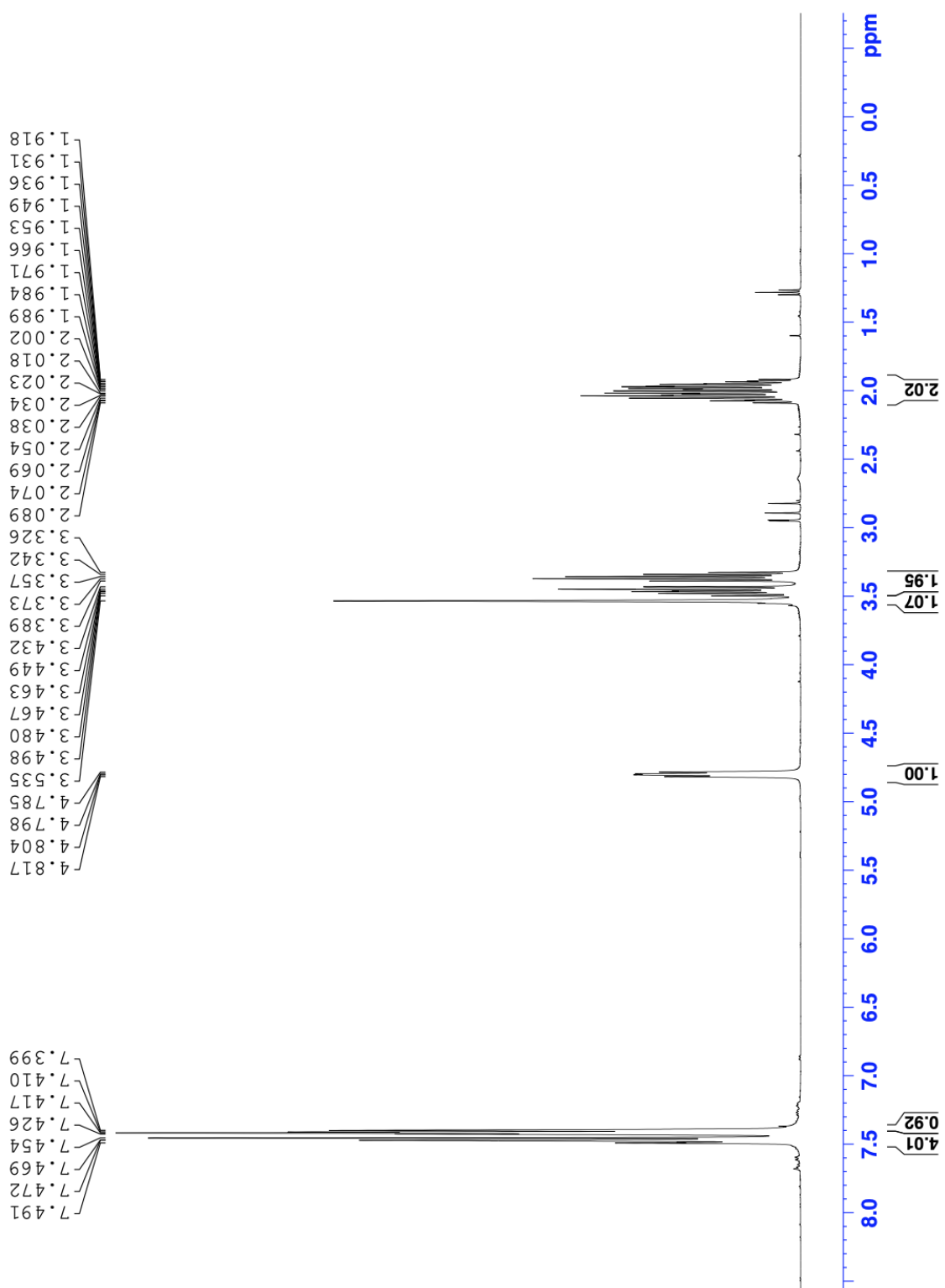
Supplementary Figure 4: ^{1}H NMR spectrum in CDCl$_3$, 400 MHz of *(S)*-3-azido-1-phenylpropanol (**2**).
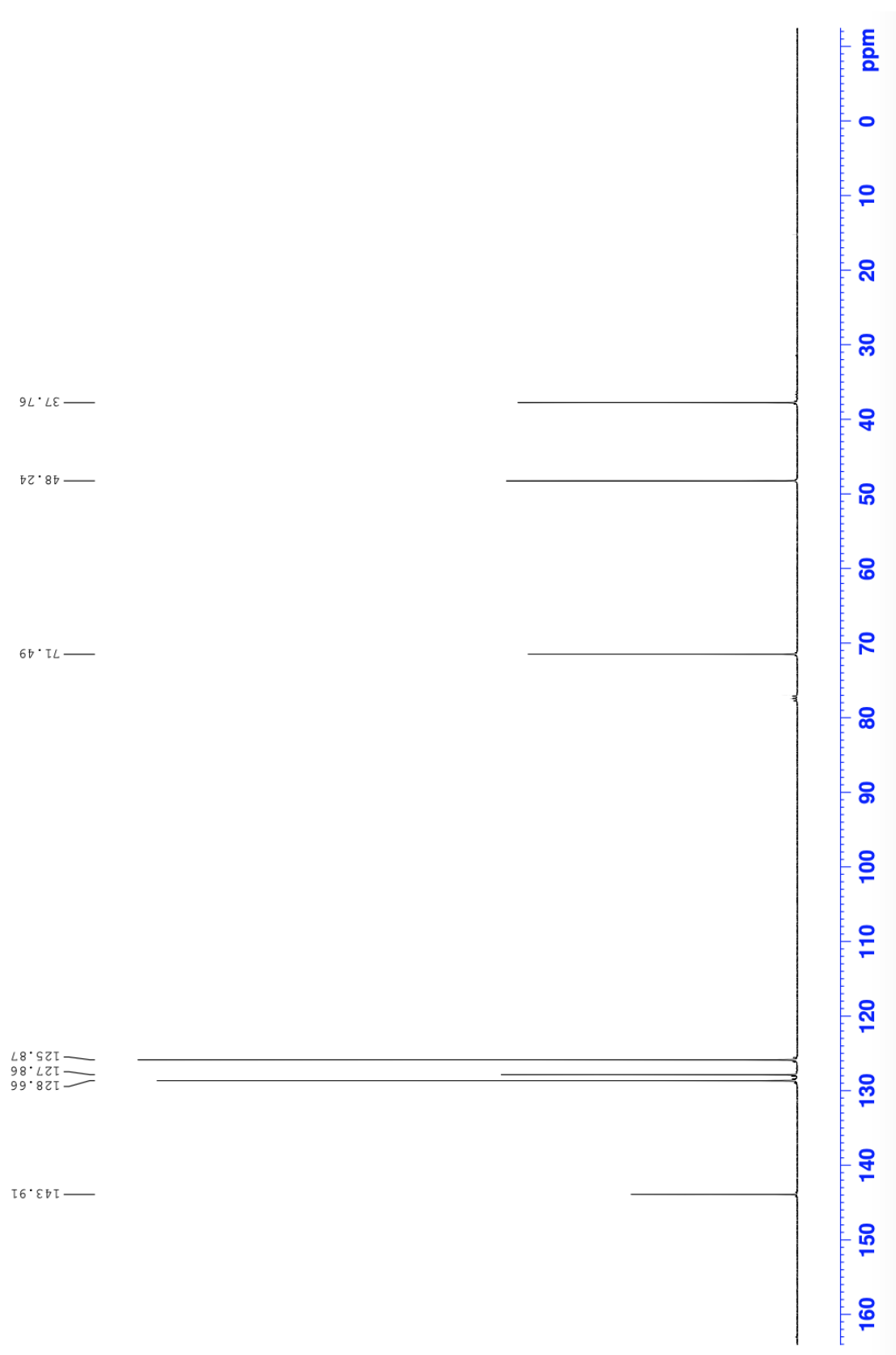
Supplementary Figure 5: ^{13}C NMR spectrum in CDCl$_3$, 100 MHz of **2**.
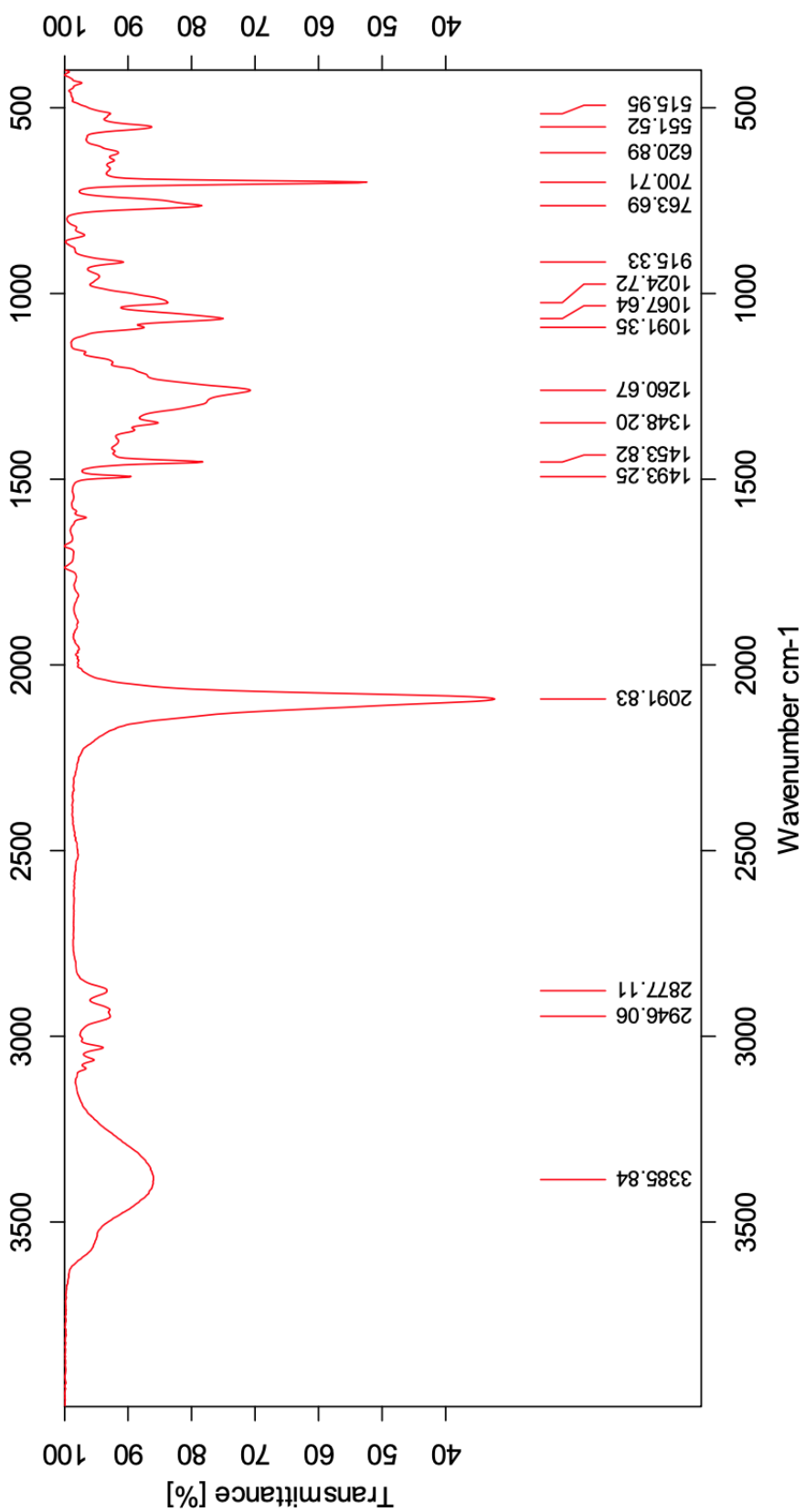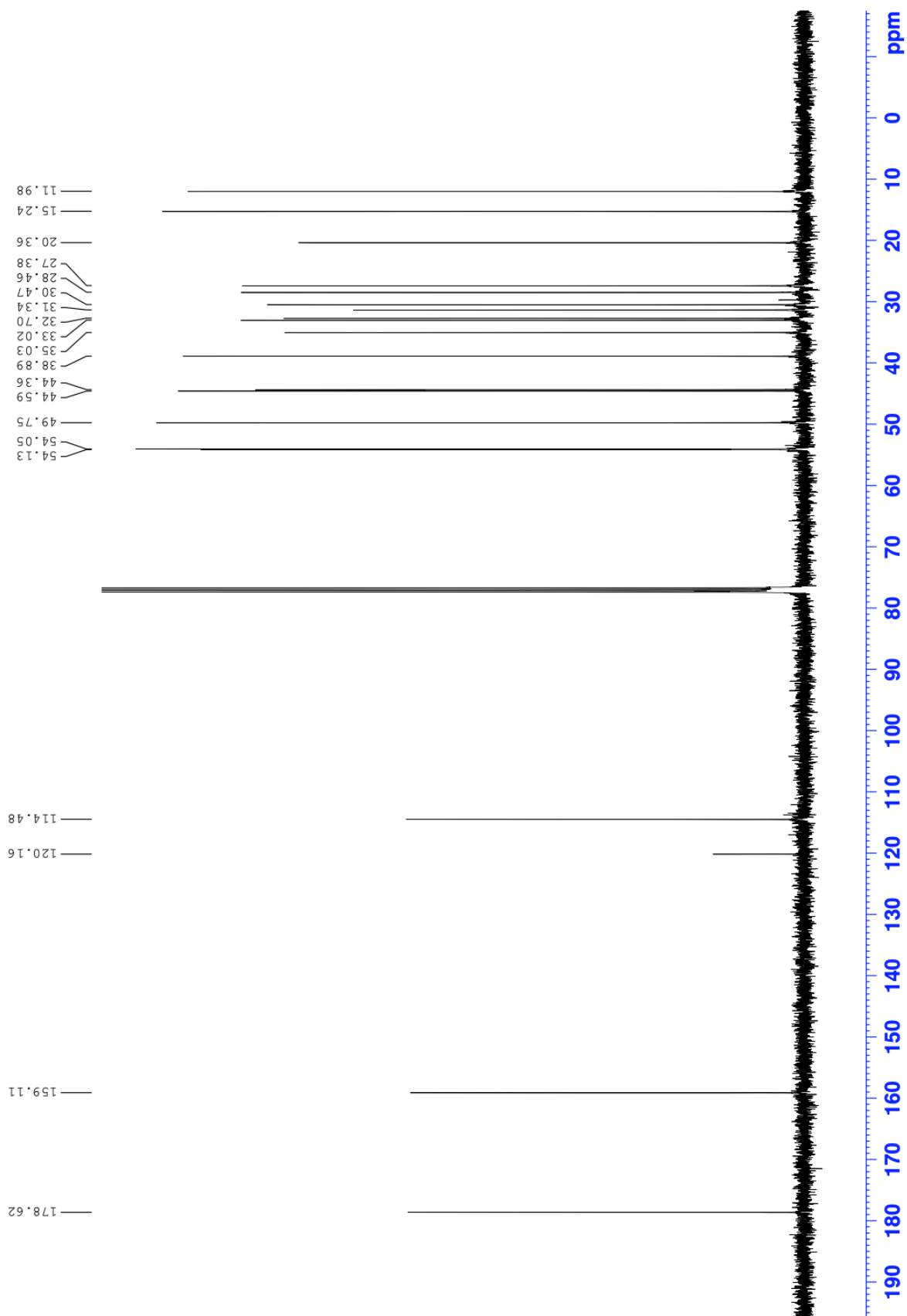
Supplementary Figure 6: IR spectrum of **2**.

C   Spectroscopic data for compound 3
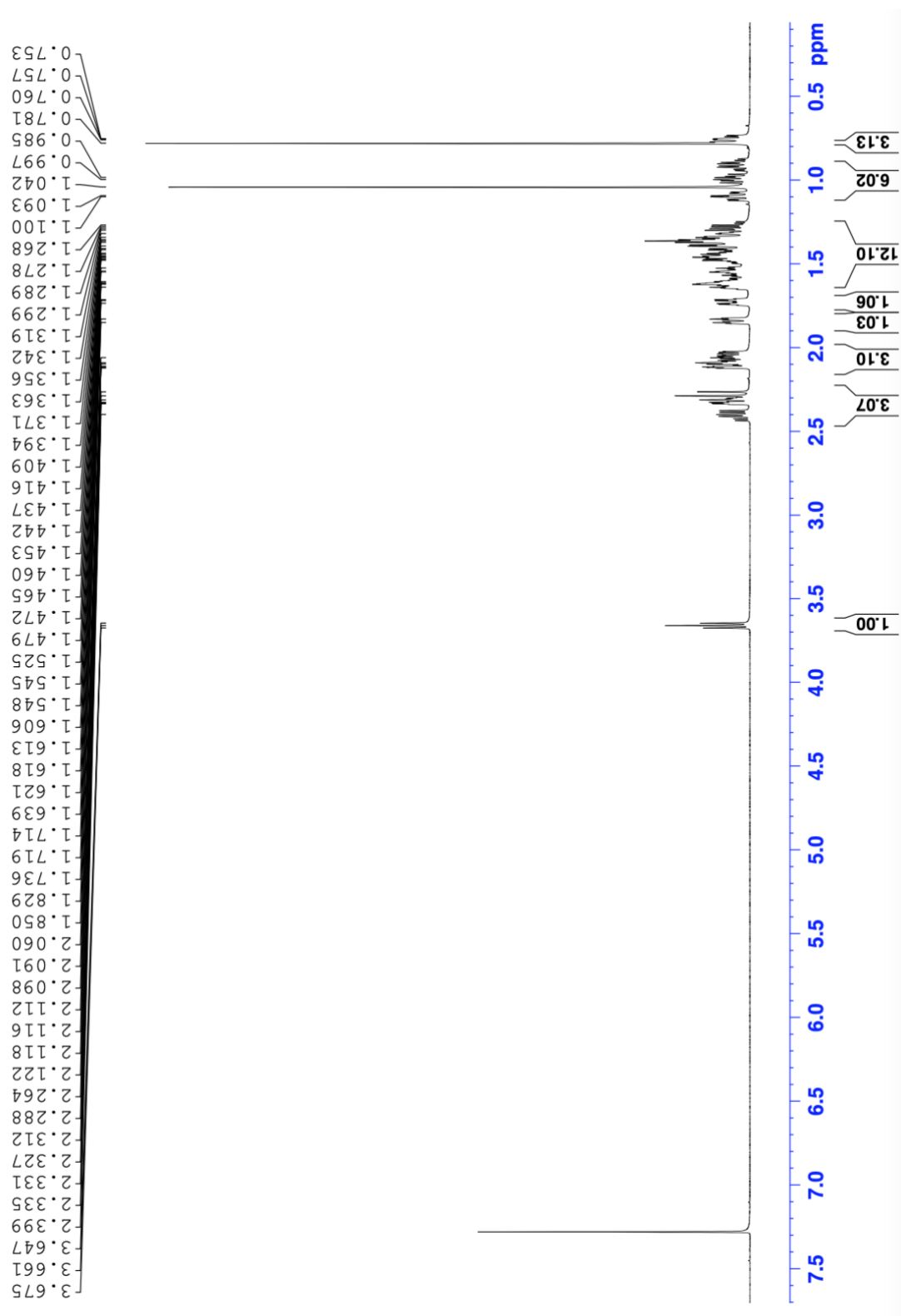
Supplementary Figure 7: ^{1}H NMR spectrum in CDCl$_3$, 400 MHz of 5α-dihydrotestosterone (**3**).
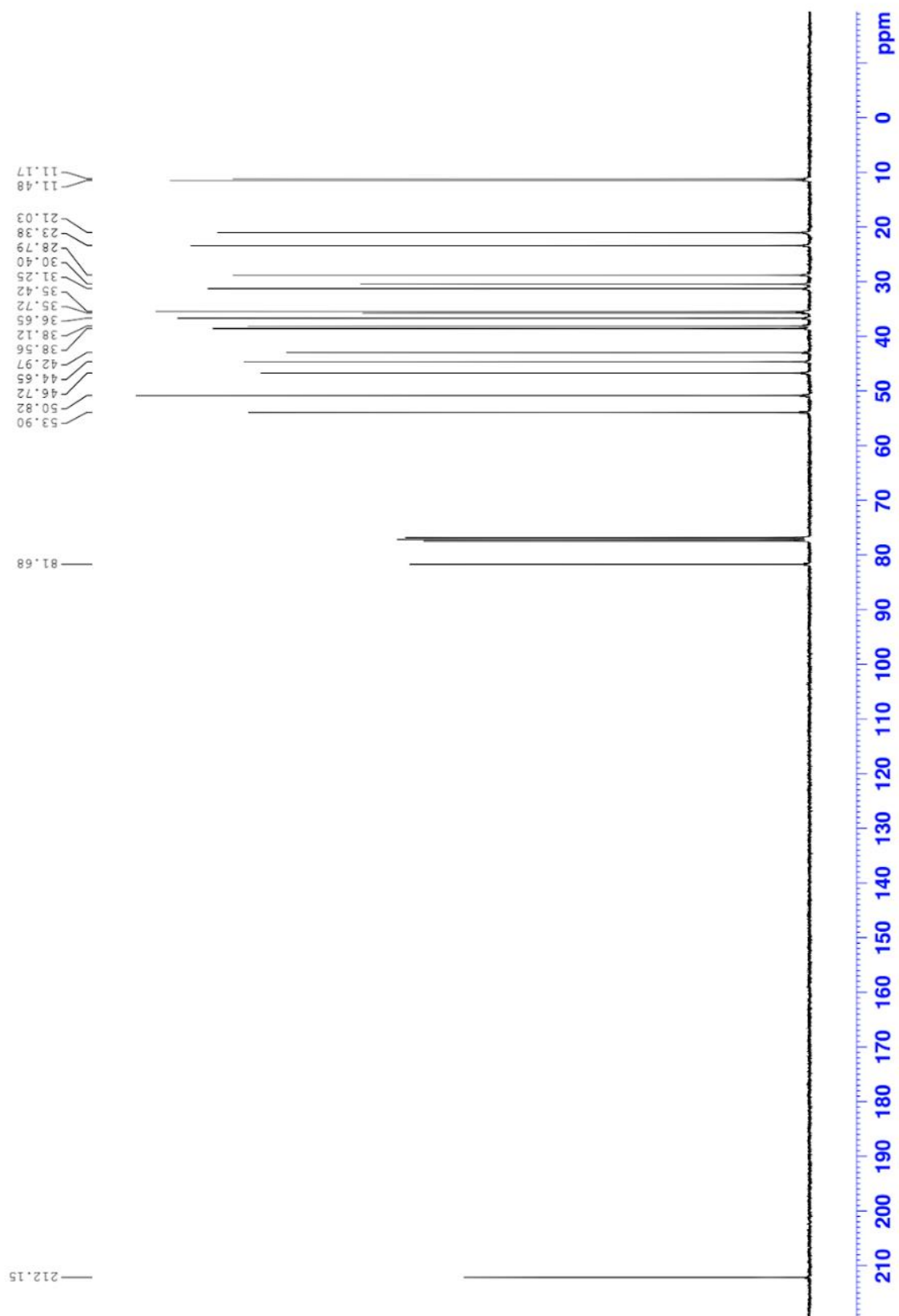
Supplementary Figure 8: ^{13}C NMR spectrum in CDCl$_3$, 100 MHz of **3**.
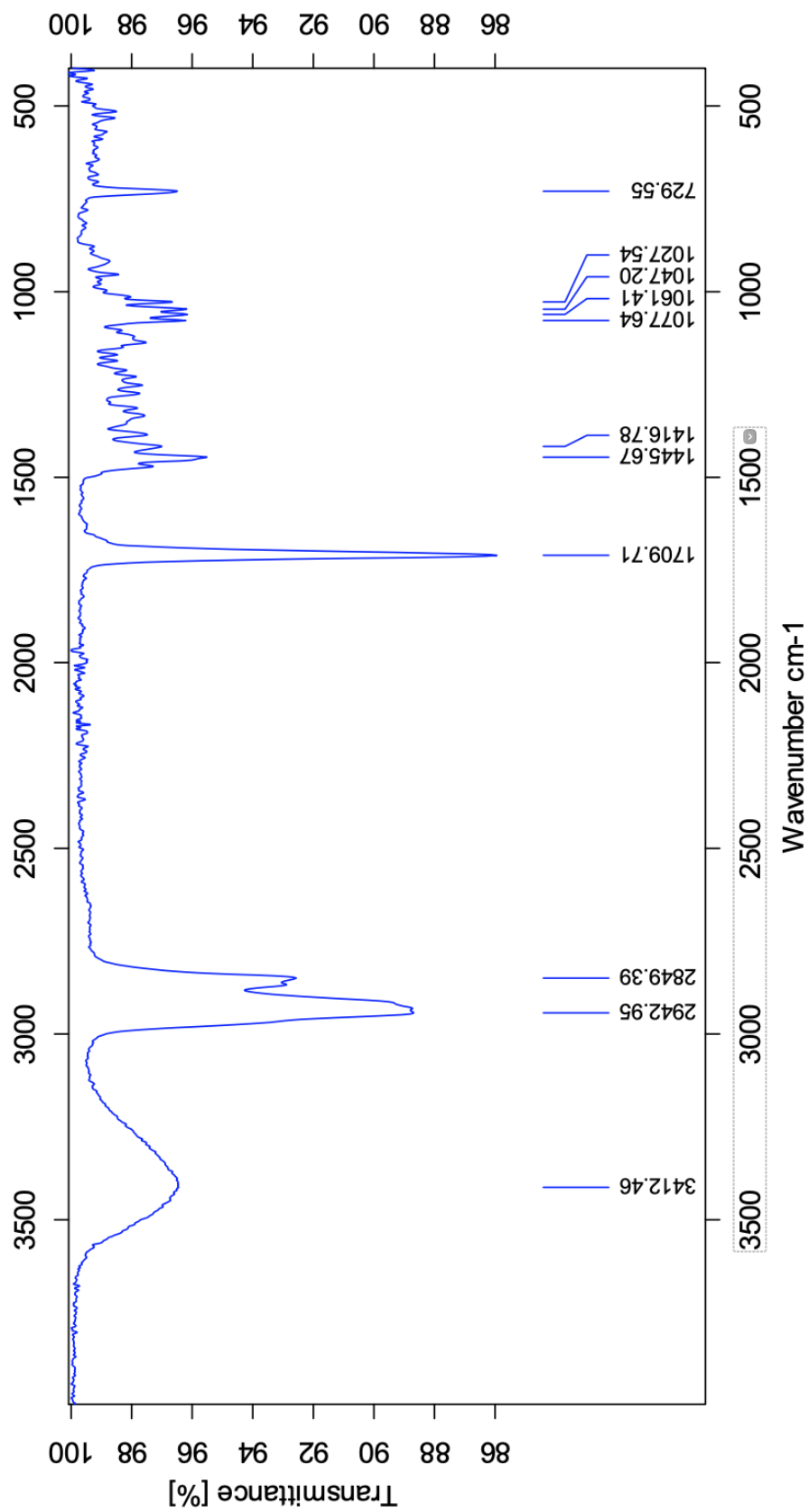
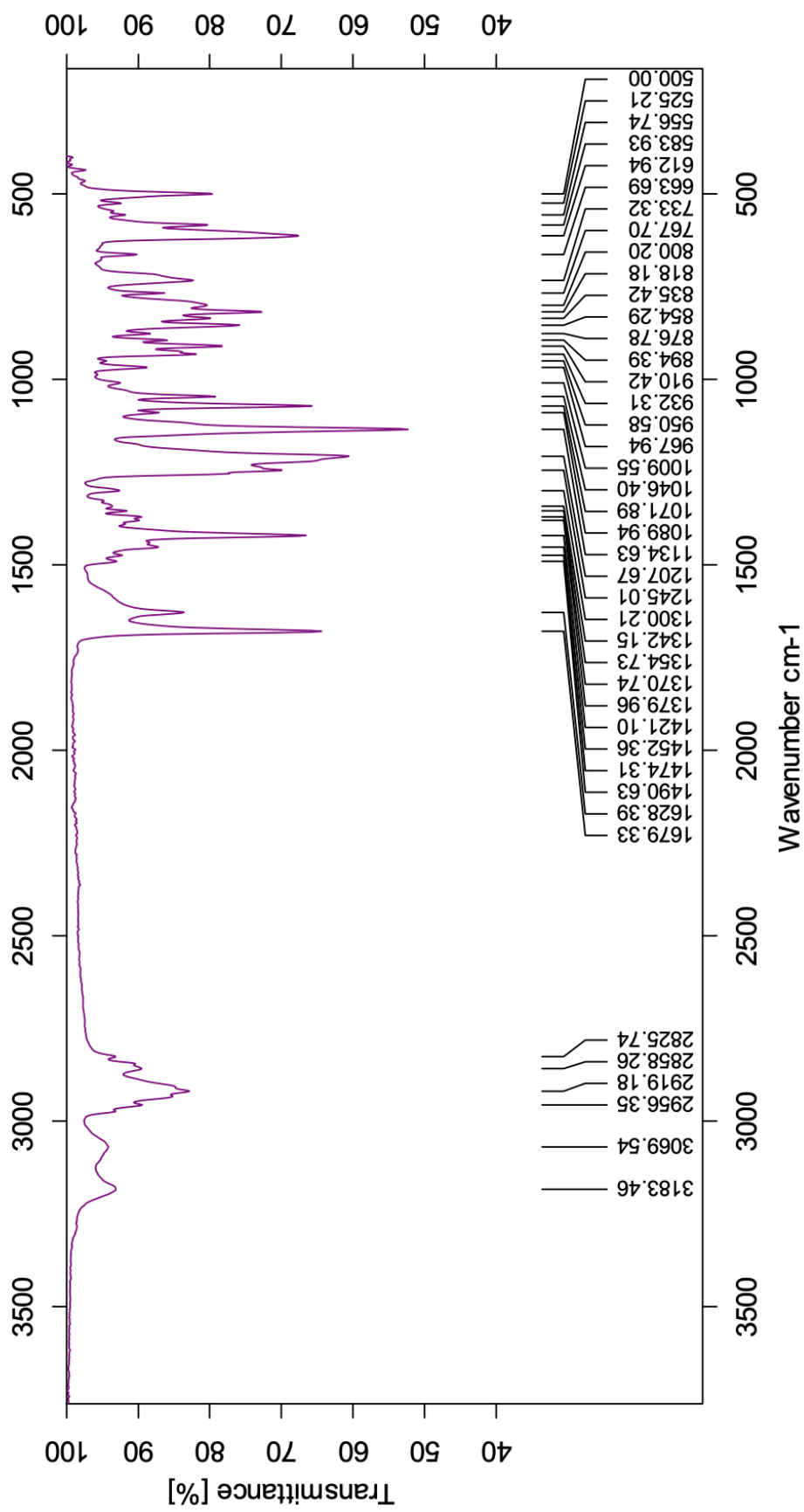**Supplementary Figure 9:** IR spectrum of **3**.

D   Spectroscopic data for compound 4
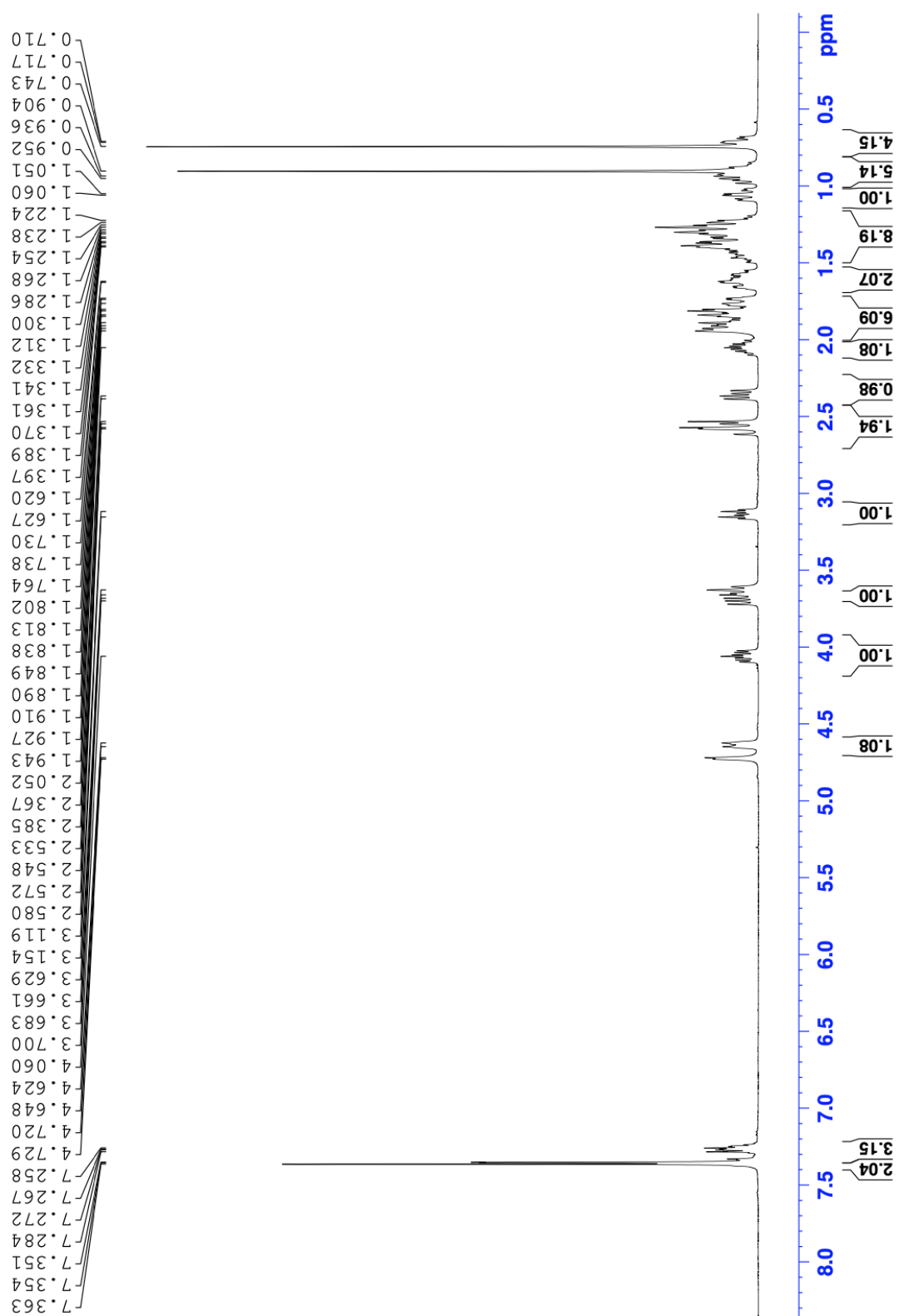
Supplementary Figure 10: [^1]H NMR spectrum in CDCl₃, 400 MHz of **4**.
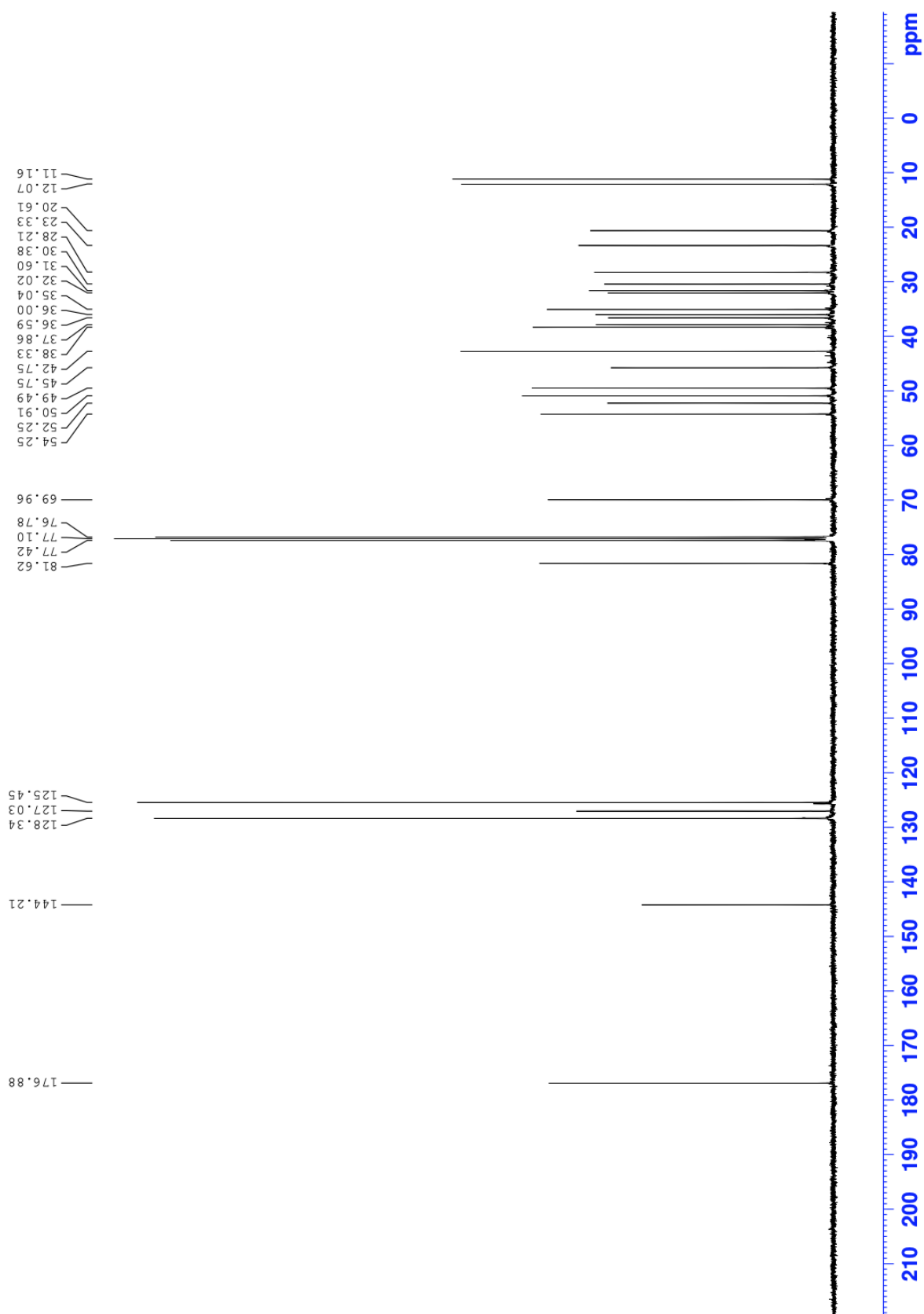
Supplementary Figure 11: ^{13}C NMR spectrum in CDCl$_3$, 100 MHz of **4**.
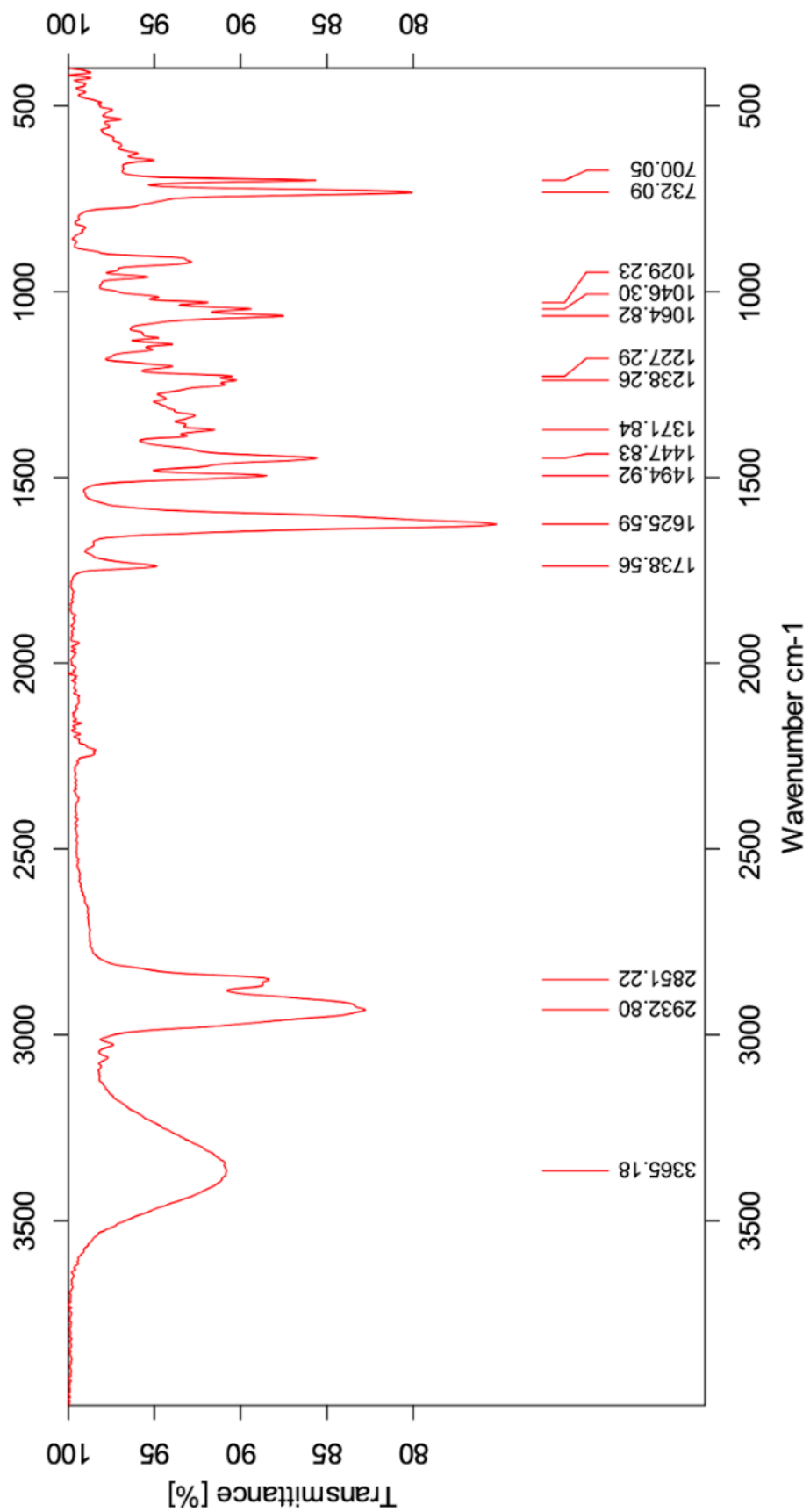
Supplementary Figure 12: IR spectrum of **4**.

E   Spectroscopic data for compound 5
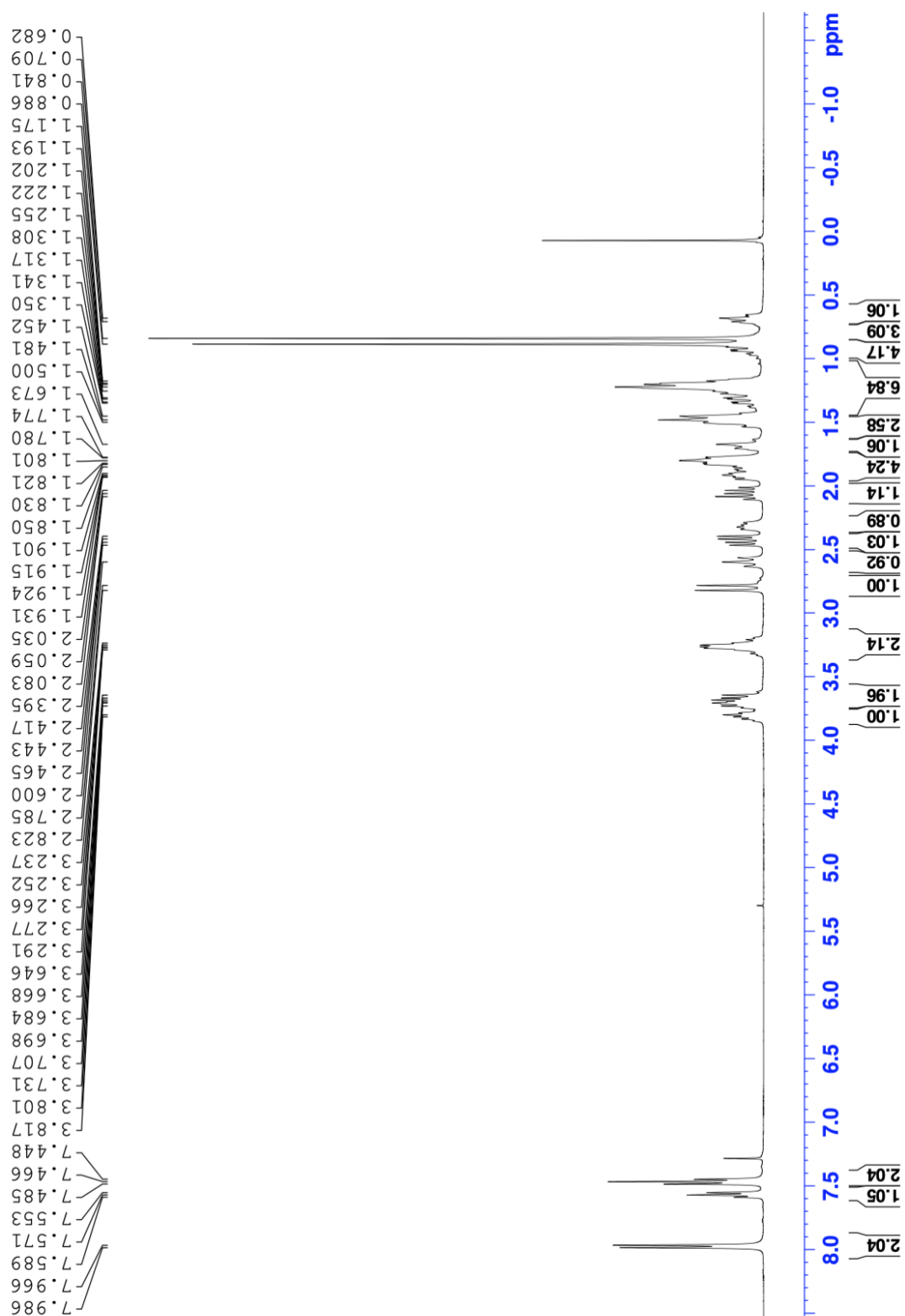
Supplementary Figure 13: ^{1}H NMR spectrum in CDCl$_3$, 400 MHz of **5**.
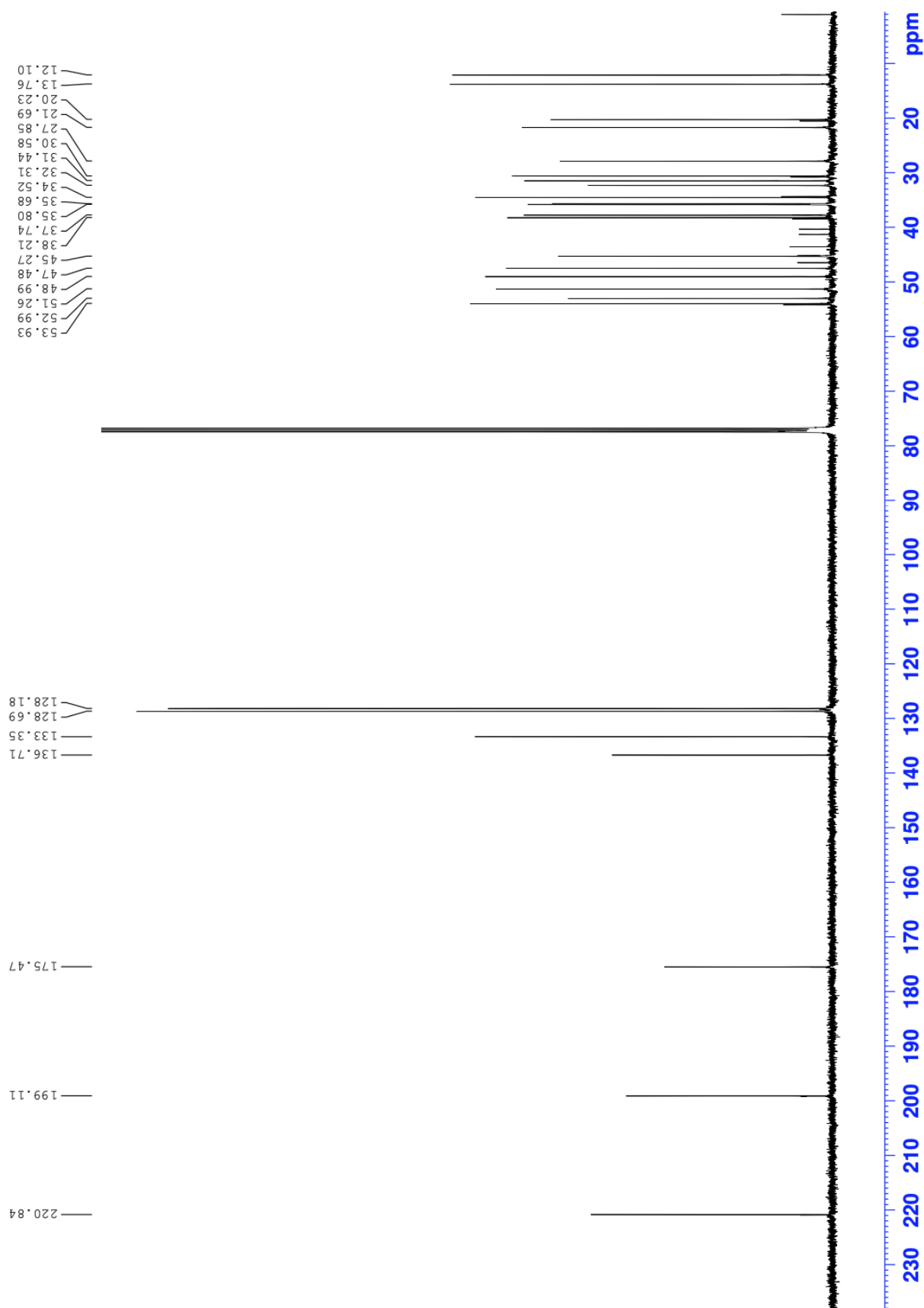
Supplementary Figure 14: ^{13}C NMR spectrum in CDCl$_3$, 100 MHz of **5**.
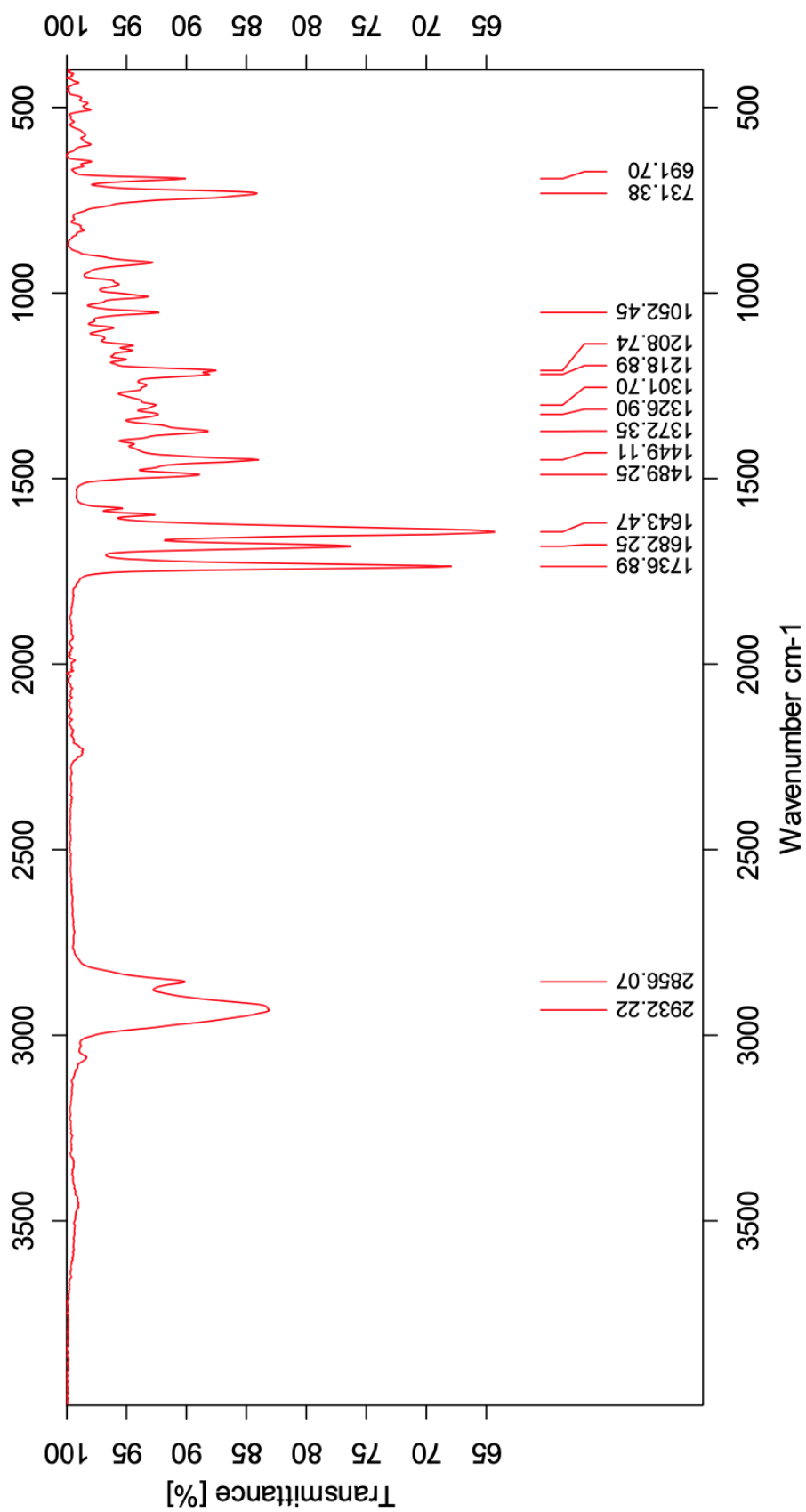
Supplementary Figure 15: IR spectrum of **5**.

F   Spectroscopic data for compound 6
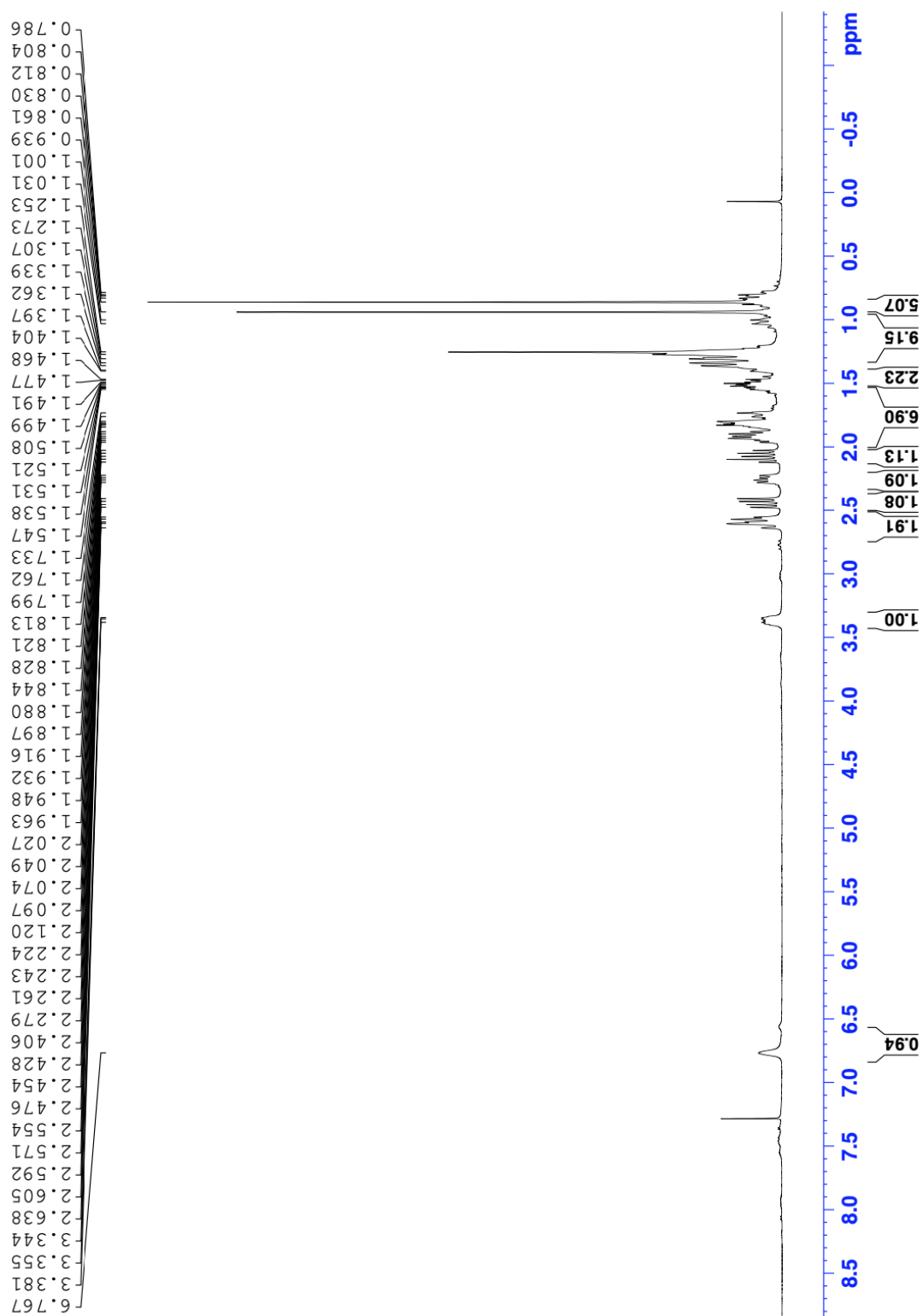
Supplementary Figure 16: ^{1}H NMR spectrum in CDCl$_3$, 400 MHz of **6**.
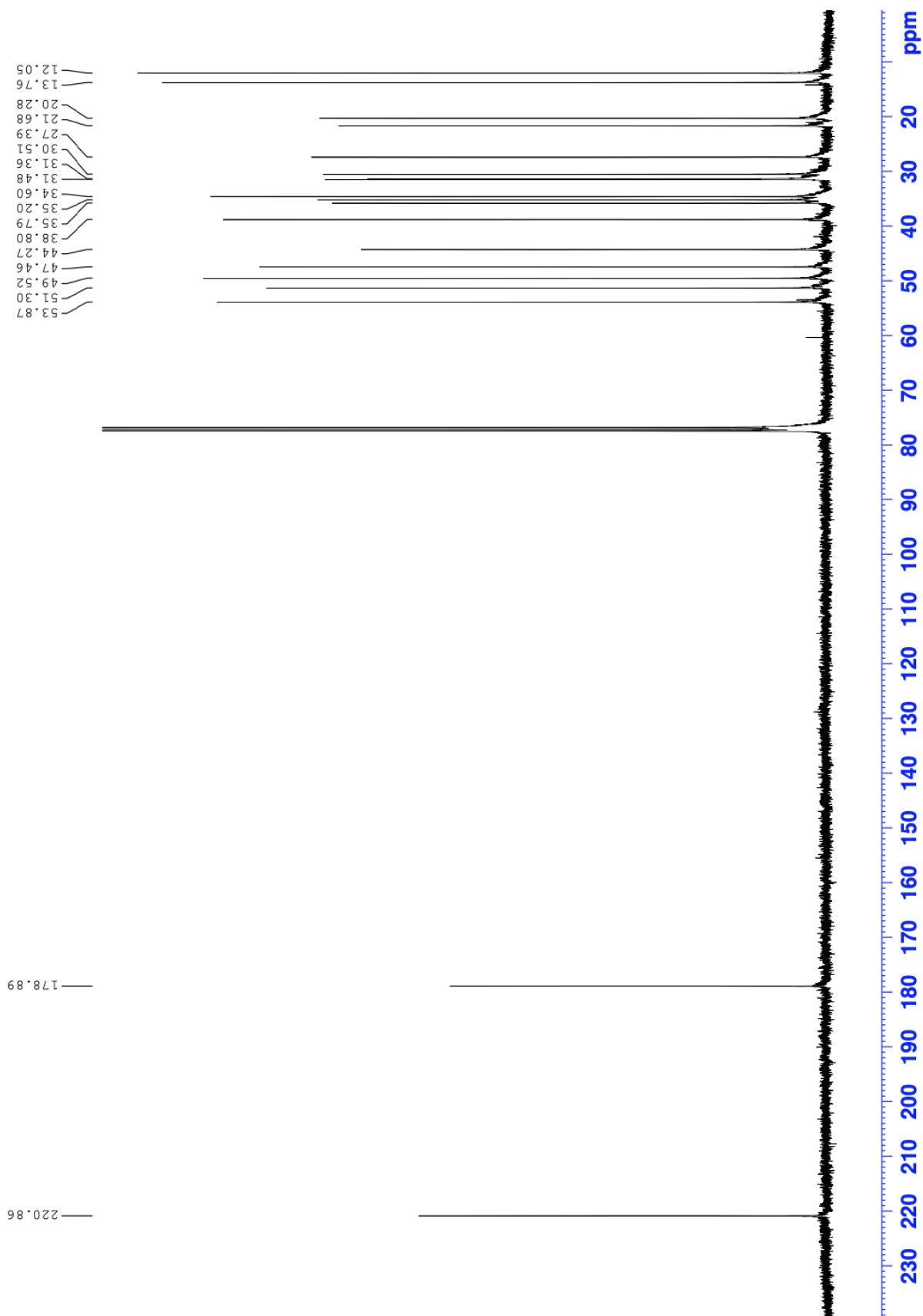
Supplementary Figure 17: ^{13}C NMR spectrum in CDCl$_3$, 100 MHz of **6**.
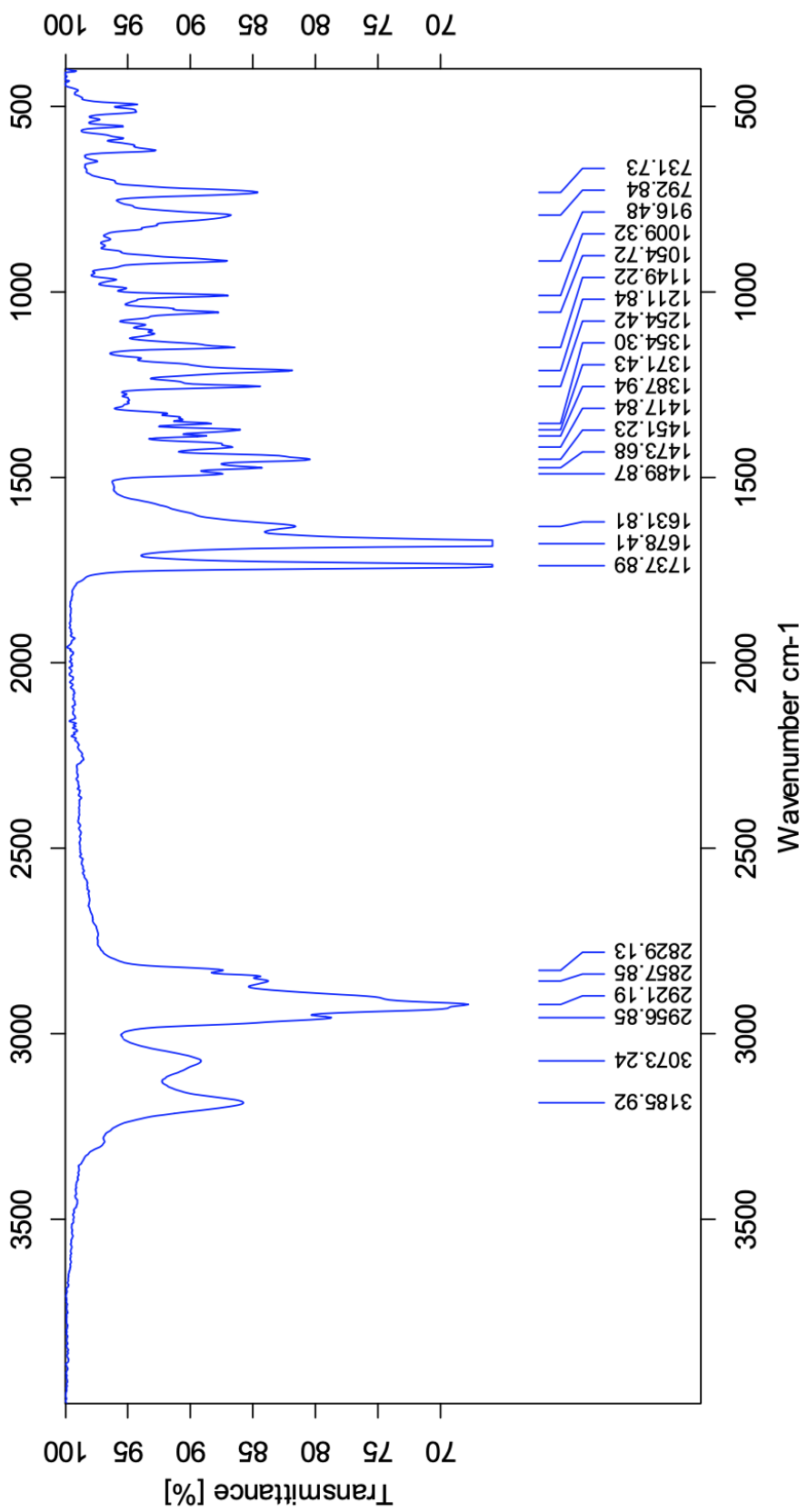
Supplementary Figure 18: IR spectrum of **6**.

G Spectroscopic data for compound 7
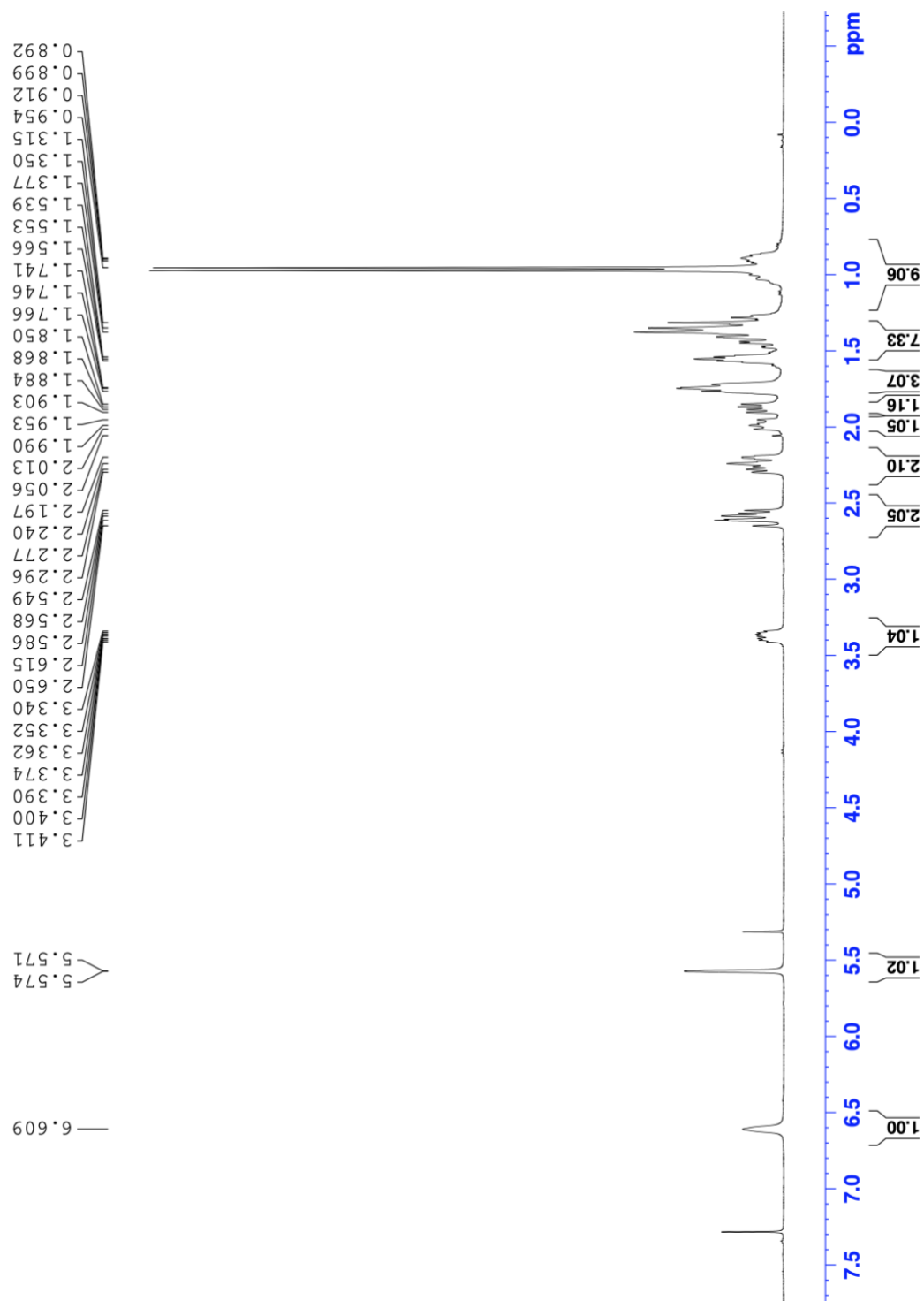
Supplementary Figure 19: ^{1}H NMR spectrum in CDCl$_3$, 400 MHz of **7**.

Supplementary Figure 20: ^{13}C NMR spectrum in CDCl$_3$, 100 MHz of **7**.

Peak labels: 11.98, 15.24, 20.36, 27.38, 28.46, 30.47, 31.34, 32.70, 33.02, 35.03, 38.89, 44.36, 44.59, 49.75, 54.05, 54.13, 114.48, 120.16, 159.11, 178.62

Supplementary Figure 21: IR spectrum of **7**.

Single Mass Analysis
Tolerance = 2.0 PPM   /   DBE: min = -10.0, max = 50.0
Element prediction: Off
Number of isotope peaks used for i-FIT = 6

Monoisotopic Mass, Even Electron Ions
1513 formula(e) evaluated with 3 results within limits (all results (up to 1000) for each mass)
Elements Used:
C: 0-100   H: 0-100   N: 0-2   O: 0-10   S: 0-1   F: 0-3

2021_338 117 (1.109) AM2 (Ar,35000.0,0.00,0.00); ABS; Cm (112:117)
1: TOF MS ES+
                                                                                    3.52e+006
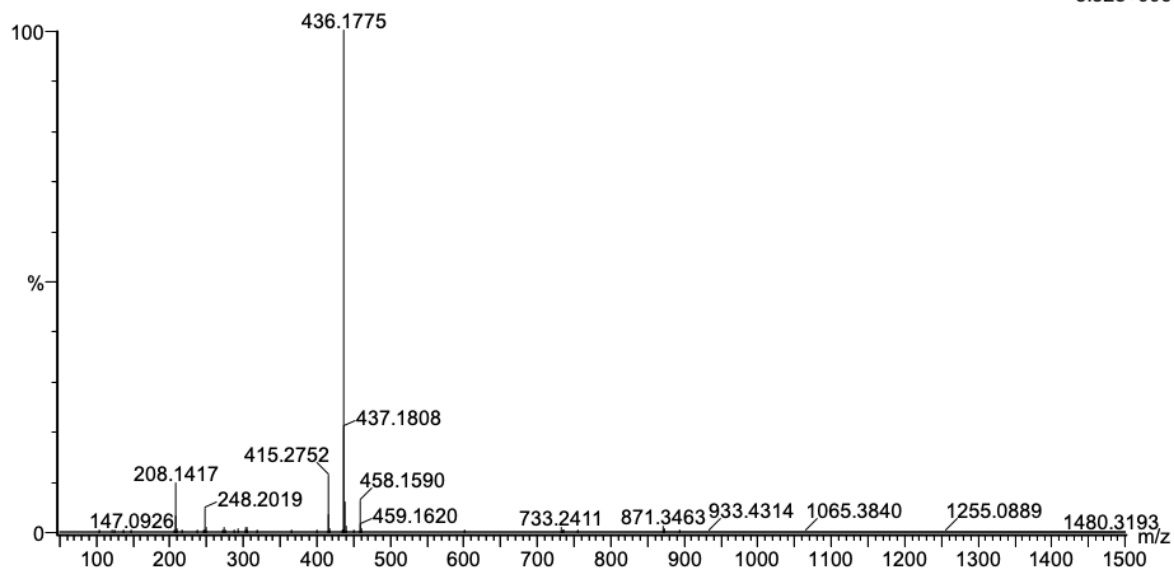
Mass	Calc. Mass	mDa	PPM	DBE	i-FIT	Norm	Conf(%)	Formula
Minimum:				-10.0				
Maximum:		5.0	2.0	50.0				
436.1775	436.1769	0.6	1.4	5.5	1691.5	0.000	100.00	C20 H29 N O4 S F3
	436.1783	-0.8	-1.8	5.5	1706.6	15.107	0.00	C19 H28 N O8 F2
	436.1772	0.3	0.7	9.5	1707.4	15.888	0.00	C22 H27 N O7 F

Supplementary Figure 22: MS spectrum of **7.** Ions observed are [M+H].
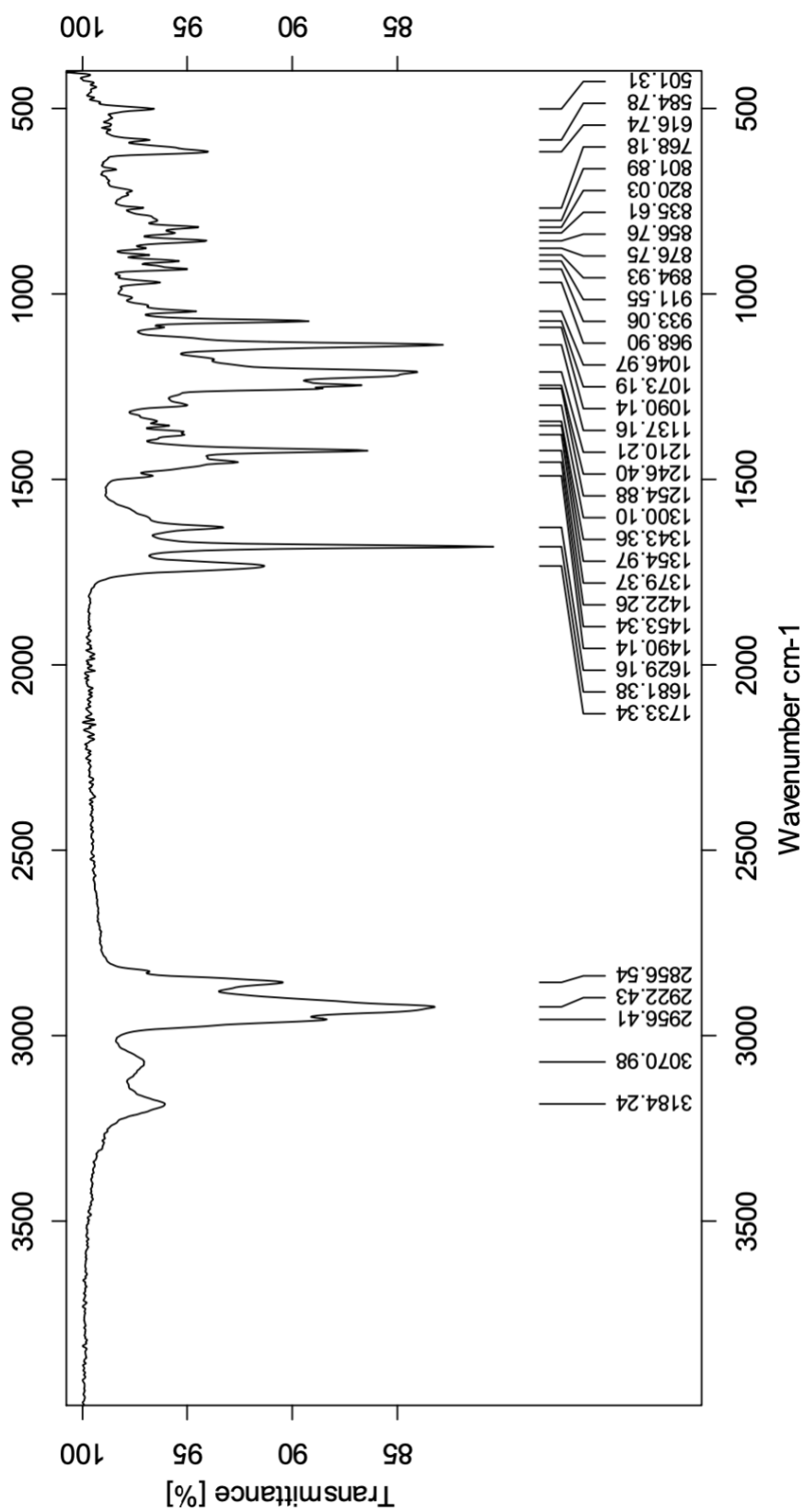
XXII

H   Spectroscopic data for compound 8a
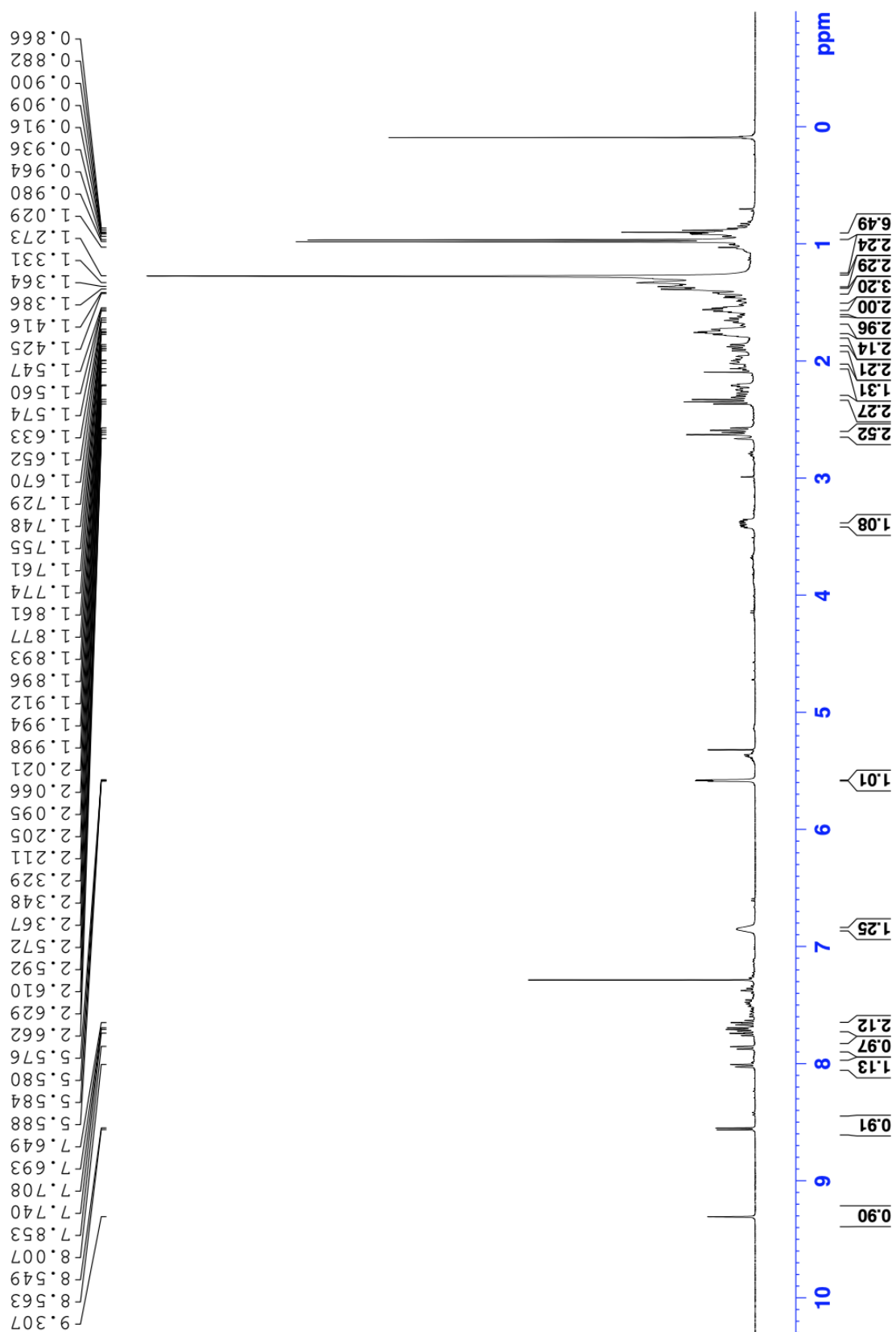
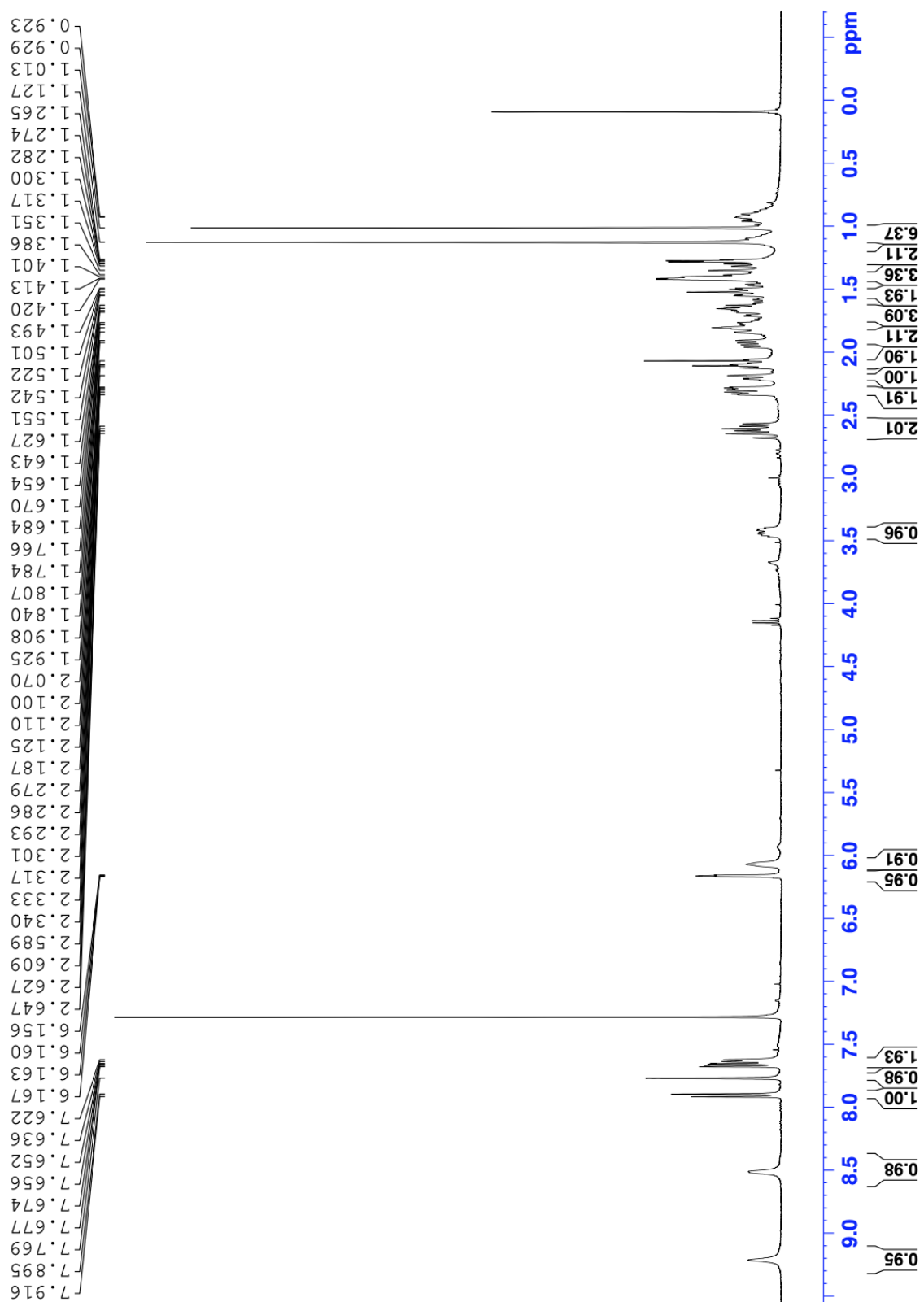**Supplementary Figure 23:** ^{1}H NMR spectrum in CDCl$_3$, 400 MHz of **8a**.
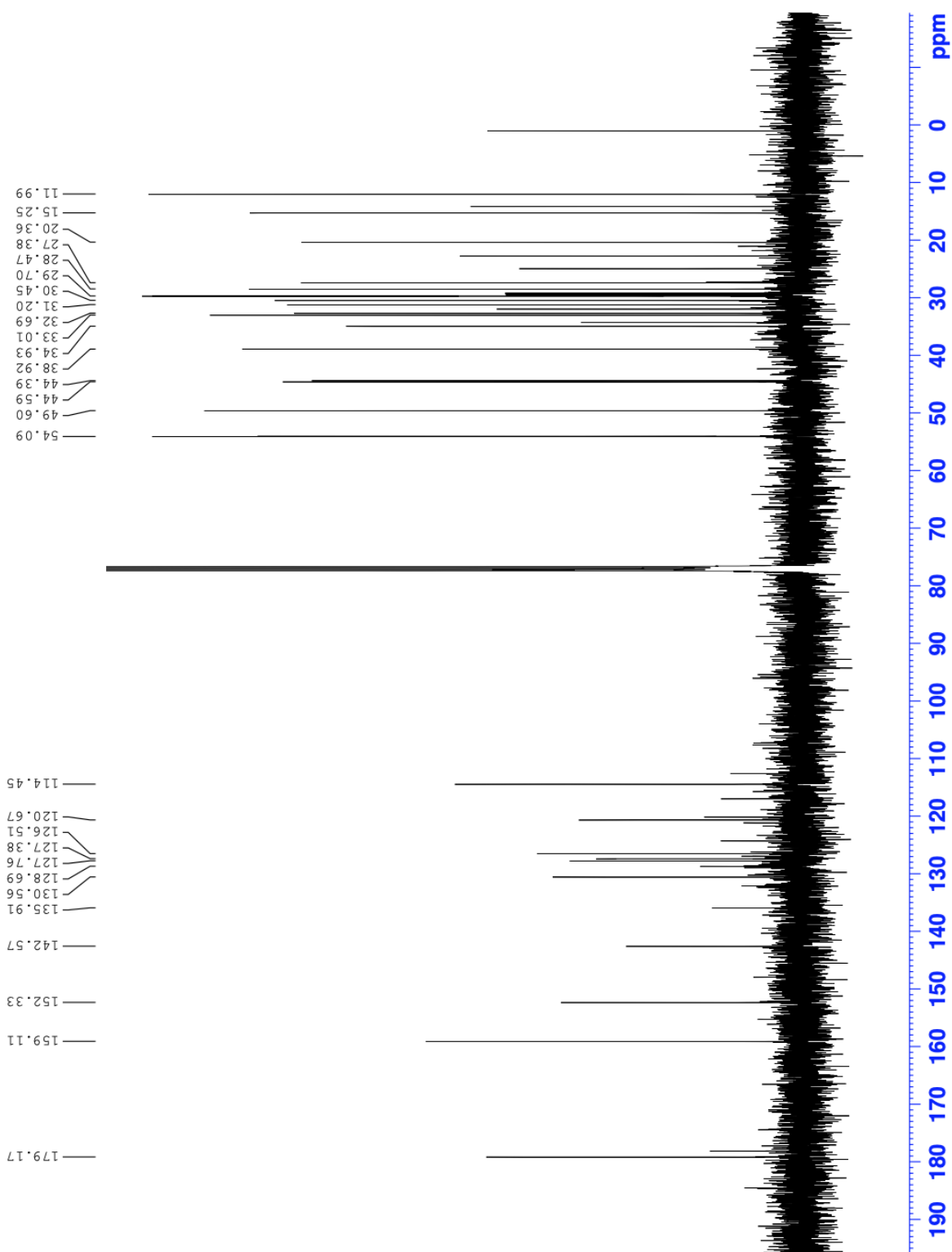
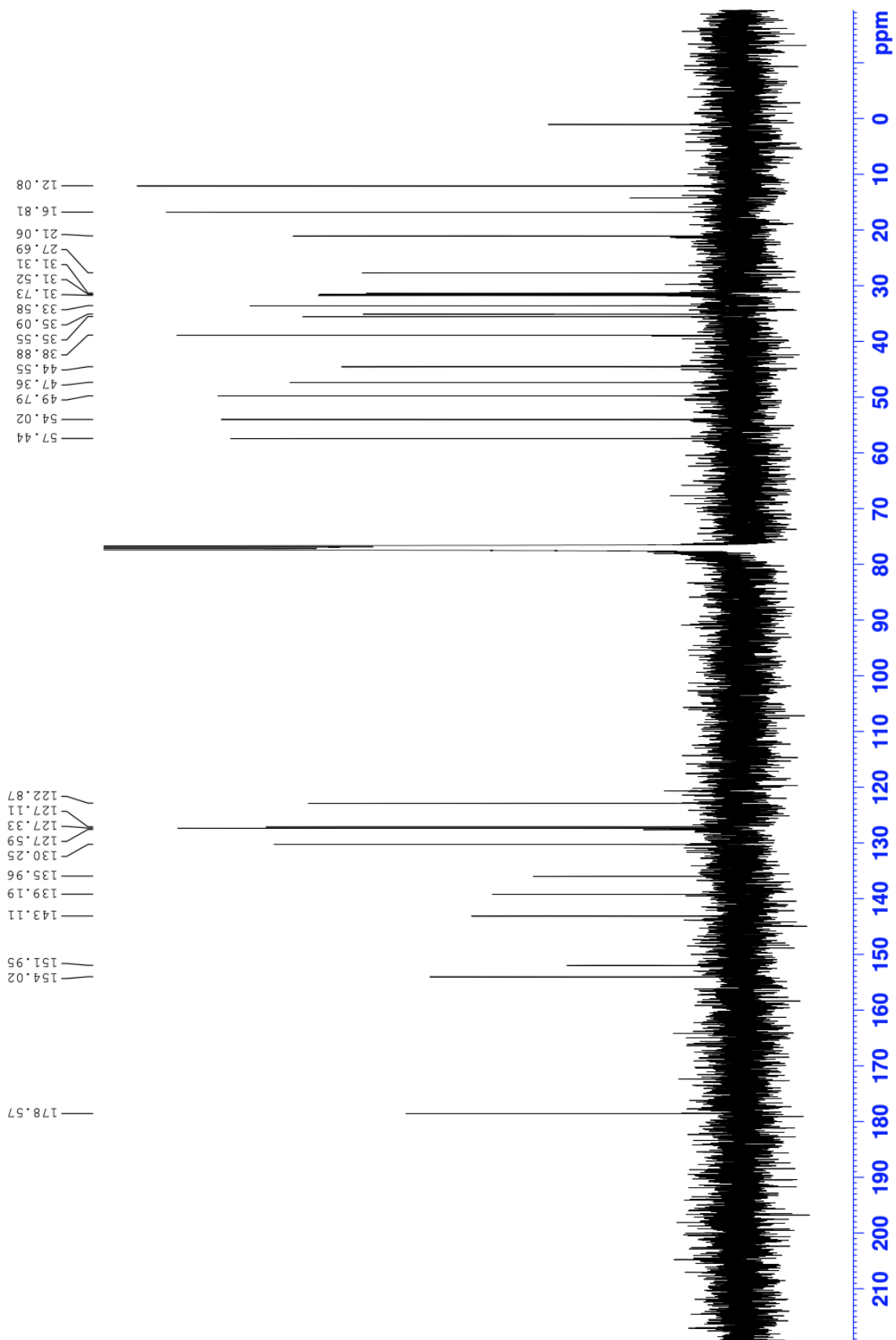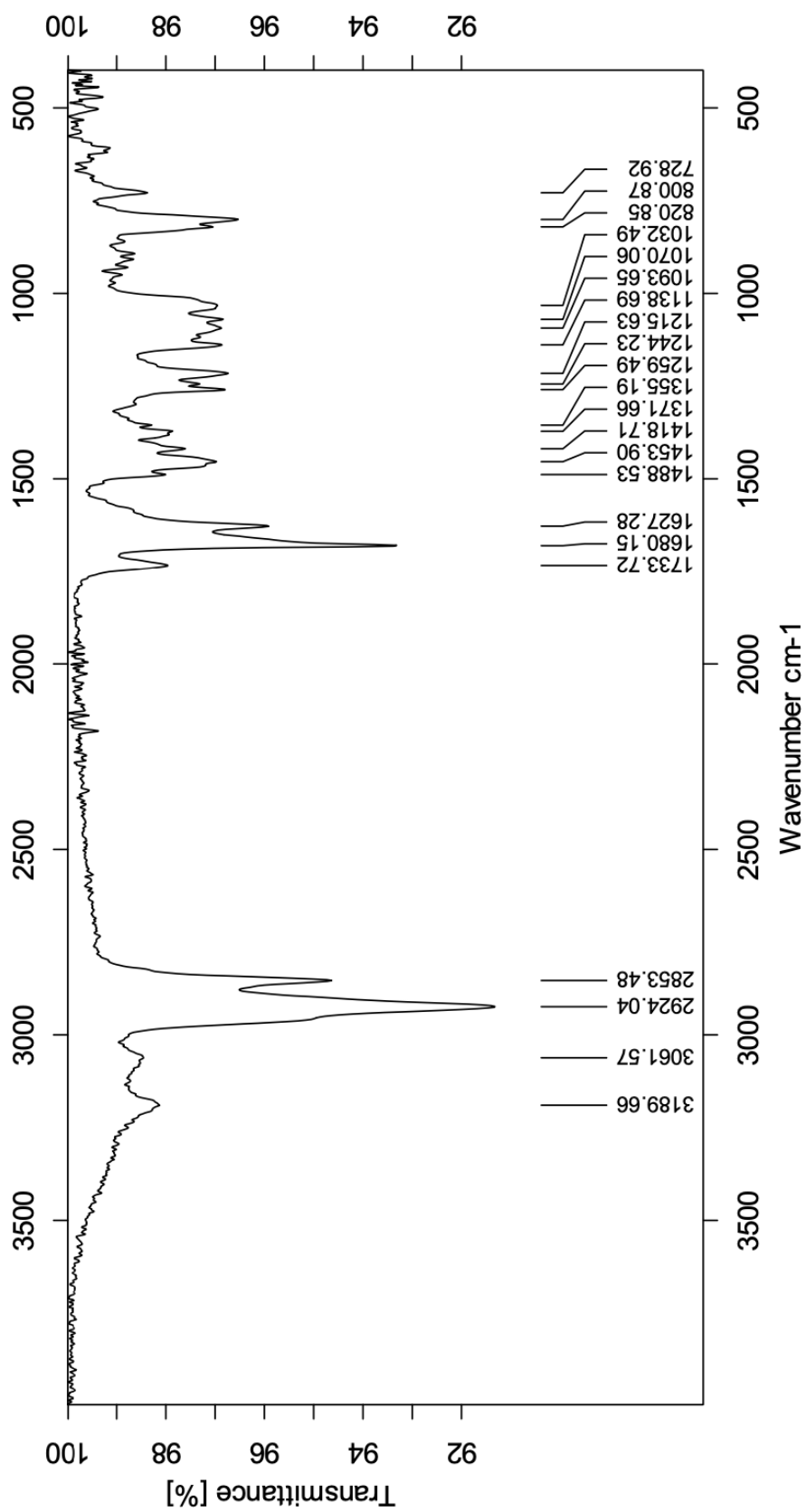**Supplementary Figure 24:** ^{13}C NMR spectrum in CDCl$_3$, 100 MHz of **8a**.

Peak labels: 11.99, 15.25, 20.35, 27.38, 28.47, 29.70, 30.45, 31.20, 32.69, 33.01, 34.93, 38.92, 44.39, 44.59, 49.60, 54.09, 114.45, 120.67, 126.51, 127.38, 127.76, 128.69, 130.56, 135.91, 142.57, 152.33, 159.11, 179.17
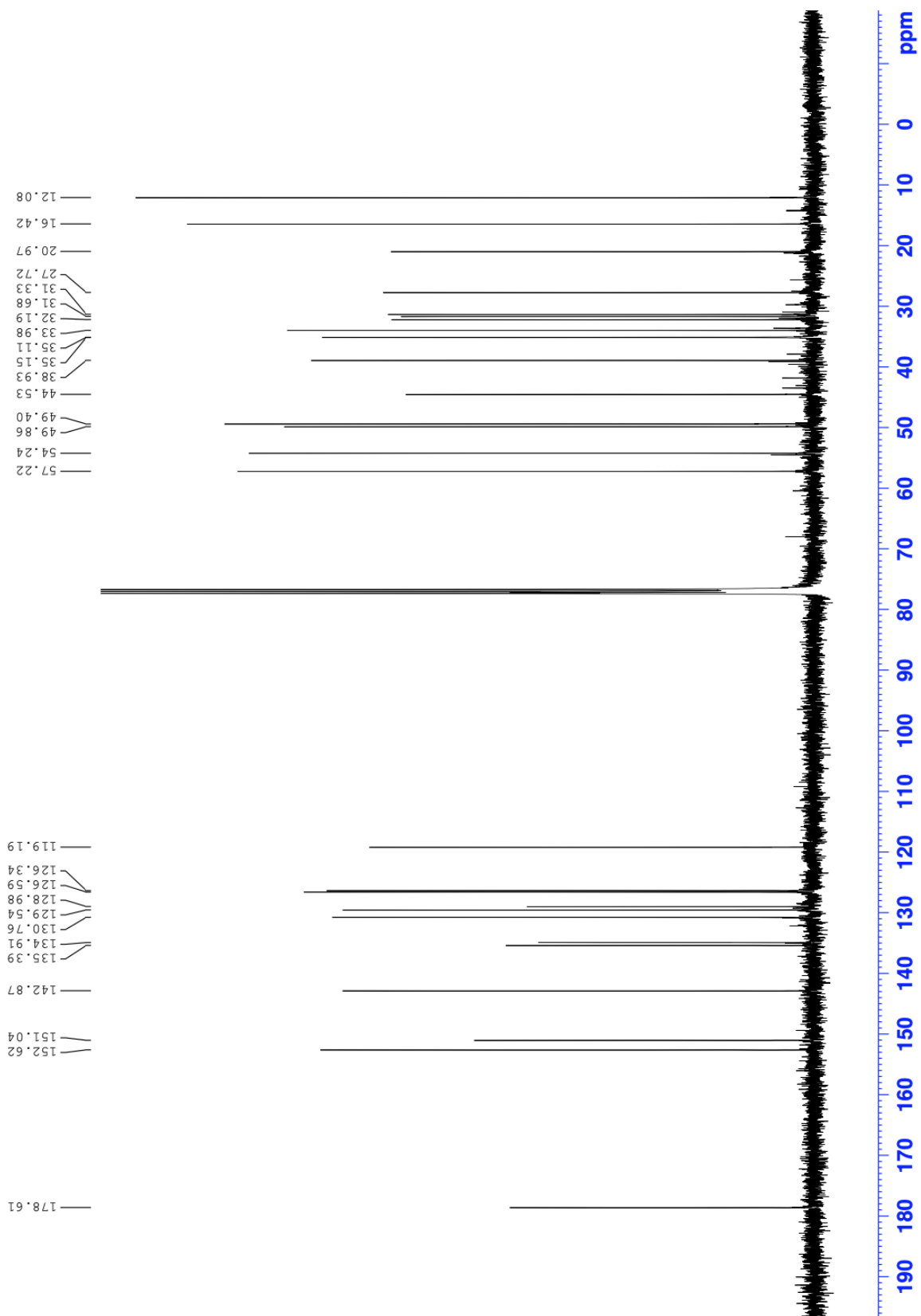
Supplementary Figure 25: IR spectrum of **8a**.

I   Spectroscopic data for compound 8b

Supplementary Figure 26: ^{1}H NMR spectrum in CDCl$_3$, 400 MHz of **8b**.

Supplementary Figure 27: ^{13}C NMR spectrum in $CDCl_3$, 100 MHz of **8b**.
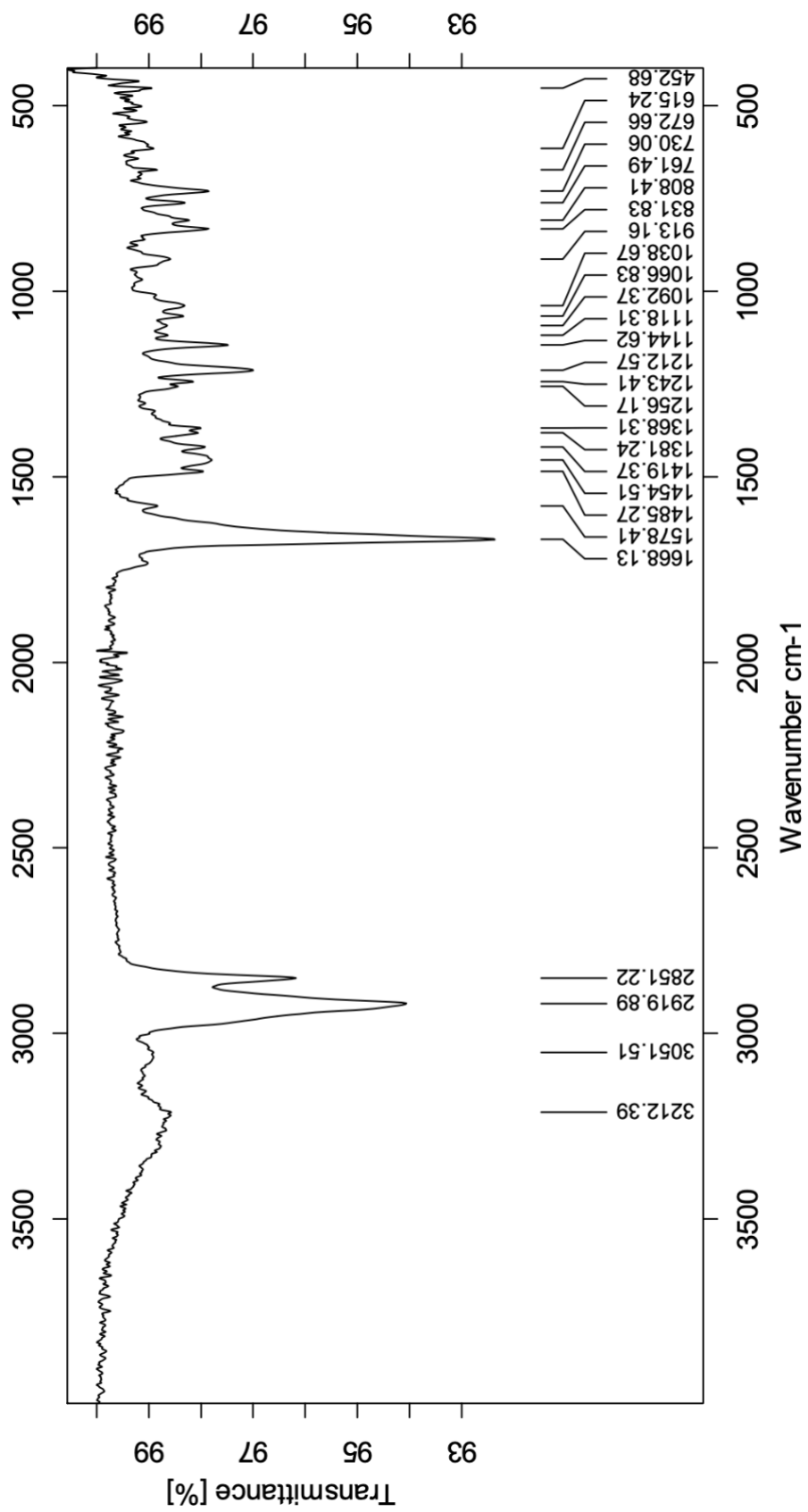
Supplementary Figure 28: IR spectrum of **8b**.

J Spectroscopic data for compound 8c
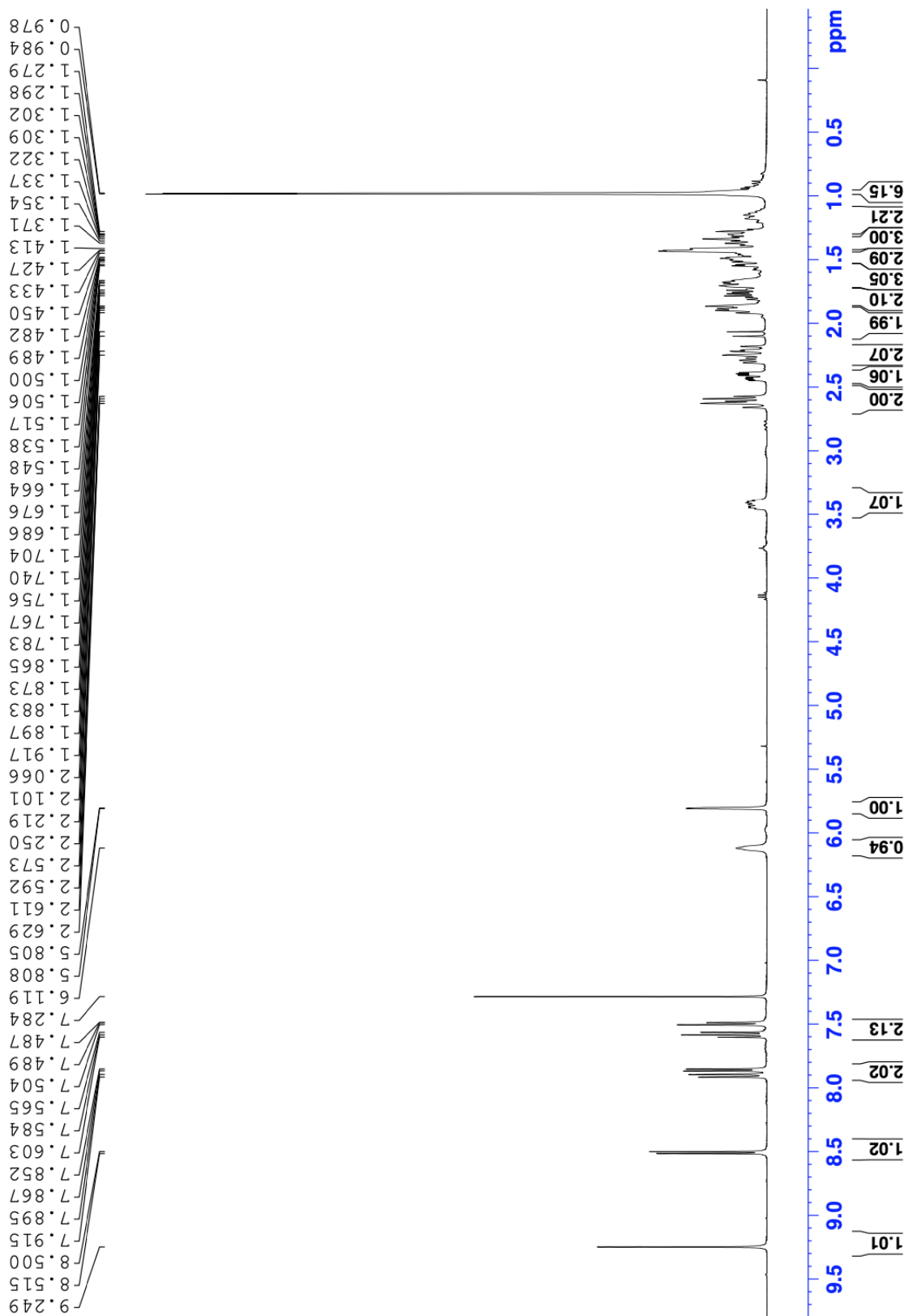
Supplementary Figure 29: ^{1}H NMR spectrum in CDCl$_3$, 400 MHz of **8c**.

Supplementary Figure 30: ^{13}C NMR spectrum in CDCl$_3$, 100 MHz of **8c**.

Supplementary Figure 31: IR spectrum of **8c**.

Single Mass Analysis
Tolerance = 2.0 PPM / DBE: min = -10.0, max = 50.0
Element prediction: Off
Number of isotope peaks used for i-FIT = 6

Monoisotopic Mass, Even Electron Ions
520 formula(e) evaluated with 1 results within limits (all results (up to 1000) for each mass)
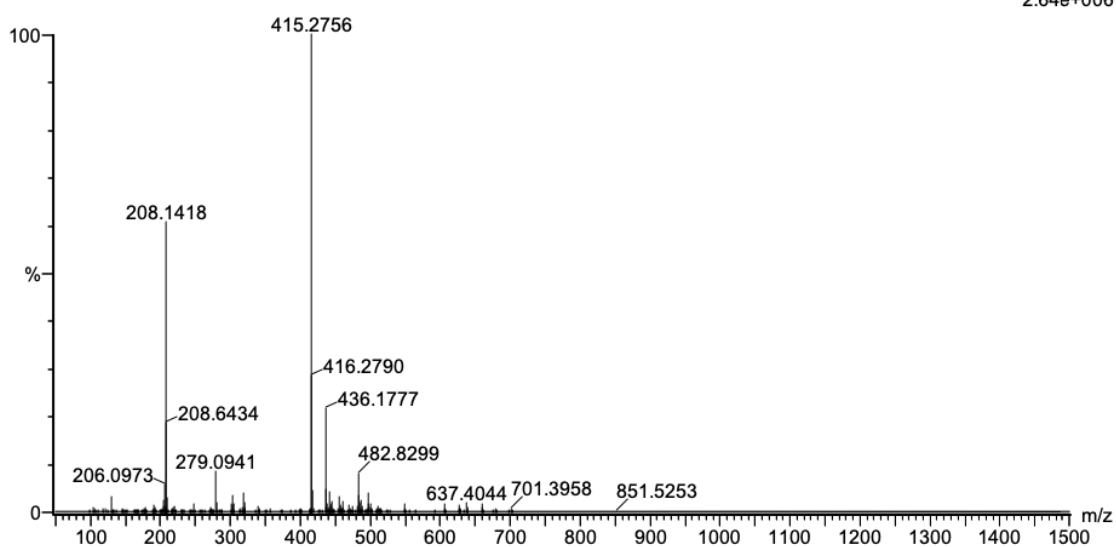Elements Used:
C: 0-100   H: 0-100   N: 0-3   O: 0-10   Na: 0-1
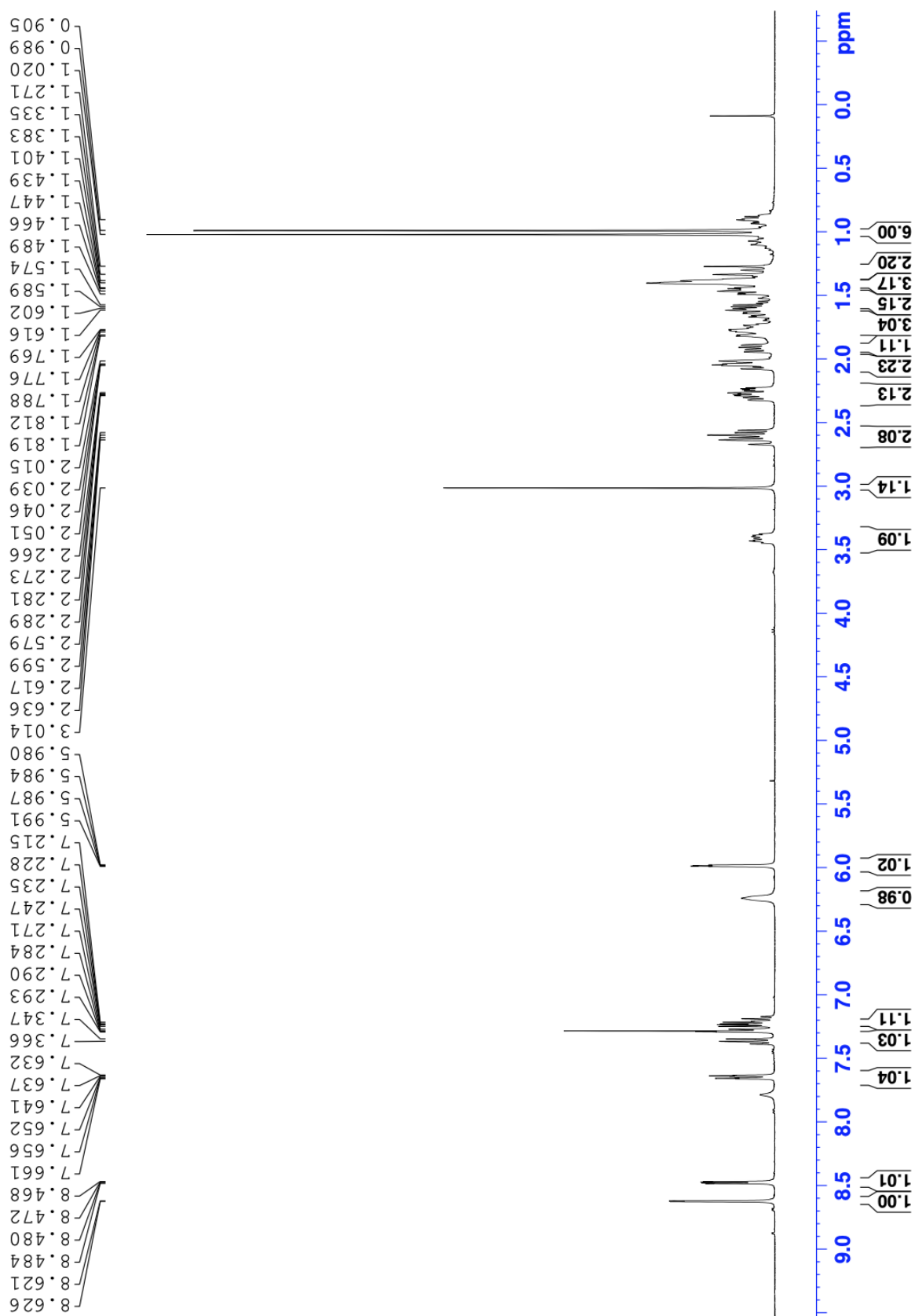2021_345 122 (1.152) AM2 (Ar,35000.0,0.00,0.00); ABS; Cm (118:122)
1: TOF MS ES+

Mass	Calc. Mass	mDa	PPM	DBE	i-FIT	Norm	Conf(%)	Formula
Minimum:				-10.0				
Maximum:		5.0	2.0	50.0				
415.2756	415.2749	0.7	1.7	12.5	1909.2	n/a	n/a	C28 H35 N2 O

Supplementary Figure 32: MS spectrum of **8c.** Ions observed are [M+H].

Supplementary Figure 33: ^{1}H NMR spectrum in CDCl$_3$, 400 MHz of **8d**.
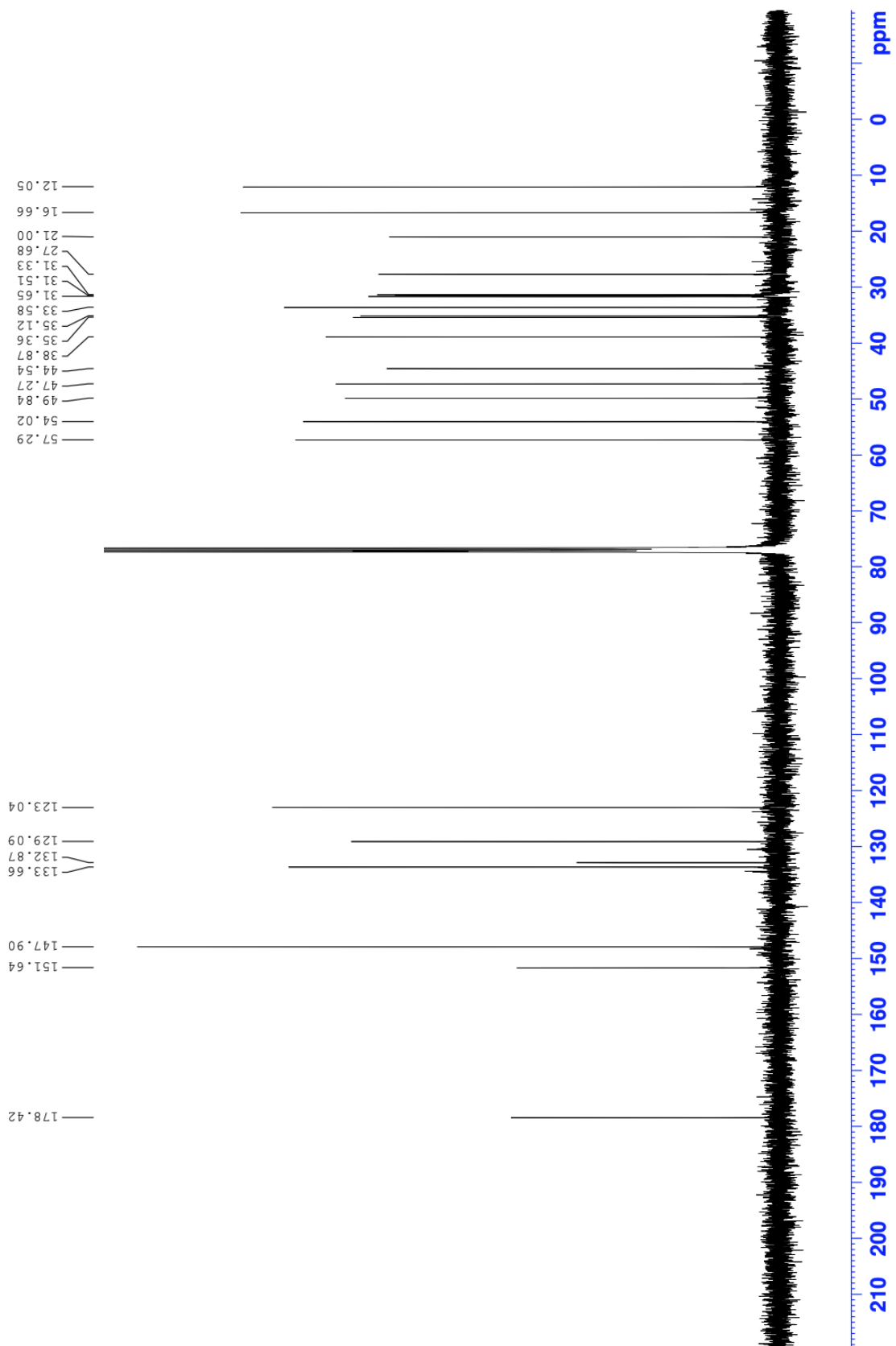
Supplementary Figure 34: ^{13}C NMR spectrum in CDCl$_3$, 100 MHz of **8d**.
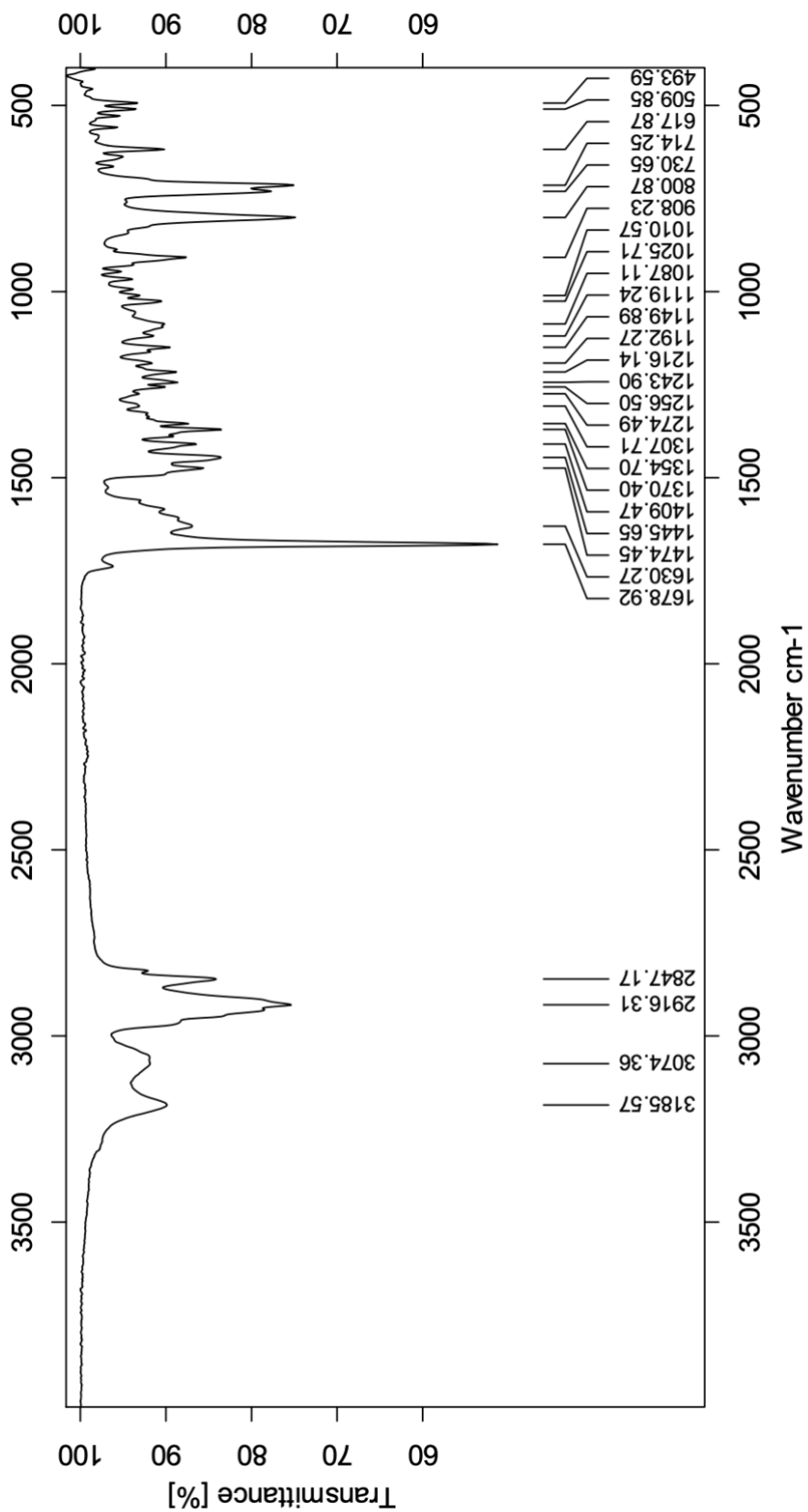
Supplementary Figure 35: IR spectrum of **8d**.

Single Mass Analysis
Tolerance = 2.0 PPM   /   DBE: min = -10.0, max = 50.0
Element prediction: Off
Number of isotope peaks used for i-FIT = 6

Monoisotopic Mass, Even Electron Ions
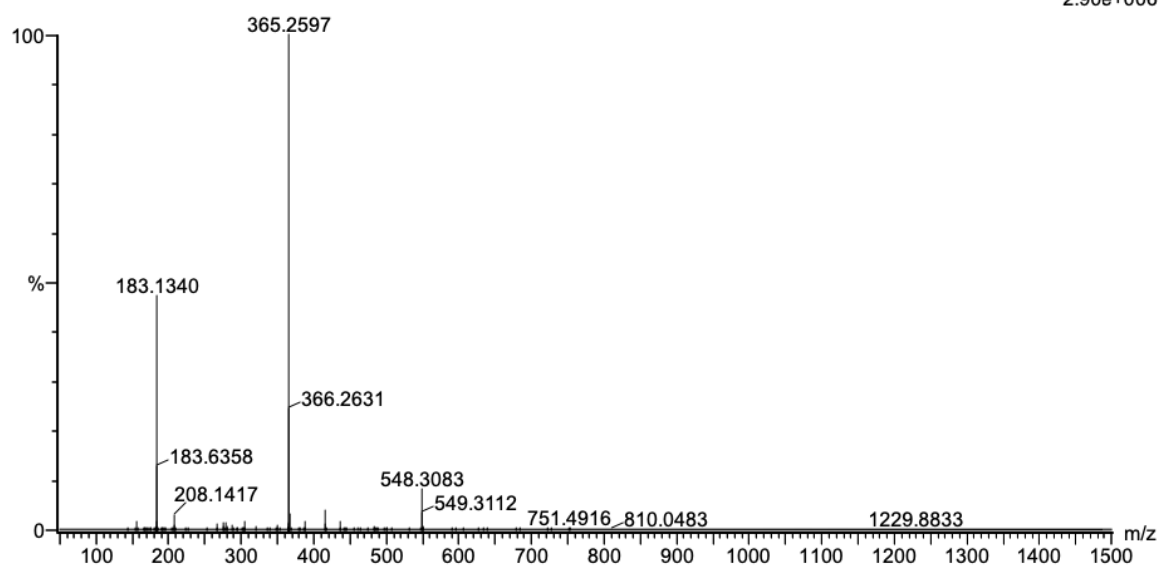470 formula(e) evaluated with 1 results within limits (all results (up to 1000) for each mass)
Elements Used:
C: 0-100   H: 0-100   N: 0-3   O: 0-10   Na: 0-1
2021_346 86 (0.813) AM2 (Ar,35000.0,0.00,0.00); ABS; Cm (86:87)
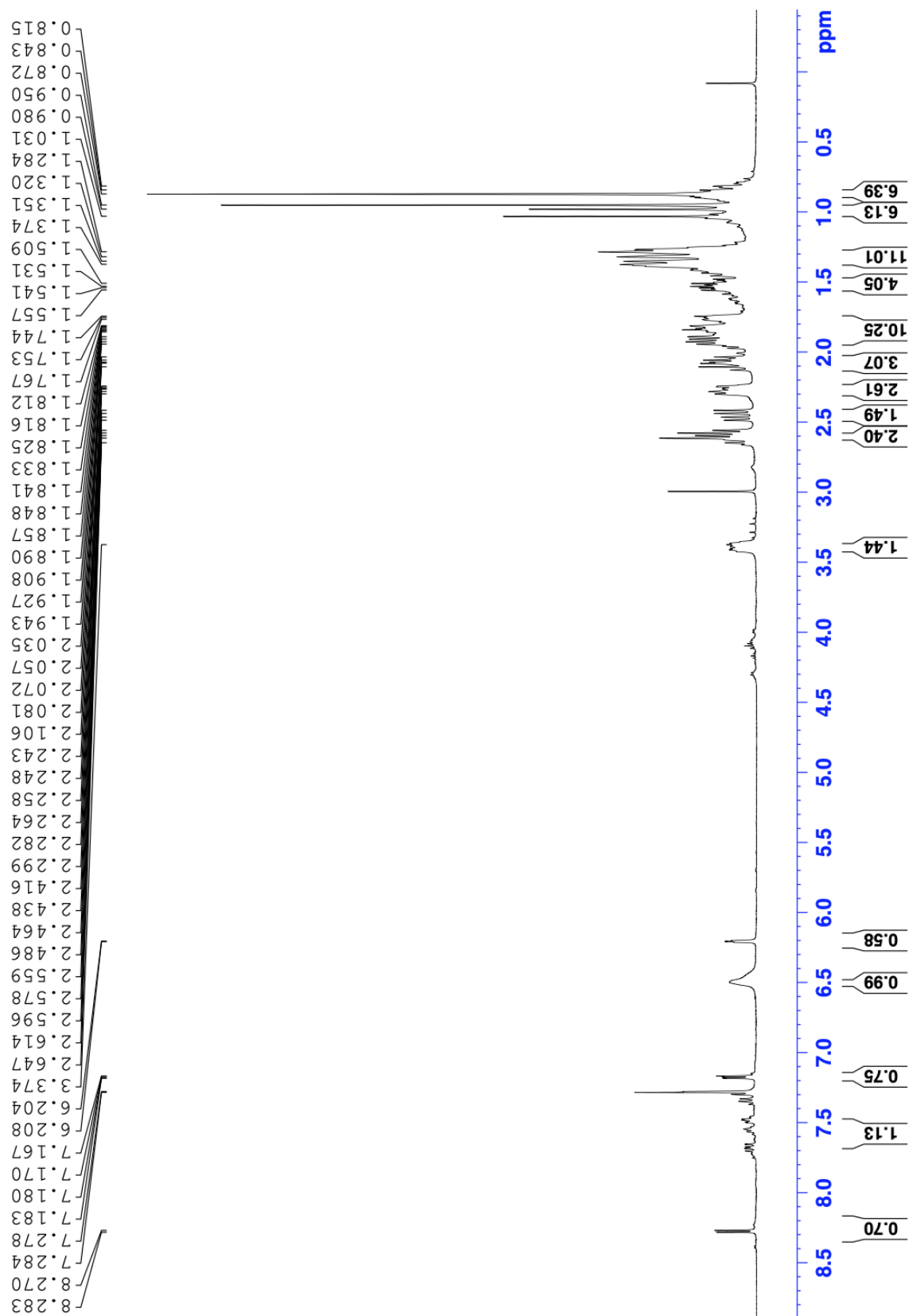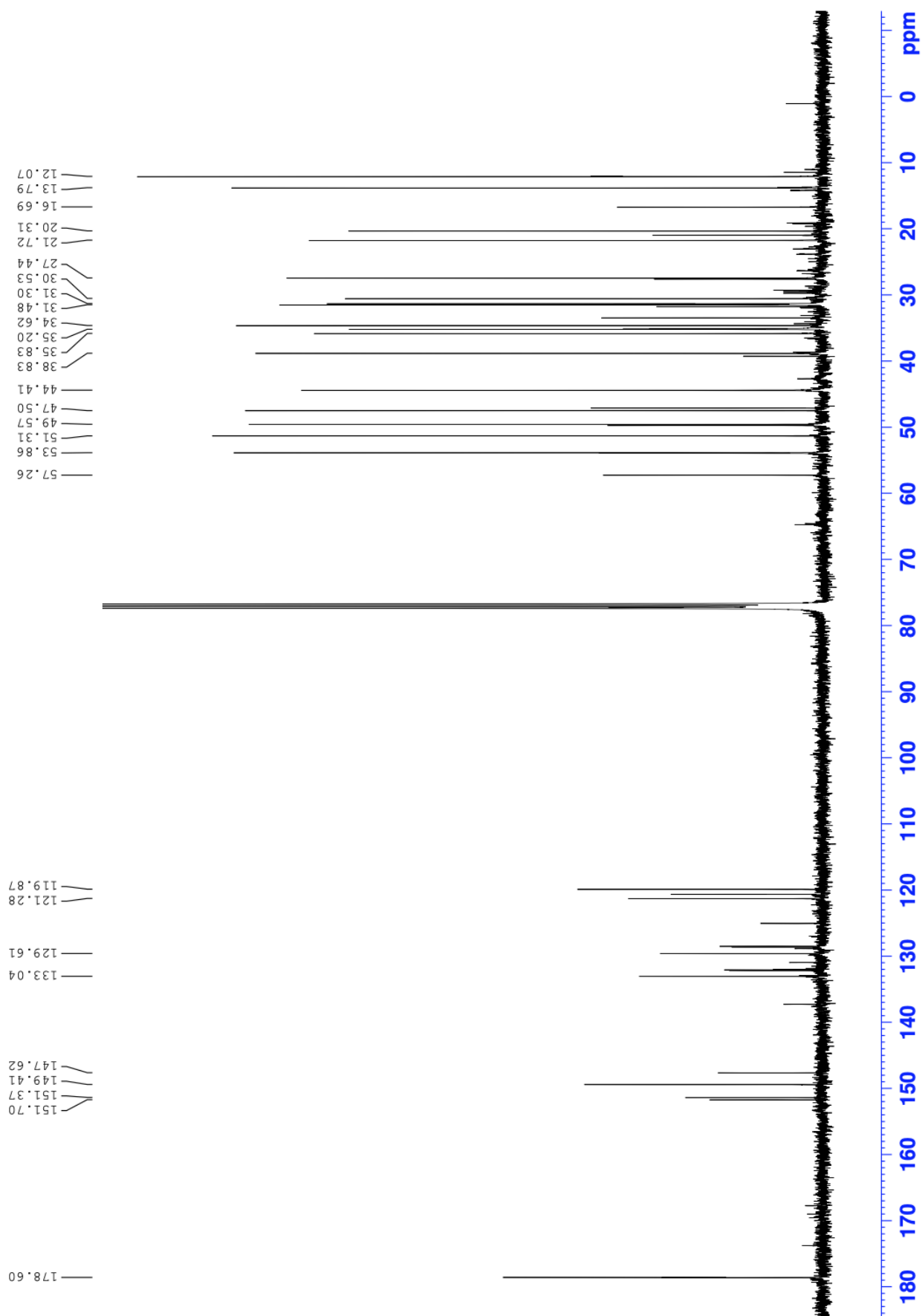1: TOF MS ES+

2.90e+006

Mass	Calc. Mass	mDa	PPM	DBE	i-FIT	Norm	Conf(%)	Formula
Minimum:				-10.0				
Maximum:		5.0	2.0	50.0				
365.2597	365.2593	0.4	1.1	9.5	2084.6	n/a	n/a	C24 H33 N2 O

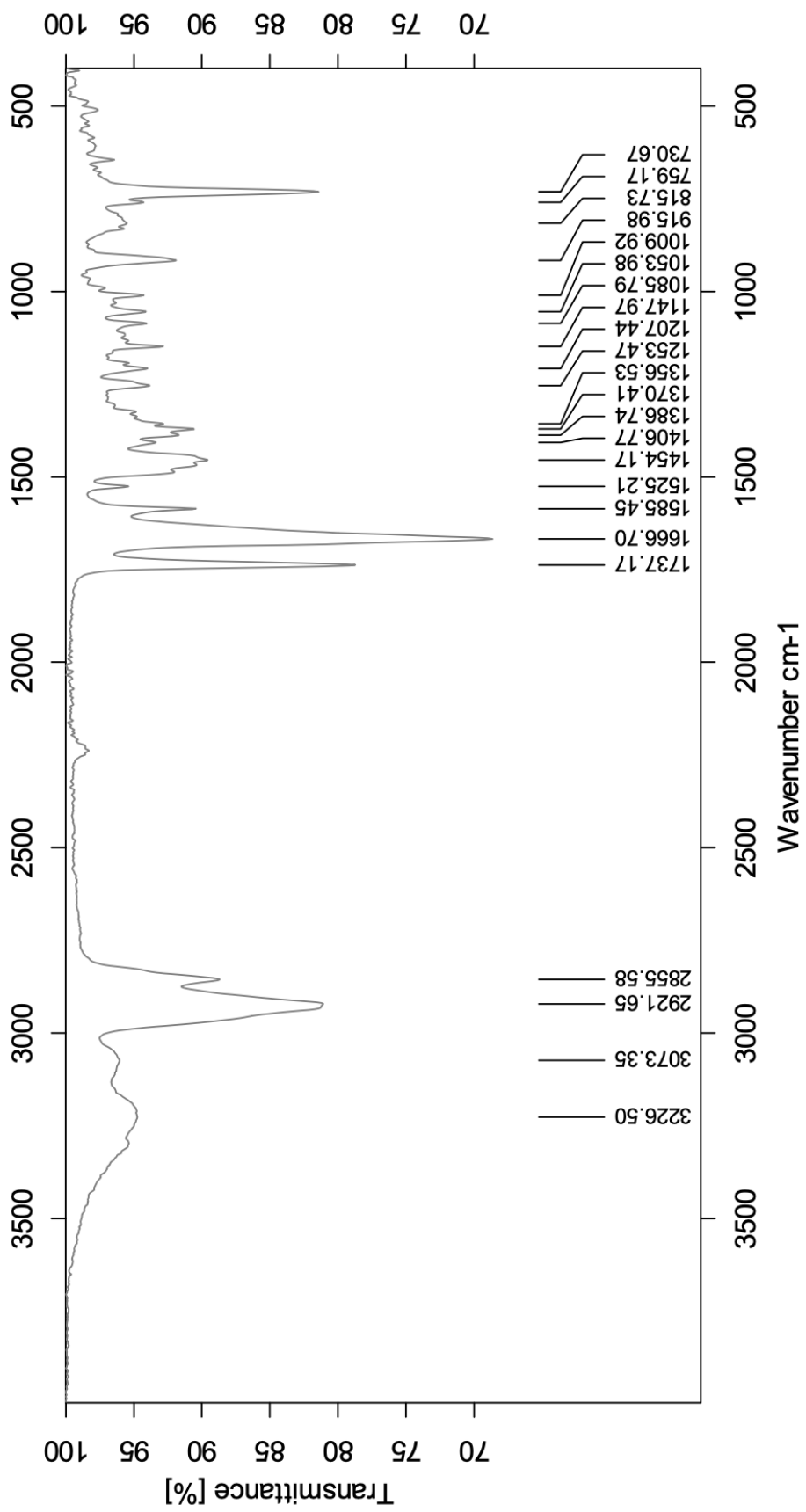**Supplementary Figure 36:** MS spectrum of **8d.** Ions observed are [M+H].

L   Spectroscopic data for compound 8e

Supplementary Figure 37: ^{1}H NMR spectrum in CDCl$_3$, 400 MHz of **8e**.

Supplementary Figure 38: ^{13}C NMR spectrum in CDCl$_3$, 100 MHz of **8e**.

Supplementary Figure 39: IR spectrum of **8e**.

Single Mass Analysis
Tolerance = 2.0 PPM   /   DBE: min = -10.0, max = 50.0
Element prediction: Off
Number of isotope peaks used for i-FIT = 6

Monoisotopic Mass, Even Electron Ions
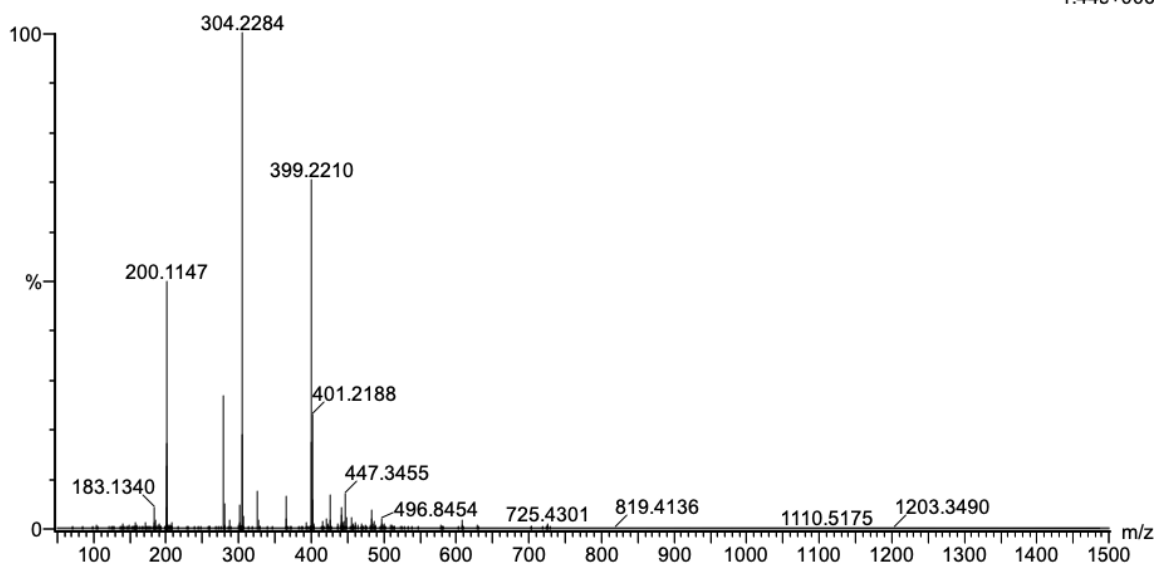1381 formula(e) evaluated with 2 results within limits (all results (up to 1000) for each mass)
Elements Used:
C: 0-100   H: 0-100   N: 0-3   O: 0-10   Na: 0-1   Cl: 0-2
2021_347 55 (0.525) AM2 (Ar,35000.0,0.00,0.00); ABS; Cm (51:55)
1: TOF MS ES+

1.44e+006

Minimum:				-10.0			
Maximum:		5.0	2.0	50.0			

Mass	Calc. Mass	mDa	PPM	DBE	i-FIT	Norm	Conf(%)	Formula
399.2210	399.2206	0.4	1.0	-2.5	2037.5	30.234	0.00	C15 H36 O10 Na
	399.2203	0.7	1.8	9.5	2007.3	0.000	100.00	C24 H32 N2 O Cl

Supplementary Figure 40: MS spectrum of **8e.** Ions observed are [M+H].

Malene Fikseth Jakobsen